PB88-234174

Effect of Relative Humidity and Additives on the Reaction of Sulfur Dioxide with Calcium Hydroxide

Texas Univ. at Austin

Prepared for

Environmental Protection Agency
Research Triangle Park, NC

Jul 88

U.S. Department of Commerce
National Technical Information Service
NTIS

PB88-234174

EPA/600/2-88/037
July 1988

Effect of Relative Humidity and Additives on the Reaction of Sulfur Dioxide with Calcium Hydroxide

by

Rosa Ruiz-Alsop and Gary T. Rochelle

The University of Texas at Austin
Department of Chemical Engineering
Austin, TX 78712

EPA Cooperative Agreement CR 812-454

EPA Project Officer
Charles B. Sedman

Air and Energy Engineering Research Laboratory
Research Triangle Park, NC 27711

AIR AND ENERGY ENGINEERING RESEARCH LABORATORY
OFFICE OF RESEARCH AND DEVELOPMENT
U.S. ENVIRONMENTAL PROTECTION AGENCY
RESEARCH TRIANGLE PARK, NC 27711

REPRODUCED BY
U.S. DEPARTMENT OF COMMERCE
National Technical Information Service
SPRINGFIELD, VA. 22161

TECHNICAL REPORT DATA
(Please read Instructions on the reverse before completing)

1. REPORT NO. EPA/600/2-88/037	2.	3. RECIPIENT'S ACCESSION NO. PB88-234174/AS
4. TITLE AND SUBTITLE Effect of Realtive Humidity and Additives on the Reaction of Sulfur Dioxide with Calcium Hydroxide		5. REPORT DATE July 1988
		6. PERFORMING ORGANIZATION CODE
7. AUTHOR(S) Rosa Ruiz-Alsop and Gary T. Rochelle		8. PERFORMING ORGANIZATION REPORT NO.
9. PERFORMING ORGANIZATION NAME AND ADDRESS The University of Texas at Austin Department of Chemical Engineering Austin, Texas 78712		10. PROGRAM ELEMENT NO.
		11. CONTRACT/GRANT NO. CR812454
12. SPONSORING AGENCY NAME AND ADDRESS **EPA, Office of Research and Development** **Air and Energy Engineering Research Laboratory** **Research Triangle Park, NC 27711**		13. TYPE OF REPORT AND PERIOD COVERED Final; 1/84 - 6/86
		14. SPONSORING AGENCY CODE **EPA/600/13**

15. SUPPLEMENTARY NOTES AEERL project officer is Charles B. Sedman, Mail Drop 4, 919/541-7700.

16. ABSTRACT

The paper gives results of a study of the reaction of SO2 with Ca(OH)2 at conditions similar to those of commercial-scale bag filters: 19-74% relative humidity (RH), 30.4-95 C, and 300-4000 ppm SO2. (NOTE: Previous results with flue gas desulfurization by spray drying of Ca(OH)2 show that a significant amount is removed in the bag filters used to collect the solids.) The study was carried out in a bench-scale reactor with powder reagent Ca(OH)2 dispersed in silica sand. The gas phase was a mixture of N2, SO2, and water vapor. The effects of Ca(OH)2 leading, temperature, RH, inlet SO2 concentration, and additives were investigated. Of the additives tried (buffer acids, and organic and inorganic deliquescents), only the deliquescent salts improved Ca(OH)2 reactivity toward SO2. The improvement depends on the type and amount of salt and on the RH. The experimental data were modelled by a shrinking core model with zero order kinetics in SO2, using an empirical correlation to account for shape and surface roughness of the Ca(OH)2 particles. The diffusion coefficient of the SO2 through the product layer (De) increases linearly with RH and the amount of additive, and the kinetic rate constant (ks) increases exponentially with RH and the amount of additive. De from 0.75E-9 to 1.20E-6 sq cm/sec and ks from 1.0E-9 to 8.23E-9 cm to the 4th power/gmol sec were used in the model.

17. KEY WORDS AND DOCUMENT ANALYSIS

a. DESCRIPTORS		b. IDENTIFIERS/OPEN ENDED TERMS	c. COSATI Field/Group	
Pollution	Temperature	Pollution Control	13B	14G
Sulfur Dioxide	Mathematical Models	Stationary Sources	07B	12A
Calcium Hydroxides				
Reaction Kinetics			07D	
Humidity			04B	
Additives			11G	

18. DISTRIBUTION STATEMENT **Release to Public**	19. SECURITY CLASS *(This Report)* **Unclassified**	21. NO. OF PAGES 218
	20. SECURITY CLASS *(This page)* **Unclassified**	22. PRICE A10 $25.95

EPA Form 2220-1 (9-73)

NOTICE

This document has been reviewed in accordance with U.S. Environmental Protection Agency policy and approved for publication. Mention of trade names or commercial products does not constitute endorsement or recommendation for use.

ABSTRACT

Previous results with flue gas desulfurization by spray drying of $Ca(OH)_2$ show that a significant amount of SO_2 removal occurs in the bag filters used to collect the solids. This research program investigates the reaction of SO_2 with $Ca(OH)_2$ at conditions similar to those of commercial scale bag filters: 19 to 74% relative humidity, 30.4 to 95°C, and 300 to 4000 ppm SO_2. The study was carried out in a bench scale fixed bed reactor, with powder reagent $Ca(OH)_2$ dispersed in silica sand. The gas phase was a mixture of N_2, SO_2, and water vapor. The effects of $Ca(OH)_2$ loading, temperature, relative humidity, inlet SO_2 concentration, and additives were investigated. Of the additives tried (buffers acids, organic deliquescents, and inorganic deliquescents), only the deliquescent salts improved $Ca(OH)_2$ reactivity towards SO_2. The improvement depends on the type and amount of salt and on the relative humidity. The experimental data was modelled by a shrinking core model with zero order kinetics in SO_2, using an empirical correlation to account for shape and surface roughness of the $Ca(OH)_2$ particles. The diffusion coefficient of the SO_2 through the product layer (D_e) increases linearly with relative humidity and amount of additive, and the kinetic rate constant (k_s) increases exponentially with relative humidity and amount of additive. D_e values ranging from 0.75E-9 to 1.20E-6 (cm^2/s) and k_s values ranging from 1.0E-9 to 8.23E-9 ($cm^4/gmol$ s) in the model simulated the experimental results.

TABLE OF CONTENTS

Abstract iii

List of Tables vii

List of Figures ix

Section 1. Project Summary 1

- 1.1. Introduction 1
- 1.2. Experimental Methods 3
  - 1.2.1. Apparatus 3
  - 1.2.2. Analysis of the Experimental Data 5
  - 1.2.3. Reagent Used 5
  - 1.2.4. Preparation of the Samples with Additives 6
- 1.3. Model 6
- 1.4. Results 11
  - 1.4.1. Effect of Relative Humidity 12
  - 1.4.2. Effect of Inlet SO_2 concentration 14
  - 1.4.3. Effect of Amount of $Ca(OH)_2$ in the Reactor 16
  - 1.4.4. Effect of Reactor Temperature 16
  - 1.4.5. Effect of Additives 18
    - 1.4.5.1. Influence of Salt Concentration 21
    - 1.4.5.2. Effect of Prehumidification of Bed 22
- 1.5. Conclusions 24

Section 2. Background of Research 27

- 2.1. Introduction 27
- 2.2. Reduction of SO_2 Emissions 29
  - 2.2.1. Change to Low Sulfur Fuel 30
  - 2.2.2. Use of Desulfurized Coal and Oil 31
  - 2.2.3. Removal of SO_2 from Flue Gases 31
- 2.3. Throwaway Dry FGD Processes 32
  - 2.3.1. Dry Injection 32
  - 2.3.2. Coal/Alkali Combustion 36

2.3.3. Injection/Humidification 36
2.3.4. Spray dryer-based processes 40
2.4. Scope of Investigation 44

Section 3. Reaction of $Ca(OH)_2$ with SO_2 48

3.1. Introduction 48
3.2. Previous Work on the Reaction of SO_2 with $Ca(OH)_2$ . . 49
3.2.1. Previous Work on Fixed Bed Reactors 49
3.2.2. Results from Spray Drying Pilot Plants 51
3.3. Experimental Apparatus 52
3.4. Analysis of the Experimental Data 55
3.5. Reagent Used 56
3.6. Experimental Results 58
3.6.1. Effect of Relative Humidity 58
3.6.2. Effect of Inlet SO_2 Concentration 61
3.6.3. Effect of Amount of $Ca(OH)_2$ in the Reactor 63
3.6.4. Effect of Reactor Temperature 65
3.6.5. Other Types of Lime 66

Section 4. Effect of Additives 68

4.1. Introduction 68
4.2. Previous Research 69
4.2.1. Bench Scale Fixed Bed Reactor 69
4.2.2. Spray Dryer Pilot Plants 70
4.3. Experimental Apparatus 73
4.4. Reactants 73
4.5. Preparation of the Samples with Additives 73
4.6. Organic Acids as Additives 74
4.7. Organic Deliquescents as Additives 74
4.8. Inorganic Deliquescents as Additives 76
4.8.1. Effect of Amount of Additive 78
4.8.2. Effect of Type of Deliquescent Salt 79
4.8.3. Effect of Prehumidification at 98% RH 80
4.8.4. Effect of Nitrogen Purity 82
4.9. Other Experimental Runs 84
4.9.1. Effect of Relative Humidity 84
4.9.2. $CaCl_2$ and Adipic Acid as Additives 84

4.9.3. Differential Experiments 86
4.9.4. Effect of NaCl in the Reactivity of Dolomitic Lime . . 88

Section 5. Modelling of the Reaction of SO_2 with $Ca(OH)_2$ 89

5.1. Summary 89
5.2. Introduction 90
5.3. Experimental 91
5.4. Model 92
5.5. Modelling Results 101
5.6. Discussion 110
5.7. Conclusions 111

Section 6. Conclusions and Recommendations 112

6.1. Conclusions 112
6.2. Recommendations 114

Appendix A. Solids Characterization 116

A.1. Coulter Counter Particle Size Distribution 117
A.2. BET Surface Area Measurement 119
A.3. Scanning Electron Microscope (SEM) 123
A.4. Energy Dispersive Spectroscopy (EDS) 124
A.5. Differential Scanning Calorimetry (DSC) 131
A.6. X-Ray Diffraction 136
A.7. Acid/Base and Iodometric Titration 150

Appendix B. Experimental Data from Sand Bed Reactor . 153

Appendix C. Model Computer Program 163

Appendix D. Sample Calculation for Lime Conversion . . . 180

Appendix E. Error Analysis and Reproducibility 186

E.1. Error Analysis 187
E.2. Reproducibility of Results 192
E.3. Quality Assurance 194

Bibliography 195

LIST OF TABLES

Table 1-1:	Particle Size and BET Surface Area of Reactant	5
Table 1-2:	Experimental Conditions	12
Table 1-3:	Effect of Deliquescent Salts in $Ca(OH)_2$ Reactivity and Deliquescent Properties of the Salts	19
Table 1-4:	Effect of Prehumidification of the Bed at 98% RH on $Ca(OH)_2$ Reactivity	23
Table 2-1:	National Estimates of Sulfur Dioxide Emissions Teragrams/year	28
Table 2-2:	Power Generation Sources: Present and Future	28
Table 2-3:	Flue Gas Desulfurization Processes	33
Table 3-1:	Particle Size and BET Surface Area of Reactant	56
Table 3-2:	Experimental Conditions	58
Table 3-3:	Reactivity of Pressure Hydrated Dolomitic Lime	67
Table 4-1:	Effect of Organic Acids and Organic Deliquescents on $Ca(OH)_2$ Reactivity	75
Table 4-2:	Effect of Deliquescent Salts in $Ca(OH)_2$ Reactivity and Deliquescent Properties of the Salts	77
Table 4-3:	Effect of Prehumidification of the Bed at 98% RH on $Ca(OH)_2$ Reactivity	82
Table 4-4:	Effect of Nitrogen Purity on Lime Reactivity	83
Table 4-5:	Effect of Adipic acid and $CaCl_2$ as Additives for $Ca(OH)_2$	86
Table 4-6:	Effect of NaCl on the Reactivity of Pressure Hydrated Dolomitic Lime	88
Table 5-1:	Modelling Experiments with Salt Additives at High Relative Humidity	107
Table 5-2:	Modelling Experiments with Salt Additives at Moderate Relative Humidity	108
Table A-1:	$Ca(OH)_2$ Particle Size Distributions	118
Table A-2:	BET Surface Area of the Solids	122

Table A-3: Elemental Analysis using EDS 131
Table A-4: X-Ray Powder Diffraction Results 146
Table B-1: Experimental Data Lime 0 154
Table B-2: Experimental Data Lime A 155
Table B-3: Experimental Data, Lime with Organic Additives 156
Table B-4: Experimental Data of Lime with Salts Additives at 74% RH 157
Table B-5: Experimental Data of Lime with Salts Additives at 54% RH 158
Table B-6: Experimental Data of Lime with Salts Additives at 17 and 35% RH 160
Table B-7: Experimental Data, Pressure Hydrated Dolomitic Lime 161
Table B-8: Differential Experiments 162
Table D-1: Conversion of $Ca(OH)_2$ versus reaction time 185

LIST OF FIGURES

Figure 1-1:	Experimental Apparatus	4
Figure 1-2:	Effect of Relative Humidity on Reaction Rate, Lime 0	13
Figure 1-3:	Effect of Relative Humidity on Model Parameters	13
Figure 1-4:	Effect of SO_2 Concentration, High Relative Humidity	15
Figure 1-5:	Effect of SO_2 Concentration, Moderate Relative Humidity	15
Figure 1-6:	Effect of $Ca(OH)_2$ Loading, 1000 ppm SO_2	17
Figure 1-7:	Effect of Reactor Temperature, Lime A	17
Figure 1-8:	Effect of Amount of Additive	21
Figure 1-9:	Effect of NaCl on the Model Parameters	22
Figure 2-1:	Diagram of the Coolside Process	38
Figure 2-2:	Typical Spray Dryer System for FGD	41
Figure 3-1:	Experimental Apparatus	53
Figure 3-2:	Lime 0, Effect of Relative Humidity	60
Figure 3-3:	Lime A, Effect of Relative Humidity	60
Figure 3-4:	Differential Experiments, Effect of Relative Humidity	61
Figure 3-5:	Effect of SO_2 Concentration, High Relative Humidity	62
Figure 3-6:	Effect of SO_2 Concentration, Moderate Relative Humidity	62
Figure 3-7:	Effect of $Ca(OH)_2$ Loading, 1000 ppm SO_2	64
Figure 3-8:	Effect of $Ca(OH)_2$ Loading, 2000 ppm SO_2	64
Figure 3-9:	Effect of Reactor Temperature, Lime A	65
Figure 4-1:	Effect of Amount of Additive on $Ca(OH)_2$ Reactivity	78
Figure 4-2:	Effect on $Ca(OH)_2$ Conversion of Decreasing Relative Humidity by Increasing Temperature, With and Without 10 mole% NaCl	85

Figure 4-3: Effect on $Ca(OH)_2$ Conversion of Decreasing Relative Humidity by Increasing Temperature, With and Without 10 mole% $NaNO_3$ 85
Figure 4-4: Differential Experiments, Effect of NaCl on $Ca(OH)_2$ Conversion 87
Figure 4-5: Differential Experiments, Effect of $CaCl_2$ on $Ca(OH)_2$ Conversion 87
Figure 5-1: Effect of Relative Humidity on Reaction Rate, Lime 0 102
Figure 5-2: Effect of Relative Humidity on Model Parameters 102
Figure 5-3: Effect of Relative Humidity on Reaction Rate, Lime A 103
Figure 5-4: Effect of SO_2 Concentration, 70% Relative Humidity 104
Figure 5-5: Effect of SO_2 Concentration, 50% Relative Humidity 104
Figure 5-6: Effect of $Ca(OH)_2$ Load on Reaction Rate 105
Figure 5-7: Effect of Temperature on Reaction Rate 106
Figure 5-8: Effect of NaCl on the Model Parameters 109
Figure A-1: SEM Micrograph: Lime 0, 400 Magnification 125
Figure A-2: SEM Micrograph: Lime 0, 4000 Magnification 125
Figure A-3: SEM Micrograph: Lime A, 400 Magnification 126
Figure A-4: SEM Micrograph: Lime A, 4000 Magnification 126
Figure A-5: SEM Micrograph: $Ca(OH)_2$ + 10 mole% NaCl, 10000 Magnification 127
Figure A-6: SEM Micrograph: Reacted Lime A + 10 mole% NaCl, 4000 Magnification, 74% RH, 500 ppm SO_2, 64.4°C, 2 hr Reaction Time, Conversion 46% 127
Figure A-7: SEM Micrograph: Ball Mill Hydrated Dolomitic Lime, 400 Magnification 128
Figure A-8: SEM Micrograph: Ball Mill Hydrated Dolomitic Lime, 4000 Magnification 128
Figure A-9: SEM Micrograph: Hydrator Hydrated Dolomitic Lime, 400 Magnification 129
Figure A-10: SEM Micrograph: Hydrator Hydrated Dolomitic Lime, 4000 Magnification 129

Figure A-11: DSC Curve for Reacted $Ca(OH)_2$ + 10 mole% NaCl, N_2 of 99.5% purity, 54% RH, 66°C, 500 ppm SO_2, 1 hr Reaction Time, Conversion 30% 133
Figure A-12: DSC Curve for Reacted $Ca(OH)_2$, O_2 Free N_2, 74% RH, 64.4°C, 500 ppm SO_2, 1 hr Reaction Time, Conversion 24.5% 134
Figure A-13: DSC Curve for Reacted $Ca(OH)_2$ + 10 mole% NaCl, O_2 Free N_2, 74% RH, 64.4°C, 500 ppm SO_2, 2 hr Reaction Time, Conversion 46% 135
Figure A-14: X-ray Diffraction Pattern: Slurried $Ca(OH)_2$ 137
Figure A-15: X-Ray Diffraction Pattern: $Ca(OH)_2$ with 20 mole% $CaCl_2 \cdot 2H_2O$ 139
Figure A-16: X-ray Diffraction Pattern: $Ca(OH)_2$ with 10 mole% NaCl 140
Figure A-17: X-ray Diffraction Pattern: $Ca(OH)_2$ with 30 mole% $NaNO_3$ 141
Figure A-18: X-ray Diffraction Pattern: $Ca(OH)_2$ with 30 mole% LiCl 142
Figure A-19: X-ray Diffraction Pattern: $Ca(OH)_2$ with 10 mole% KCl 143
Figure A-20: X-ray Diffraction Pattern: $Ca(OH)_2$ with 20 mole% $BaCl_2 \cdot 2H_2O$ 144
Figure A-21: X-ray Diffraction Pattern: $Ca(OH)_2$ with 10 mole% NaBr 145
Figure A-22: X-ray Diffraction Pattern: Reacted $Ca(OH)_2$, 21% Conversion, 500 ppm SO_2, 74% R H, 64.4°C, 1 hr reaction 147
Figure A-23: X-ray Diffraction Pattern: Reacted $Ca(OH)_2$ with 10 mole% NaCl, 74% R H, 64.4°C, 500 ppm SO_2, 2 hr Reaction, 46% Conversion 148
Figure A-24: X-ray Diffraction Pattern: Pressure Hydrated Dolomitic Lime 149
Figure D-1: Raw Data from Experiment 132 182
Figure E-1: Reproducibility of results, pure $Ca(OH)_2$ 193
Figure E-2: Reproducibility of results, $Ca(OH)_2$ with 10 mole% NaCl 193

Section 1

Project Summary

1.1 Introduction

Flue gas desulfurization by spray drying of $Ca(OH)_2$ slurry has become increasingly important in recent years as an alternative to the more traditional wet lime or limestone scrubbing. During spray drying, the SO_2 containing flue gas is contacted in the dryer with a finely atomized aqueous solution or slurry of an alkali (typically slaked lime or soda ash), which absorbs and neutralizes the SO_2. Simultaneously, the water is evaporated from the slurry droplets leaving a solid material which can be collected using conventional solids collection equipment such as bag filters or electrostatic precipitators. Bag filters are the preferred collection equipment because the unreacted $Ca(OH)_2$ present in the solids reacts with SO_2 in the bag filters, thus producing additional SO_2 removal (Kelly and Dickerman, 1981, Kelly et al., 1983, Stevens, 1981, Samuel et al., 1983, Samuel et al., 1984, Bresowar et al., 1981, Blythe and Rhudy, 1984). The reaction between lime solids and SO_2 taking place in the ducts and bag filters of a spray dryer system is the subject of the present research.

Most of the information available in the literature for this reaction is reported results of SO_2 removal across the bag filters of pilot and demonstration spray dryer plants (Blythe and Rhudy, 1984, Bresowar et al., 1981, Samuel et al., 1984, Yeh et al., 1983, Jankura et al., 1984, Lewis and Gehri, 1983, Parsons et al., 1981, Robards et al., 1985, Kelly et al., 1983, Gustke et al., 1984, Donnelly et al., 1985). These results are difficult to interpret because the conditions of the flue gas entering the bag filters are dependent on the spray absorber behavior. Any variable changes that affect the SO_2 removal across the spray absorber will change the concentration of SO_2 entering the bag filters. Therefore, two variables will have effectively been changed in the bag filters and the contribution of each one can not be isolated.

Two bench scale studies regarding the reaction of interest have been reported, one at the Lund Institute of Technology-Sweden (Klingspor, Karlsson, and Bjerle, 1983, 1984) and one at EPA (Jorgensen et al., 1986). However, the characterization of this reaction is far from complete.

The present study was carried out in a bench scale fixed bed reactor, operated at conditions similar to those found in bag filters of commercial spray drying systems, and using powder reagent $Ca(OH)_2$ as the sorbent. The effect of $Ca(OH)_2$ loading, temperature, SO_2 concentration, and relative humidity was studied. Also, additives that improve the lime reactivity towards SO_2 were identified.

1.2 Experimental Methods

1.2.1 Apparatus

The general design of the experimental apparatus is given in Figure 1-1. A simulated flue gas was synthesized by combining nitrogen and sulfur dioxide from gas cylinders. The gas flow rates were measured using rotameters. Water was added to the system by means of a syringe pump (Sage Instruments, Model 341A) and evaporated at 120°C in a stainless steel evaporation chamber before mixing with the gas stream.

The reactor was made of glass, and it had a diameter of 4 cm and 12 cm height. The reactor was packed with a mixture of silica sand and $Ca(OH)_2$ reactant in a weight ratio of 40:1. The addition of sand is necessary to avoid channeling caused by lime agglomeration (Karlsson et al., 1983). The silica sand (between 80 and 115 mesh) was obtained from Martin Marietta Aggregates.

The reactor was immersed in a water bath that maintained the system temperature within 0.1°C. Tubing upstream from the reactor was heated to prevent the condensation of moisture on the walls. Before going to analysis, the gas was cooled and the water vapor then condensed out by cooling water and an ice bath . The gas was analyzed for SO_2 using a pulsed fluorescent SO_2 analyzer (Thermoelectron Corporation model 40), and the SO_2 concentration was continuously recorded. The SO_2 analyzer was calibrated using a calibration standard (a mixture of 2000 ppm SO_2 and N_2). The reactor was equipped with a bypass, to allow the bed to be preconditioned and to allow the gas flow to be stabilized at the desired SO_2 concentration before beginning

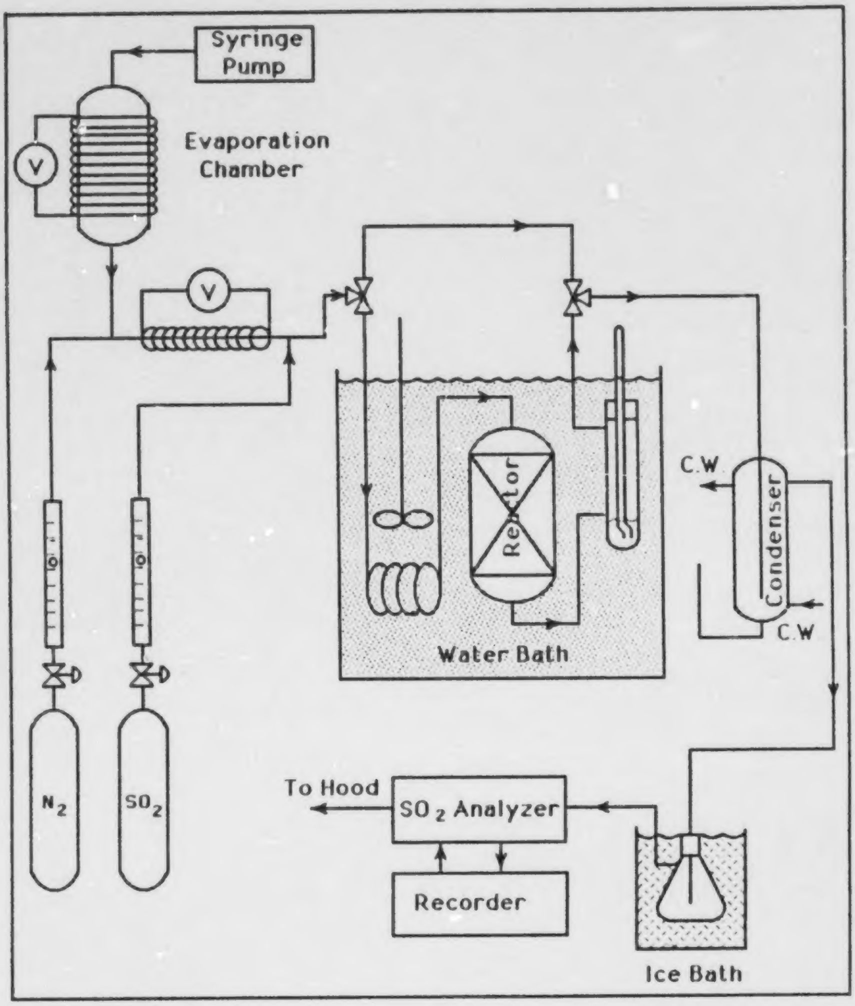
Syringe Pump
Evaporation Chamber
V
V
Reactor
C.W
Condenser
C.W
Water Bath
N2
SO2
To Hood
SO2 Analyzer
Recorder
Ice Bath

Figure 1-1: Experimental Apparatus

the experimental run. Prior to each experimental run the bed was humidified by flushing first with pure nitrogen at a relative humidity of about 98% for 10 minutes and then later with pure nitrogen for 8 minutes at the relative humidity at which the experiment was to be performed. This was done to simulate the moisture conditions encountered in the bag filters where the solids are originally slurry droplets.

The reaction time was normally 1 hour. The raw data from each experimental run were curves of SO_2 concentration leaving the reactor versus time. These curves were given by the recorder of the SO_2 analyzer.

1.2.2 Analysis of the Experimental Data

The raw data from the experiments were SO_2 concentrations from the reactor as a function of time. By integration of the SO_2 concentration over time and a mass balance on the reactor, the average fraction of $Ca(OH)_2$ converted were calculated at each time. As a backup, the reacted solids were analyzed for sulfite and hydroxide using acid/base and iodine titrations.

1.2.3 Reagent Used

Most of the experimental work was done using reagent grade $Ca(OH)_2$ as a reactant. Two batches of $Ca(OH)_2$ that will be identified as lime 0 and lime A were used. These two batches of $Ca(OH)_2$ differ slightly in particle size and BET surface area as shown in Table 1-1.

Table 1-1: Particle Size and BET Surface Area of Reactant

Reactant	Coulter Counter Median Particle Size (μm)	BET Surface Area (m^2/g)
lime 0	7.4	8.2
lime A	5.6	9.4
lime A (slurried)	-	8.8

The BET surface area of a sample of 1 g of $Ca(OH)_2$ A, after slurrying with 5 ml of distilled water and drying at 75°C, is also shown in Table 1-1. The slurrying and drying process caused a slight decrease in the surface area of $Ca(OH)_2$.

1.2.4 Preparation of the Samples with Additives

An aqueous solution containing the desired additive was prepared. Five ml of this solution were then added to 1 g of $Ca(OH)_2$ and slurried. The sample was placed in a oven to dry at 75°C for about 14 hours, and then later sieved to separate the individual $Ca(OH)_2$ particles prior to mixing with the silica sand and being placed in the reactor.

1.3 Model

The equations that describe the absorption of a component from a moving gas stream by a fixed solid in a packed bed consist of two differential equations obtained from material balances in the gaseous and solid phases.

Schematically:

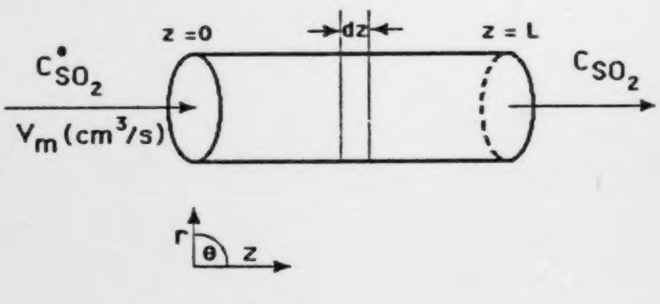

Assuming uniform SO_2 and $Ca(OH)_2$ concentrations in the r and θ directions, and neglecting SO_2 diffusion and dispersion in the z direction as well as the time derivative of the SO_2 concentration (von Rosenberg et al., 1977), the following equations are obtained:

$$\frac{v_m \, dC_{SO_2}}{A \, dz} = r_{SO_2} \tag{1.1}$$

$$\frac{dC_{lime}}{dt} = r_{SO_2} \tag{1.2}$$

with boundary and initial conditions:

$$\text{At } z = 0 \qquad C_{SO_2} = C^{o}_{SO_2} \tag{1.3}$$

$$\text{At } t = 0 \qquad C_{lime} = C^{o}_{lime}$$

Where:

v_m = volumetric flow rate of gas (cm^3/sec)

C_{SO_2} = concentration of SO_2 in the gas phase ($gmol/cm^3$)

A = cross sectional area of the reactor (cm^2)

z = length of the reactor (cm)

r_{SO_2} = rate of disappearence of SO_2 ($gmol/cm^3$ sec)

C_{lime} = $Ca(OH)_2$ concentration ($gmol/cm^3$)

t = time (sec)

The rate equation for r_{SO_2} will depend on the model selected to represent the kinetics of the reaction.

A shrinking core model with kinetics of zero order in SO_2 was chosen to fit the experimental data. The shrinking core model or unreacted core model assumes that the reaction takes place at the exterior surface of the particle. As the reaction proceeds, the surface of reaction will move into the interior of the solid leaving behind a layer of inert product. The external radius of the particle remains the same, assuming no shrinkage or swelling of the product layer.

The shrinking core model was originally developed by Yagi and Kunii (1961) for the isothermal reaction of spherical solid particles. The $Ca(OH)_2$ particles are non-spherical and have a rough surface, so their surface area is much higher than that of spherical particles of the same volume. An empirical expression was introduced to account for the decrease in roughness as the reaction progresses. A dimensionless roughness parameter was defined as:

$$\sigma = \frac{A}{A_\phi} \tag{1.4}$$

Where:

A = actual surface area of the lime (m^2/g)

A_ϕ = surface area of spherical particles of equal mass (m^2/g)

When the lime is unreacted, σ can be estimated as the ratio of the BET surface area of the lime and the surface area calculated from the Coulter Counter particle size distribution assuming spherical particles. As the reaction progresses, σ should decrease and approach the limit $\sigma = 1.0$ when all the lime has reacted.

An empirical expression of the form:

$$\sigma = 1.0 + \exp(a X_{lime} + b) \qquad (1.5)$$

where X_{lime} is the fraction of lime unreacted, was used to describe the change of roughness with the reaction. Equation (1.5) must satisfy the condition:

$$\text{At } X_{lime} = 1.0 \qquad \sigma = \sigma_o = \text{BET area}/A_\phi \qquad (1.6)$$

To force σ to decrease more rapidly at high values of X_{lime} and to simulate the experimental results, the following additional condition was imposed:

$$\text{At } X_{lime} = 0.8 \qquad \sigma = 2.0 \qquad (1.7)$$

For the two batches of $Ca(OH)_2$ used in the experiments, namely lime 0 and lime A which differ slightly in surface area and particle size, the constants a and b in Equation (1.5) took slightly different values (a was 12.878 for lime 0 and 13.428 for lime A, while the values of b were -10.302 and -10.742 respectively).

Using the roughness parameter σ, the following equations can be obtained for the rate of disappearence of SO_2 assuming that chemical reaction, or SO_2 diffusion through the gas film and product layer are the rate controlling steps.

$$r_{SO_2} = \frac{1}{V}\, 4\pi R^2 N \sigma \rho_{lime} k_s X_{lime}^{2/3} \qquad (1.8)$$

$$r_{SO_2} = \frac{1}{V} \frac{C^g_{SO_2}}{\dfrac{X_{lime}^{-1/3} - 1}{4\pi D_e N R (\sigma\sigma_o)^{1/2}} + \dfrac{1}{4\pi R^2 k_g N \sigma_o}} \qquad (1.9)$$

where:

V = reactor volume (cm^3)

R = Radius of the particle (cm)

N = number of $Ca(OH)_2$ particles

ρ_{lime} = $Ca(OH)_2$ molar density ($gmol/cm^3$)

k_s = kinetic rate constant (cm/sec)

$C^g_{SO_2}$ = SO_2 concentration at the gas bulk ($gmol/cm^3$)

D_e = diffusivity of SO_2 through product (cm^2/sec)

k_g = mass transfer coefficient (cm/sec)

If the chemical reaction is slow, the rate of disappearance of SO_2 will be given by Equation (1.8). If the chemical reaction is fast, all of the SO_2 that reaches the surface of the core will be immediately consumed and the concentration of the SO_2 at the surface of the unreacted core will become zero. At these conditions the rates of diffusion of the SO_2 through the gas film and product layer will become the limiting steps, and Equation (1.9) will become important.

Of equations (1.8) and (1.9), the one that gives the lowest rate of SO_2 disappearance will determine the overall kinetic rate. The parameters of the model are k_g, D_e, and k_s. The integration of Equations (1.1) and (1.2) with the rate of disappearence of SO_2 given by equations (1.8) or (1.9), was carried out by assuming an average particle size of the lime particles which gave the same surface area as the measured particle size distribution assuming spherical particles. The mass transfer coefficient, k_g was not used as an adjustable parameter because at the conditions at which the experiments were performed, gas film diffusion is not likely to be important. The only effect of gas film diffusion is that it provides a limit to the rate expression (1.9) at the beginning of the reaction where product layer resistance is zero as there is no product formed. The value of k_g (544 cm/sec) was estimated using a Sherwood number of 2 corresponding to mass transfer from spherical particles in an stagnant fluid (Sherwood et al., 1975).

Thus D_e and k_s were the only parameters used to fit the experimental data. Depending on whether mass transfer or chemical reaction is the controlling step, only one of these parameters may be important.

A computer program with variable step size in time and in distance along the reactor was written to model the reaction. This computer program uses the IMSL integration routine DGEAR to carry out the integration, and the IMSL interpolation routine ICSCCU to provide interpolated values of lime conversion needed for each time integration step.

1.4 Results

The effects of relative humidity, temperature, inlet SO_2 concentration, and amount of lime in the reactor on the reaction of SO_2 with powdered reagent $Ca(OH)_2$ were studied. The experimental conditions are listed in Table 1-2.

Table 1-2: Experimental Conditions

Relative Humidity:	17 - 90%
SO_2 Inlet Concentration:	500 - 4000 ppm
Reactor Temperature:	30.5 - 95°C
Nitrogen Flow Rate:	4600 cm^3/min (0°C, 1 atm)
Amount of Lime:	1.0 - 4.0 g

1.4.1 Effect of Relative Humidity

Relative humidity was found to have a dramatic effect on the rate of reaction of SO_2 with $Ca(OH)_2$ as illustrated by Figure 1-2. The full lines correspond to experimental results at 2000 ppm inlet SO_2 and 66°C using 4 g of lime 0. Figure 1-2 shows that for all relative humidities, 100% of the SO_2 entering the reactor is being removed during the first one or two minutes of reaction, then the reaction rate (represented by the slope of the conversion versus time curves) decreases quickly at low relative humidities but slower at high relative humidities.

The broken lines in Figure 1-2 correspond to the model prediction for these experiments. Figure 1-3 shows the dependence of the rate constant and solid diffusion coefficient on relative humidity. At high relative humidity, the chemical reaction is the controlling step and k_s is the parameter that determines the rate of reaction. Any value of D_e greater than 8.0E-8 cm^2/sec will give essentially the same result. SO_2 diffusion through the product layer becomes more important as the

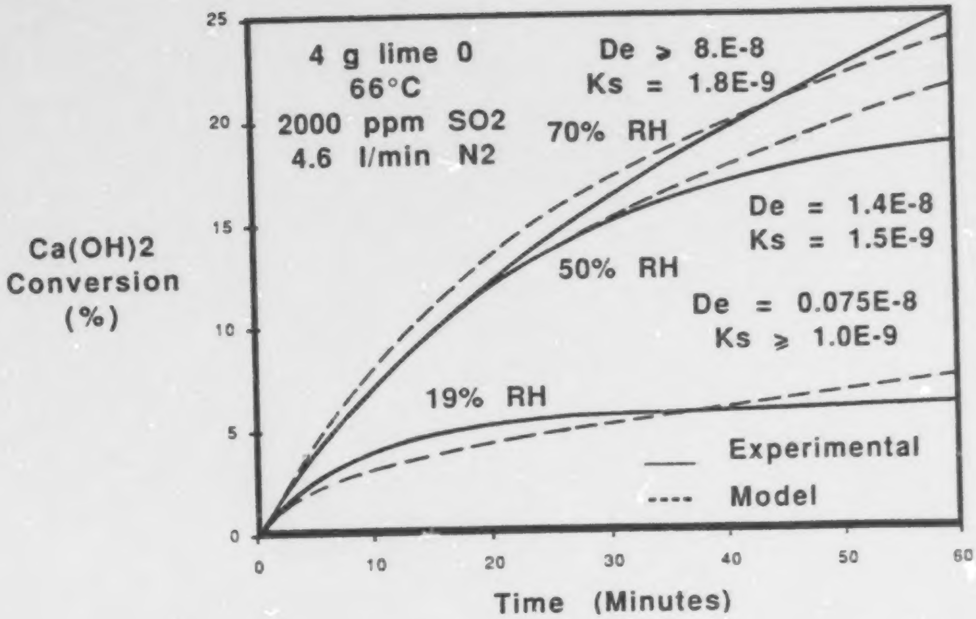

Figure 1-2: Effect of Relative Humidity on Reaction Rate, Lime 0

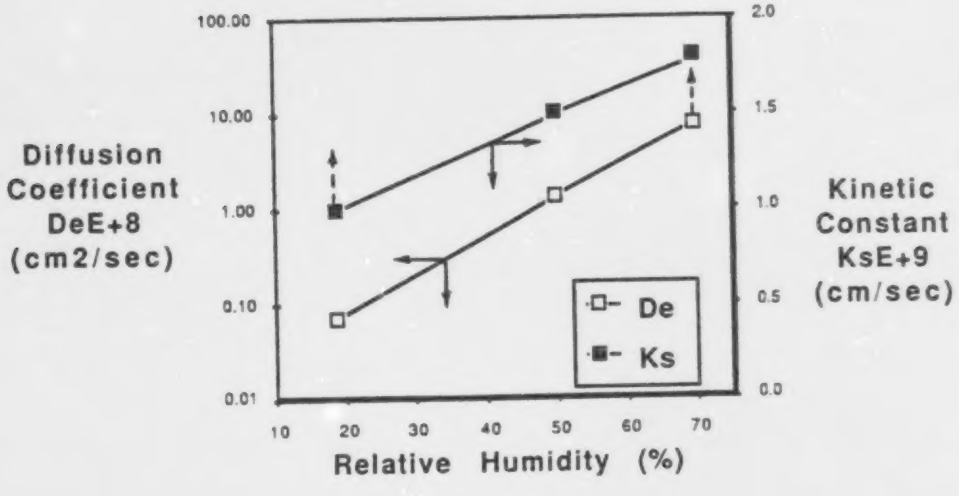

Figure 1-3: Effect of Relative Humidity on Model Parameters

relative humidity decreases. At 19% relative humidity, D_e is the parameter that determines the rate of adsorption of SO_2. At 19% relative humidity, any value of k_s greater than 1.0E-9 cm/sec will give essentially the same results. Both D_e and k_s are affected by the relative humidity, but in the range of relative humidities studied k_s increases approximately linearly while D_e increases exponentially. Because the SO_2 diffusion coefficient changes more rapidly than the kinetic constant, a change in the controlling mechanism occurs when the relative humidity is increased. The strong effect of relative humidity on reaction rate has also been reported by other researchers (Klingspor et al., 1984, Jorgensen et al., 1986).

1.4.2 Effect of Inlet SO_2 concentration

The effect of the inlet SO_2 concentration on the reaction rate was found to depend on the relative humidity. Figures 1-4 and 1-5 illustrate the effect of inlet SO_2 concentration at 70 and 50% relative humidity, respectively. The full lines in these figures correspond to experimental results, and the broken lines to the model predictions. At 70% relative humidity, the $Ca(OH)_2$ conversion was practically independent of the inlet SO_2 concentration as can be seen in Figure 1-4. At lower relative humidity the reaction rate is not affected by the SO_2 concentration if the SO_2 concentration is high. However, at lower levels of SO_2 the reaction rate is affected by the SO_2 concentration as illustrated by Figure 1-5. The observed effect of SO_2 concentration can be explained by assuming that the reaction rate has zero order kinetics in SO_2, but at low relative humidity and/or low SO_2 concentrations, SO_2 diffusion becomes the controlling step instead of chemical reaction. As can be seen from Figures 1-4 and 1-5, the model is able to predict the SO_2 effect with reasonable accuracy.

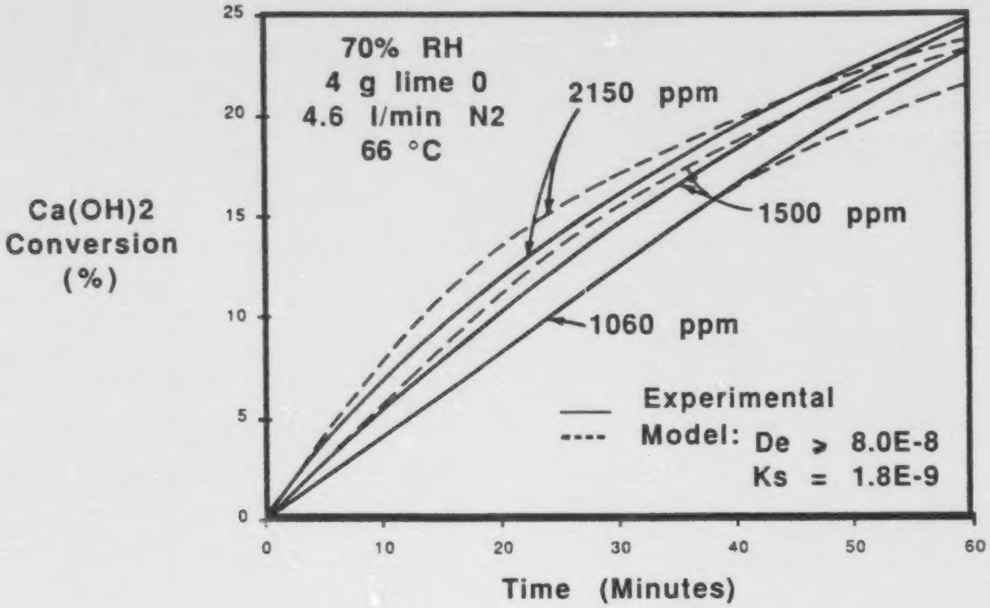

Figure 1-4: Effect of SO_2 Concentration, High Relative Humidity

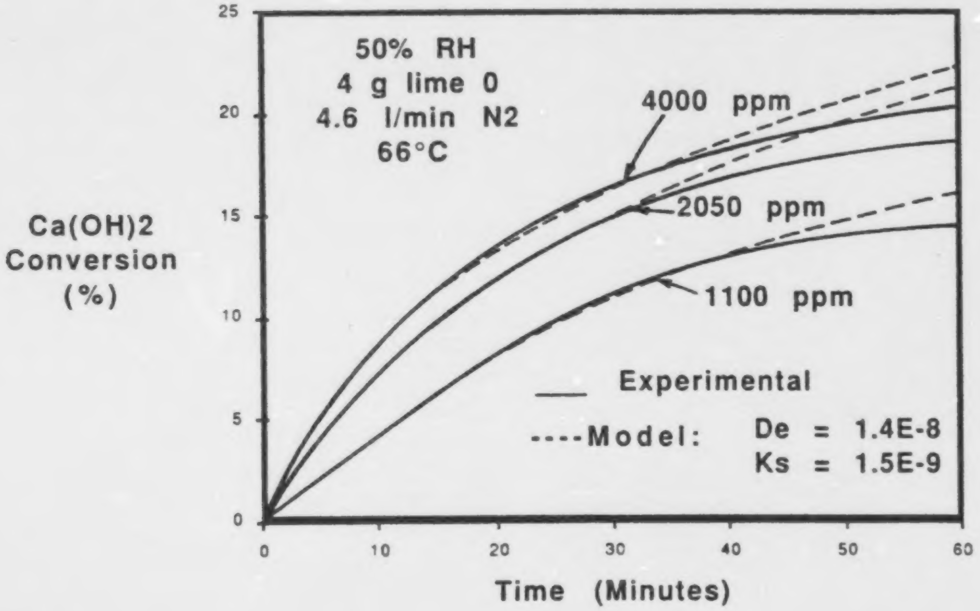

Figure 1-5: Effect of SO_2 Concentration, Moderate Relative Humidity

1.4.3 Effect of Amount of $Ca(OH)_2$ in the Reactor

The effect on the average $Ca(OH)_2$ conversion of changing the amount of $Ca(OH)_2$ in the reactor is illustrated by the full lines in Figure 1-6 which show the experimental $Ca(OH)_2$ conversion when the amount of lime 0 in the reactor was reduced from 4 to 1 g at 1000 ppm SO_2, 50% relative humidity. From the figure it can be seen that the amount of $Ca(OH)_2$ present in the reactor makes a difference during the first minutes of reaction, but the effect is less marked at later times. These results are consistent with the effect of SO_2 concentration discussed in the previous subsection. When more $Ca(OH)_2$ is present in the reactor, more SO_2 is removed at the entrance of the reactor, so the $Ca(OH)_2$ present farther down in the reactor "sees" a lower concentration of SO_2, and the reaction rate is slower. At later times when the SO_2 removal is lower, the amount of $Ca(OH)_2$ present will not be as important.

1.4.4 Effect of Reactor Temperature

Reactor temperature has a very moderate effect on $Ca(OH)_2$ reactivity, as illustrated by the full line in Figure 1-7, which shows the effect on $Ca(OH)_2$ conversion when the reactor temperature was increased from 30.4 to 64.4°C while keeping all other variables constant. The relative humidity was 74%, so in this region the reaction is expected to be kinetically controlled.

The broken lines in Figure 1-7 are the model predictions for the experiments run at the two different temperatures. At the conditions at which the experiments were performed, the reaction rate is kinetically controlled, so k_s is the only important adjustable parameter in the

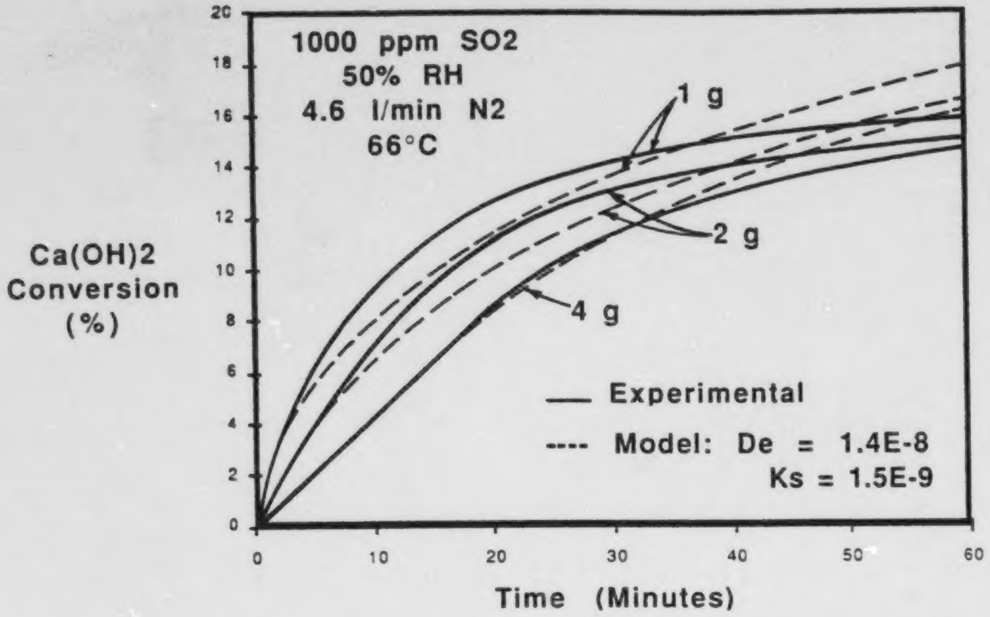

Figure 1-6: Effect of $Ca(OH)_2$ Loading, 1000 ppm SO_2

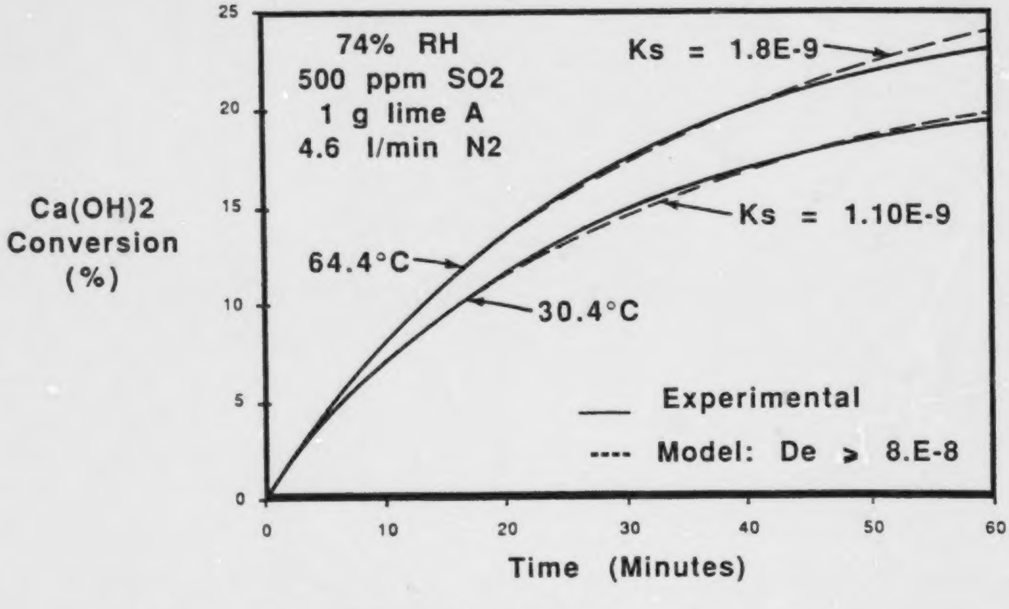

Figure 1-7: Effect of Reactor Temperature, Lime A

model. By using the values of k_s given by the model, an apparent activation energy of 2.9 kcal/gmol can be estimated for $Ca(OH)_2$. This value of activation energy is somewhat lower than the value of 6 kcal/gmol reported by other sources for this reaction (Jorgensen et al., 1986).

A very weak dependence of the reaction rate with temperature was also reported by other researchers (Klingspor et al., 1984, Jorgensen et al., 1986).

1.4.5 Effect of Additives

Two organic acids (adipic acid, and glycolic acid) and three organic deliquescents (ethylene glycol, tri-ethylene glycol, and mono-ethanolamine) were selected as test additives for $Ca(OH)_2$. All of them proved to be detrimental to the reaction of SO_2 with $Ca(OH)_2$.

A number of deliquescent salts were also tested as additives at 74 and 54% RH (Table 1-3). The beneficial effect of the salts depends on the type and amount of salt and the relative humidity. At high relative humidity (74%), all the deliquescent salts tried were successful in increasing the reactivity of the $Ca(OH)_2$ towards SO_2. At a lower relative humidity (54%), some of the salts do not perform as well, and some, such as $Ca(NO_3)_2$, do not have any beneficial effect at all.

Also presented in Table 1-3 is the water activity over saturated solutions of the salts at 70°C and 1 atm. The water activity is approximately equal to the fractional relative humidity of the gaseous phase that would be in equilibrium with a saturated solution of the salt at that temperature. If one of these deliquescent salts is contacted with

Table 1-3: Effect of Deliquescent Salts in $Ca(OH)_2$ Reactivity and Deliquescent Properties of the Salts

500 ppm SO_2, 1.0 g lime A, 4.6 l/min N_2 (0°C,1 atm)

Additive (Mole%)	$Ca(OH)_2$ Conversion at 60 minutes (%) 74% RH 64.4°C	54% RH 66°C	a_w[a] at 70°C	Model Constants at 74% RH D_eE+8 (cm^2/sec)	k_sE+9 (cm/sec)	at 54% RH D_eE+8 (cm^2/sec)	k_sE+9 (cm/sec)
None	22.4	11.8	-	$\geq$ 8.0	1.8	1.5	$\geq$ 1.5
5% Na_2SO_4	28.3	-	.887[d]	$\geq$ 18.0	2.7	-	-
5% Na_2SO_3	29.8	16.1	-	$\geq$ 17.0	2.6	3.3	$\geq$ 1.7
5% $CaCl_2$[c]	34.6	16.4	.69[d]	$\geq$ 73.0	5.4	2.9	$\geq$ 1.6
10% NaCl	38.5	27.0	.751[e]	$\geq$ 85.0	6.1	$\geq$ 18.0	2.75
5% $Ca(NO_3)_2$[c]	39.4	12.3	.553[b,d]	$\geq$ 85.0	7.0	1.6	$\geq$ 1.5
5% $Co(NO_3)_2$	-	13.2		-	-	1.9	$\geq$ 1.5
10% $NaNO_2$	40.0	-	.593[e]	$\geq$ 80.0	7.0	-	-
10% $NaNO_3$	41.5	27.2	.657[e]	$\geq$ 95.0	7.6	$\geq$ 18.0	2.75
5% $BaCl_2$	-	19.4	.876[d]	-	-	4.5	$\geq$ 1.9
5% $Na_2S_2O_3$	-	21.6	.298[d]	-	-	6.6	2.15
10% KCl	-	37.3	.80[e]	-	-	$\geq$ 80.0	4.8
10% NaBr	-	42.0	.507[e]	-	-	$\geq$ 90.0	7.7
10% LiCl	-	43.9	.099[d]	-	-	$\geq$ 120.	8.23
100% SO_2 Removal		48.2	48.2				

---

[a] Activity of water over saturated solutions of the salt

[b] data at 100°C.

[c] Solid phases were $CaCl_2 \cdot Ca(OH)_2 \cdot H_2O$ and $Ca_2N_2O_7 \cdot 2H_2O$ respectively.

[d] Source (National Research Council, 1930)

[e] Source (Lange, 1961)

a gaseous phase of relative humidity greater than the water activity, the salt will capture water from the gas phase and become a solution. This tendency to capture water has been extensively documented in the literature by studies of the growth of salt containing aerosols as a function of the atmospheric relative humidity (Winkler, 1973, Ferron, 1977, Tang, 1976, Tang et al., 1977, Tang and Munkelwitz, 1977, Tang et al., 1978). From the data presented in Table 1-3 it is clear that based on deliquescence alone most of the salts tested, specifically $NaNO_3$ and all the chlorides with exception of LiCl, should not have any beneficial effect at 54% relative humidity. Nevertheless, these salts are among the ones that behave the best at that moderate relative humidity. A possible explanation for this finding would be a hysteresis phenomenon, and this will be discussed later.

Table 1-3 also shows the values of the diffusion coefficient of SO_2 through the product layer (D_e), and the kinetic constant (k_s) that can be used to simulate the experimental runs using salt additives. D_e values ranging from 1.5E-8 to 120E-8 (cm^2/s) and k_s values from 1.5E-9 to 8.23E-9 ($cm^4/gmol\ s$) were used in the simulation of the salt experiments. Depending on the amount and type of salt added, chemical reaction or SO_2 diffusion can become the controlling step. A reasonably good agreement was found between the predictions of the model and the experimental results. The maximum percentage of error between the experimental data and predicted values was below 10% in most cases with a few exceptions where it was below 20%.

1.4.5.1. Influence of Salt Concentration

The influence of the salt concentration on the SO_2 reaction rate is illustrated by Figure 1-8. The salts used were NaCl and $NaNO_3$ in concentrations ranging from 1 to 15 mole%. The experiments were carried out at a relative humidity of 54%, and a reactor temperature of 66°C. As can be seen from the figure, the conversion increases with increasing concentration of additive until about 10 mole%. After this the curve levels off. The optimum concentration of additive is then about 10 mole% for 1:1 electrolytes like NaCl and $NaNO_3$.

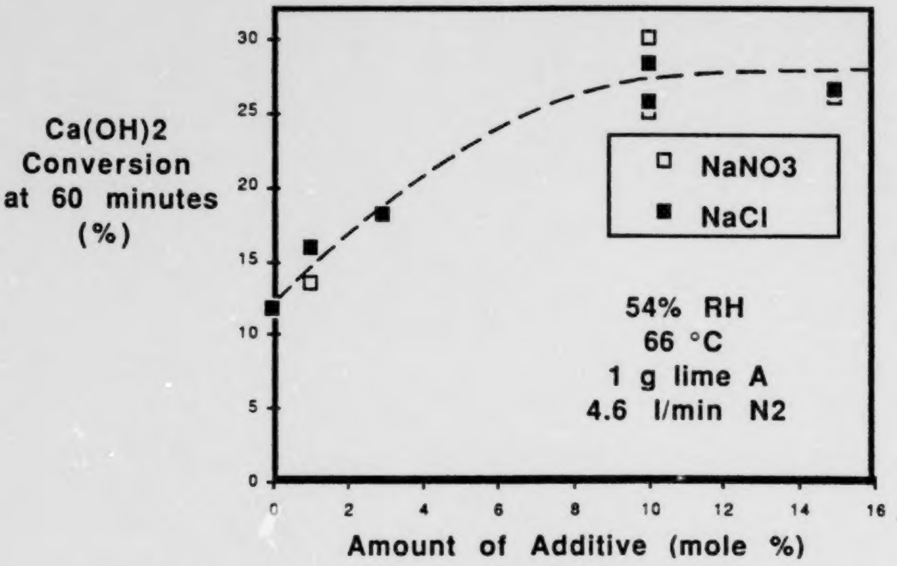

Figure 1-8: Effect of Amount of Additive

The deliquescent salts affected the model parameters in a similar way to the relative humidity, the diffusion coefficient increasing more rapidly than the kinetic constant by the addition of the salts.

Figure 1-9 illustrates the effect of NaCl on the model parameters. The kinetic constant increased linearly when NaCl concentration was increased from 0 to 10 mole%, while the diffusion coefficient increased exponentially after a sharp increase from 0 to 1 mole% NaCl.

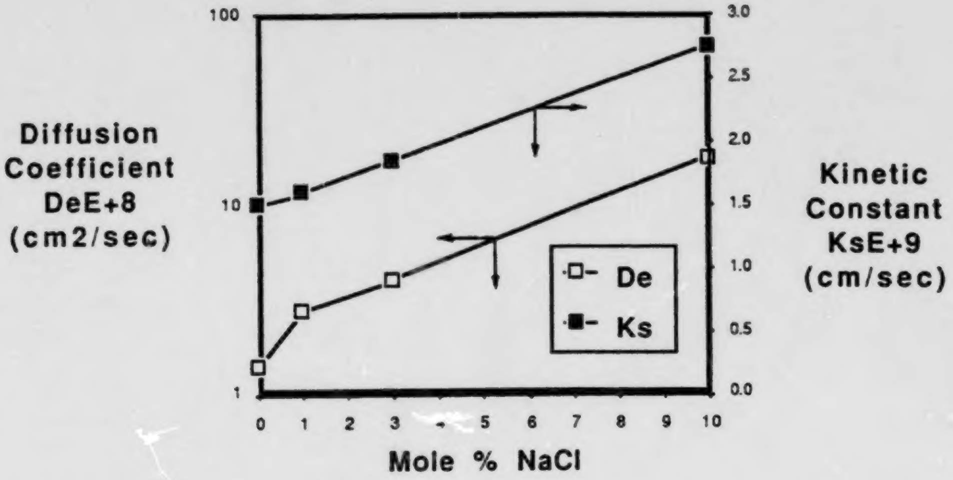

Figure 1-9: Effect of NaCl on the Model Parameters

1.4.5.2. Effect of Prehumidification of Bed

As was mentioned in the experimental apparatus subsection, before each experimental run the fixed bed was prehumidified by flushing with pure nitrogen at a relative humidity of about 98% for 10 minutes before flushing with nitrogen at the relative humidity at which the experiment was to be performed.

This prehumidification step could be the reason why some of the salts were still effective at a relative humidity lower than the one predicted from equilibrium considerations. Due to hysteresis it is possible that when the relative humidity was lowered to the experimental conditions after the prehumidification, some excess water remained in the solids. Strong hysteresis effects have been reported in NaCl aerosols (Tang and Munkelwitz, 1977).

To check if hysteresis was responsible for the beneficial effect of some salts at low relative humidities, experimental runs were made omitting the prehumidification step. Table 1-4 shows the results obtained at 54 and 17.4% relative humidity with and without prehumidification of the bed at 98% relative humidity.

Table 1-4: Effect of Prehumidification of the Bed at 98% RH on $Ca(OH)_2$ Reactivity

500 ppm SO_2, 1.0 g $Ca(OH)_2$ A, 4.6 l/min (0°C,1 atm) N_2

	Average $Ca(OH)_2$ Conversion after 1 hr (%)			
	54% RH		17.4% RH	
	66°C		95°C	
Additive	Prehumidified		Prehumidified	
(Mole%)	Yes	No	Yes	No
None	11.2	-	4.0	-
10% NaCl	27.0[a]	23.2	9.7	4.0
10% $NaNO_3$	27.2[a]	23.7	11.9	-
10% KCl	37.3	19.3	3.4	-

a Average of two experimental runs

The additives used were NaCl, $NaNO_3$, and KCl. At 54% relative humidity even when some decrease of the $Ca(OH)_2$ conversion was found without the prehumidification, the results with additives were still far superior to the pure $Ca(OH)_2$ case. Hysteresis then, can not explain all the beneficial effect observed at 54% relative humidity. At 17.4% relative humidity all the beneficial effect in the case of the NaCl appears to be due to the prehumidification of the bed, i.e., due to a hysteresis phenomenon.

1.5 Conclusions

As shown in the results subsection, the relative humidity of the gaseous phase is the most important variable in the reaction of SO_2 with $Ca(OH)_2$ solids. This result is in agreement with results reported in the literature for SO_2 removal in the bag filters of spray dryer pilot and commercial plants (Blythe and Rhudy, 1984, Bresowar et al., 1981, Robards et al., 1985, Samuel et al., 1983, Stevens, 1981, Stevens et al., 1982), and bench scale studies (Klingspor et al., 1983, Klingspor et al., 1984, Jorgensen et al., 1986). The other variables tested (i.e., temperature, amount of $Ca(OH)_2$, and SO_2 concentration) have a lesser impact on the reaction rate. The different effect of SO_2 concentration at low and high relative humidity can be explained by assuming that the reaction has zero order kinetics in SO_2 and that at low relative humidity the reaction rate is mass transfer controlled while at high relative humidities the reaction is controlled by reaction kinetics.

Most of the deliquescent salts tried were effective in increasing $Ca(OH)_2$ reactivity towards SO_2. The extent of the beneficial effect was a function of the type of salt, the salt concentration, and the relative humidity. Some salts are effective at a lower relative humidity than would be predicted from their deliquescent properties. Hysteresis due to the prehumidification of the bed appears to be partially responsible for this behavior, but it can not explain all the reactivity improvement observed at 54% relative humidity. An alternate explanation proposed is that the chlorides and $NaNO_3$ modify the properties of the product $CaSO_3 \cdot 1/2H_2O$ layer that is formed as the reaction takes place, thereby facilitating the access of the SO_2 to the unreacted $Ca(OH)_2$ which remains in the interior of the particle. NaCl and $CaCl_2$ have been reported to enhance the sulfur dioxide reactivity of limestones in fluidized bed combustion by affecting the the pore structure of the lime during calcination, which then increases the extent of sulfation of the limestone (Chopra et al., 1980).

The only previous modelling effort for this reaction was the work of Klingspor et al. (1983, 1984). Their work used an integral shrinking core model with only reaction kinetics to explain the dependence of reaction rate on lime conversion. Their experimental data fit this integral shrinking core model only after a certain lime conversion had been reached. They attributed the sharp decrease on reaction rate observed at initial times to a decrease in surface roughness, but did not attempt to correlate this decrease in surface roughness with lime conversion. Their model neglected the effects of SO_2 diffusion through the product layer, and the SO_2 concentration and lime concentration profiles in the fixed bed reactor. All of these factors will be more important at initial times, when the SO_2 removal is higher, so it is not surprising that they were able to fit the the experimental data only at later times.

The simple model presented here seems able to predict with reasonable accuracy the effect of all the process variables tested and explain the trends observed in the experimental data. The experimental data are estimated to have ± 11% experimental error, so the predictions of the model are well within the range of experimental error in most cases. The values of the diffusion coefficient used in the modelling (from 0.75E-9 to 1.20E-6) seem reasonable for diffusion of SO_2 in a solid, as they are of the same order of magnitude of the diffusivities of gases in polymers (Vieth and Amini, 1974, Brzozowski and Kumins, 1974, MacDonald and Haung, 1981, McBride et al., 1979, Minoura et al., 1981).

The relative humidity affects both the diffusion coefficient of SO_2 and the kinetic constant. In the range of relative humidity studied (19 to 74%), the kinetic constant increased linearly with relative humidity while the diffusion coefficient increased exponentially. This dependence of the parameters on the relative humidity leads to a change in the reaction controlling mechanism as the relative humidity decreases. At high relative humidity and/or high SO_2 concentration, the reaction rate is kinetically controlled and the reaction rate is independent on the SO_2 level. At low relative humidity and/or low SO_2 concentration the controlling step is the diffusion of the SO_2 through the $CaSO_3 \cdot 1/2H_2O$ product layer. At these conditions the overall reaction rate becomes affected by the SO_2 concentration which is the driving force for diffusion.

The addition of deliquescent salts increases the diffusion coefficient and the kinetic constant in a similar way to the relative humidity, the diffusion coefficient increasing more rapidly than the rate constant. When increasing amounts of the same salt (NaCl) were added, k_s increased linearly and D_e nearly exponentially. Depending on the amount and type of salt additive, chemical reaction or gas diffusion can be the controlling mechanism.

The kinetic constant was a very weak function of temperature. The estimated activation energy was 2.9 kcal/gmol.

Section 2

Background of Research

2.1 Introduction

Sulfur dioxide is one of the most abundant pollutants in the United States. The estimated yearly emissions of sulfur dioxide for the years 1972, 1975, 1977, 1979 and 1981 are presented in Table 2-1. Most of the SO_2 emissions originate from the combustion of fossil fuels, the electric utilities being the most important source (over 50%). Over 90% of the SO_2 emissions due to electric utilities are from coal-fired boilers. Table 2-2 shows the contribution of different sources to the power generation in the United States during 1982 and the prediction for 1991.

Sulfur is a component of all natural oil and coal, with compositions varying from 0.1 to over 5%. The total SO_2 emissions will vary considerably depending on the nature and origin of the fuel. Power plant gases generally contain low concentrations of SO_2, but they are emitted at large volumetric rates. Typical concentrations of SO_2 in power plant gases with 15% excess air range from 0.11 to 0.35% SO_2 by volume, depending on the type of fuel (Seinfeld, 1975, Clarke, 1980).

Once in the atmosphere, SO_2 is partly oxidized to sulfur trioxide or sulfuric acid and its salts by photochemical or catalytic

Table 2-1: National Estimates of Sulfur Dioxide Emissions Teragrams/year

Source	1972	1975	1977	1979	1981
Transportation	0.6	0.6	0.8	0.9	0.8
Stationary Fuel Combustion					
Electric Utilities	15.8	16.5	16.9	15.8	14.8
Industrial	3.5	2.7	2.8	2.7	2.3
Residential, Commercial	1.2	1.0	1.1	0.8	0.7
Industrial Processes	6.4	4.8	4.4	4.3	3.9
Others	0.2	0.0	0.0	0.0	0.0
TOTAL	27.7	25.6	26.0	24.5	22.5

Source: (EPA Report 450/4-82-012, 1982)

Table 2-2: Power Generation Sources: Present and Future

	Percentage of Generation Power						Total Generating
	Coal	Nuclear	Oil	Hydro	Gas	Other	Capacity (GW)
Dec. 1982	42	11	23	12	11	1	656
Dec. 1991	44	16	19	11	9	1	799

Source: (Melia et al., 1983)

reactions (Seinfeld, 1975). It is difficult to isolate the environmental impacts of sulfur compounds alone, as they are often associated with other pollutants. The most damaging effects attributed to atmospheric air pollution are produced by oxides of sulfur in combination with particulate matter and moisture.

Sulfur compounds are held responsible for damage to a number of building materials including limestone, marble, roofing slate, and mortar. Textiles, especially nylon, can be weakened by SO_2 or sulfuric acid (Wark and Warner, 1981). Finally, sulfuric acid accounts for 60 to 70% of the acidity of acid rain (Wark and Warner, 1981), so SO_2 emissions are undoubtedly linked with this phenomena. Several detrimental environmental effects have been attributed to acid rain such as acidification of natural water sources, leaching of nutrients from the soil, direct damage to vegetation, and increase in the corrosion of building materials. The severity of the damage caused by acid rain depends on the type of minerals present in a given region. Regions that contain rocks such as limestone or similar minerals are buffered against the onslaught of acid rain. Since it is very difficult to alter the effects of acid rain once they have occurred in a region, the best solution is to control the SO_2 emissions at the source.

2.2 Reduction of SO_2 Emissions

Four possible methods or alternatives may be used to reduce the effects of SO_2 emissions from fossil fuels. These potential methods are:

A. Switch to low-sulfur fuel

B. Desulfurize coal and oil

C. Desulfurize flue gas.

2.2.1 Change to Low Sulfur Fuel

Shifting to low-sulfur fuel was a method widely used in the United States in the early 70's when air pollution regulations were established by the Environmental Protection Agency (EPA) limiting sulfur dioxide emissions (Marchello, 1976). Nevertheless, the substitution of low sulfur fuel is only a short term solution because of the limited supply, especially of natural gas and low sulfur oil (Zareski, 1973, Morrell et al., 1973). The United States does have large reserves of low sulfur coal, but its geographical location is not ideal. Most of the coal consuming utilities are in the East and Midwest, while 90% of the low sulfur coal reserves (less than 1% sulfur) are in the West (Hunter, 1973, Wark and Warner, 1981). This means high transportation cost for this low sulfur coal. The technical factors and power plant modifications needed for low sulfur coal have been discussed in detail by Schwartz (1984).

An intermediate solution, the blending of low-sulfur western coal with local high sulfur coal has been long been practiced by some midwestern Utilities. Another form of fuel blending that can be accomplished more easily with little capital expenditure is the augmentation of pulverized coal with natural gas, a procedure which has been termed the "select use" of gas (Green, 1984).

2.2.2 Use of Desulfurized Coal and Oil

Sulfur is contained in coal in organic and inorganic forms. Inorganic sulfur, in the form of iron pyrite (FeS_2), is present in discrete lumps through the coal and due to its greater density can be separated from the coal by gravity washing. About 40 to 60% of a given coal's sulfur is in the form of pyrites (Moriber, 1974), and up to 84% of the pyritic sulfur can be eliminated by crushing and gravity washing (Cavallaro et al., 1974). Sulfur in the organic form is chemically bound to the coal, and it can not be removed without chemically changing the nature of the coal. Consequently, more costly and complex processes are required to remove the organic sulfur from the coal. Examples of such processes are coal gasification, and coal liquefaction. Several coal gasification and coal liquefaction techniques are under development (Belt and Roder, 1973, Qader and Hill, 1973, Yavorsky et al., 1974, Akhtar et al., 1974), and the technical feasibility of these processes has been established. Their economic feasibility remains yet to be proven.

The desulfurization of natural oil can be accomplished by several commercially available processes (Johnson et al., 1973, Gregoli and Hartos, 1973), and although desulfurization is expensive, there is no technological deterrent (Barthel et al., 1974).

2.2.3 Removal of SO_2 from Flue Gases

The removal of SO_2 from flue gases has probably been subject to more research than any other gas-purification operation, and numerous processes have been developed. Flue gas desulfurization (FGD) processes can be grouped as 1) throwaway or regenerative and 2) wet or dry. Throwaway processes are those in which a waste product is formed which must be discarded. As a result, fresh chemicals must be continuously added. In regenerative processes, as the name indicates, the SO_2 removal agents are continuously regenerated in a close-loop system with sulfur or sulfur acid produced as a saleable product. The difference between wet and dry FGD processes is that the scrubbed flue gas in a wet process is saturated with water vapor while in a dry process the cleaned gas in unsaturated with water vapor. Table 2-3 lists the most important flue gas desulfurization processes. Dry flue gas desulfurization processes will be reviewed in detail in the following subsections.

2.3 Throwaway Dry FGD Processes

2.3.1 Dry Injection

Dry injection processes involve pneumatically introducing a dry powdery alkaline material into the flue gas stream, followed by particulate collection either using fabric filters or electrostatic precipitators. The injection point can vary from the boiler furnace area all the way to the entrance to the solids collection equipment (Kelly and Dickerman, 1981, Kelly and Shareef, 1981, Kelly et al., 1983, Blythe et al., 1980). The most commonly used sorbents are nahcolite, trona and refined trona (Genco et al., 1975, Genco and Rosenberg, 1976, Bechtel Corporation, 1976, Lutz et al., 1979, Veazie and Kielmeyer, 1970, Bagwell et al., 1969, Muzio et al., 1980, Muzio et al., 1983, Ablin, 1984). Pressure hydrated lime and dolomitic lime have also been tested, but they give a lower SO_2 removal than nahcolite and trona (Weber et al., 1984, Bobman et al., 1985).

Table 2-3: Flue Gas Desulfurization Processes

Process Generics	Process Operations	Key Sulfur Product
A. Throwaway Scrubbing		
1. Lime or limestone	Slurry scrubbing	$CaSO_3/CaSO_4$
2. Sodium Carbonate	Na_2SO_3 solution	Na_2SO_4
3. Double Alkali	Na_2SO_3 solution, regenerated by CaO or $CaCO_3$	$CaSO_3/CaSO_4$
4. Magnesium-promoted lime/limestone	$MgSO_3$ solution, regenerated by CaO or $CaCO_3$	$CaSO_3/CaSO_4$
B. Regenerative scrubbing		
1. Magnesium Oxide	$Mg(OH)_2$ slurry	15% SO_2
2. Wellman-Lord	Na_2SO_3 solution	S, H_2SO_4
3. Citrate	Sodium Citrate solution	Sulfur
4. Ammonia	Ammonia solution, conversion to SO_2	Sulfur (99.9%)
C. Dry throwaway		
1. Dry injection	Alkali injection in flue gas	Na_2SO_3
2. Coal/Alkali combustion	Burning Coal/limestone	$CaSO_3/CaSO_4$ mixture
3. Injection/humidification	Alkali injection/gas humidification	$CaSO_3/CaSO_4$
4. Spray dryer	Absorption with slaked lime solutions	$CaSO_3/CaSO_4$

Nahcolite is a naturally occurring mineral containing up to 90% sodium bicarbonate. Large reserves of this mineral are found in Northwest Colorado and Southwest Wyoming (Samuel and Lapp, 1980). Trona is another natural mineral composed of sodium carbonate and bicarbonate, with two moles of hydration water ($NaHCO_3 \cdot Na_2CO_3 \cdot 2H_2O$). Trona is also found in relative abundance in Southwestern Wyoming and Owens Lake, California. Refined trona is bicarbonate-enriched trona.

The overall reactions for the removal of SO_2 using nahcolite or trona are:

$$2NaHCO_3 + SO_2 \rightarrow Na_2SO_3 + H_2O + 2CO_2$$

$$Na_2CO_3 + SO_2 \rightarrow Na_2SO_3 + CO_2$$

Sodium bicarbonate is more reactive than sodium carbonate; thus, at comparable sodium injection ratios trona is less effective in removing SO_2 than nahcolite. The higher reactivity of $NaHCO_3$ has been attributed to thermal decomposition of the $NaHCO_3$ into highly reactive Na_2CO_3 which simultaneously reacts with SO_2. As the sodium bicarbonate decomposes, new surface continually becomes available for reaction with SO_2. The decomposition of the $NaHCO_3$ may also provide a moisture layer which serves as a reaction medium and increases the reaction rate (Mueller and Winston, 1985). Seventy percent SO_2 removal has been achieved with nahcolite at a stoichiometric ratio of 1.05 (2 moles of total Na/mol SO_2), while a refined trona stoichiometric ratio of 1.6 was required to reach the same removal. The maximum SO_2 removal observed with trona has been 50% (Samuel and Lapp, 1982).

Both baghouses and electrostatic precipitators have been tested for collection of solids in dry injection processes. Fabric filters have longer solids residence time an are better than electrostatic precipitators because additional reaction can take place between unspent sorbent collecting on the bag surface and the SO_2 remaining in the flue gas, thus increasing overall SO_2 removal (Kelly and Shareef, 1981).

Data collected in bench-scale and pilot-scale experiments support the technical feasibility of dry injection as an SO_2 control alternative, and the process appears to have economic advantages over other currently available FGD technologies when applied to western power plants burning low sulfur coal (Lutz et al., 1979, Samuel and Lapp, 1982).

No commercial dry sorbent injection system for SO_2 control are currently operational in the U. S. However, 22 MW and 100 MW demonstrations at utility electric generating stations have been conducted with technical success (70% or better SO_2 removal for low sulfur western coals when using sodium compounds).

There are, nevertheless, two major restraints to development of commercial dry injection systems. First, the uncertainty in sorbent availability, and second and most important, the difficulty of disposal of the solid wastes. The waste products in the case of sodium compounds are water soluble sodium sulfate and sodium sulfite which if disposed without stabilization or insolubilization present the environmental danger of leaching and contamination of underground water reserves. These two problems must be solved via economic means before dry injection can be commercialized.

2.3.2 Coal/Alkali Combustion

Two processes based on the combustion of coal/alkali fuel mixtures to control SO_2 emissions are under development. Combustion of coal/limestone pellets in an industrial stoker-fired boiler, and combustion of pulverized coal/limestone mixture in a low NO_x burner (limestone injection into multistage burner or LIMB process). Tests at the pilot scale have demonstrated that both of these processes are able to achieve at least 50% SO_2 removal (Kelly and Shareef, 1981 and 1981a, Kelly et al., 1983, Lisauskas et al., 1985). Coal/alkali combustion is a low cost alternative to other FGD processes, but before these two processes can be applied at a commercial scale, work remains to be done to fully characterize the impact of these technologies on boiler operation and particulate control design and operation. Also the New Source Performance Standards for coal-fired boilers ($\geq$ 200×10^6 Btu/hr heat input) must be amended as they currently require 70% or more SO_2 removal, depending on coal sulfur content. A review of these technologies has been given by Maloney (1980), and some kinetic studies of the reactions in the LIMB burner by Borgwardt (1984).

2.3.3 Injection/Humidification

Injection/humidification techniques involve humidification of the flue gas and capture of the SO_2 by a dry sorbent injected in the ductwork downstream of the air preheater, followed by removal of the spent sorbent along with coal fly ash in the particulate collection system (bag filters or ESP) of a coal fired power plant. The SO_2 reacts with the entrained sorbent particles in the ductwork and with the dense sorbent bed collected in the particulate removal system. Injection/humidification differs from dry injection processes in that it involves humidification of the gas by water spraying either before or after the SO_2 sorbent has been injected. This humidification lowers the temperature of the flue gas so the SO_2 absorption takes place at a much lower temperature and higher relative humidity than in the dry injection case.

Two injection/humidification processes have been reported in the literature, the coolside process (Stouffer et al., 1985) and hydrate addition at low temperature (Forsythe and Kaiser, 1986).

In the coolside process the proposed sorbent is high surface area hydrated lime promoted by the addition of a sodium compound such as sodium hydroxide or sodium carbonate. Boiler Limestone Injection flyash has also been demonstrated to be an effective coolside sorbent after a simple activation step and/or flue gas humidification. This possibility may allow the use of the coolside technique in combination with Boiler Limestone Injection to minimize overall SO_2 control cost.

Diagrams of the straight coolside process using hydrated lime as the sorbent, as well as the Boiler Limestone Injection recycle option are depicted in Figure 2-1. Conoco Coal Research Division made a 1 MW field trial of this process using a 3000-4000 CFM flue gas slipstream from a coal-fired industrial boiler at du Pont's Martinsville Nylon Plant. The slipstream was diverted through a pilot-scale humidifier and ESP provided by Research Cottrell. Injection of a commercial hydrated lime with sodium-based additives (selected based on laboratory work) gave an SO_2 removal up to 80% with up to 40% sorbent utilization on a once-through basis. The water droplets sprayed into the humidifier played a key role in the observed high SO_2 removal. Additionally, humidification

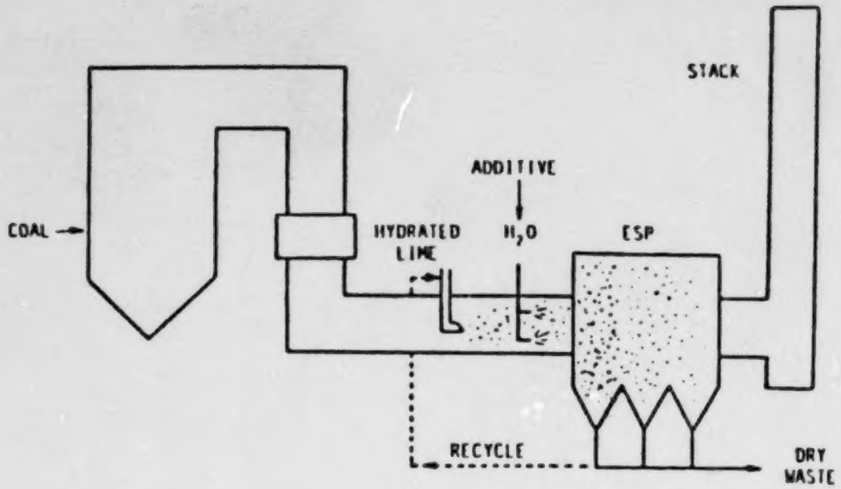
STACK
ADDITIVE
COAL
HYDRATED LIME
H_2O
ESP
RECYCLE
DRY WASTE

A. Hydrated lime as sorbent

Source: (Stouffer et al., 1985)

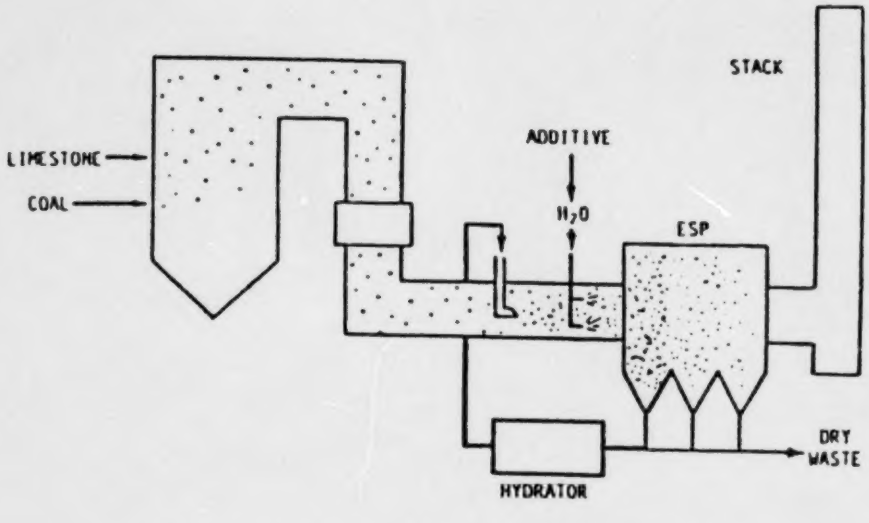
STACK
ADDITIVE
LIMESTONE
COAL
H_2O
ESP
DRY WASTE
HYDRATOR

B. Boiler Limestone Injection Recycle Option

Source: (Stouffer et al., 1985)

Figure 2-1: Diagram of the Coolside Process (Humidification of flue gas after dry sorbent injection)

was an effective method of conditioning the flue gas for efficient ESP operation, allowing removal of the higher loadings of high resistivity solids caused by the sorbent injection. The combination of coolside and limestone injection technologies also showed significant SO_2 removal across the humidifier and ESP.

The "hydrate addition at low temperature" (HALT) technology uses prepared $Ca(OH)_2$ particles as the injected sorbent. Additives, such as $CaCl_2$, calcium silicate, di-calcium silicate, and calcium aluminate in the water used produce the hydrate together with careful selection of hydration conditions combine to give the particles a surface chemistry and morphology designed to enhance SO_2 capture. Preliminary tests conducted in a 255 CFM test system at the Sammis Plant of the Ohio Edison Co. showed that up to 85% SO_2 removal could be achieved by optimizing the process parameters (Forsythe and Kaiser, 1986). Further work is necessary to demonstrate the full capabilities of the process.

Injection/humidification techniques have the potential of providing low cost control options attractive for retrofit applications under more stringent SO_2 regulation. They would require significantly lower capital investment and space than the conventional wet limestone slurry or lime spray dryer processes (Stouffer et al., 1985, Forsythe and Kaiser, 1986). The SO_2 removal that can be achieved though, is lower than in either of these processes, and they seem to require higher sorbent stoichiometries.

2.3.4 Spray dryer-based processes

Figure 2-2 is a schematic diagram of a typical spray drying FGD system. The flue gas containing fly ash and SO_2 enters the spray dryer where it is contacted with a finely atomized aqueous solution or slurry of an alkali (typically soda ash or lime). During the approximately 10 seconds of residence time in the dryer, sulfur dioxide is absorbed in the slurry droplets (lime is predominantly used) and neutralized by the alkali. Simultaneously, the thermal energy of the gas evaporates the water in the slurry droplets, adiabatically humidifying the flue gas to about 11 °C above the saturation temperature. The product leaving the spray dryer (a mixture of sulfite, sulfate, carbonate, and some unreacted lime) together with the fly ash is removed in collection equipment, such as a fabric filter or electrostatic precipitator (ESP). Since not all the water is removed from the solids in the spray dryer, the remaining moisture promotes further reaction with SO_2 in the ducts leading to the particulate collector and in the bag house when used. Due to this additional SO_2 removal capability bag filters are preferred for spray dryers.

In a straight-through process, the solids collected in the bag filters will go directly to solid waste disposal, while the clean flue gas is released to the atmosphere through the stack. In recycle of the solids to improve sorbent utilization and process operation, a portion of the collected solids are re-slurried for return to the spray dryer. Recycle is discussed further below.

Parametric studies in a number of pilot and demonstration plants indicated that the main variables affecting SO_2 removal in a spray drying system are the sorbent stoichiometric ratio (moles of

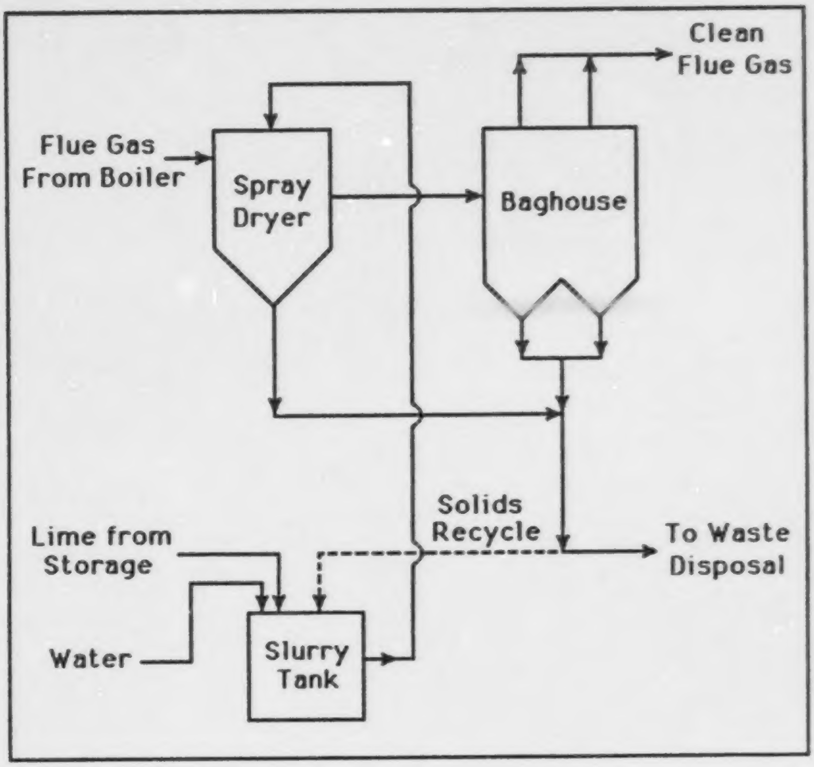
Clean
Flue Gas
Flue Gas
From Boiler
Spray
Dryer
Baghouse
Solids
Recycle
Lime from
Storage
To Waste
Disposal
Water
Slurry
Tank

Figure 2-2: Typical Spray Dryer System for FGD

lime/moles SO_2 inlet) and the approach to the adiabatic saturation temperature at the spray absorber outlet (Blythe and Rhudy, 1984, Bresowar et al., 1981, Samuel et al., 1984, Yeh et al., 1983, Jankura et al., 1984). Degree of atomization, gas flow rate, inlet SO_2 concentration, temperature, and gas retention time in the spray absorber also affect SO_2 removal, but to a lesser degree (Gustke et al., 1984, Bresowar et al., 1981, Lewis and Gehri, 1983, Samuel et al., 1984). Finally, partial recycle of spray dryer absorber and/or baghouse solids has been found to have a significant beneficial effect on SO_2 removal (Jankura et al., 1984, Parsons et al., 1981, Robards et al., 1985, Blythe and Rhudy, 1984, Kelly et al., 1983, Gustke et al., 1984, Donnelly et al., 1985). The dry waste recycle is added to the fresh lime slurry delivered from the slaker or the dry waste may be slurried before being added to the fresh lime slurry.

Spray drying with partial recycle of solid products has been patented by Niro Atomizer (Felsvang, Hansen and Rasmussen, 1981). The beneficial effect of solids recycle has been attributed to several factors (Kaplan and Felsvang, 1980). First, the recycled material contains unreacted lime which can be further utilized when introduced into the spray drying system more than once. Secondly, the spray dried products provide a surface on which slaked particles can agglomerate, thereby exposing more surface area of the fresh lime and enhancing the absorption reaction. A third benefit is from the recirculated fly ash, which, depending on its alkalinity, can allow a reduction of the system stoichiometry resulting in a decrease in the amount of fresh lime required. Jozewicz and Rochelle (1985 and 1985a) have also shown that fly ash can react with $Ca(OH)_2$ during slurrying of recycle solids with fresh lime, producing high surface area calcium silicates, which are more reactive towards SO_2 than $Ca(OH)_2$.

Spray dryer flue gas desulfurization systems have received much attention during the last decade, especially for low sulfur coal applications. They present several advantages over conventional lime and limestone wet scrubbing methods that have dominated the market for flue gas desulfurization during past years (Felsvang et al., 1978, Hollett, 1979, Masters, 1980, Shah, 1982, Kaplan and Felsvang, 1980):

- Spray drying systems produce a dry, solid waste that can be handled by conventional fly ash handling systems eliminating the need for sludge handling systems.
- Dry systems should have lower maintenance costs, because they require less equipment (Thickeners, centrifuges, vacuum filters and mixers required to handle the wet sludge waste are not longer required). Also, the slurry pumping requirements are much lower for spray drying. Finally keeping the gas warm minimizes risk of erosion, corrosion, and scaling, thus allowing the use of carbon steel as the construction material in most equipment.
- The spray dryer absorber is flexible in operation with regard to varying boiler load. Feed rates can be adjusted immediately to maintain a constant emission load.
- A typical spray dryer absorber can be installed in an area where space is limited.

Pilot and demonstration plants have been tested by various FGD system vendors (Stevens, 1981, Stevens et al., 1982, Martin et al., 1980, Grutle and Gehri, 1981, Hurst and Bielawski, 1981, Gunther et al., 1981, Samuel et al., 1983, Blythe and Rhudy, 1984, Blythe et al., 1983, Yeh et al., 1983, Bresowar et al., 1981, Kaplan and Felsvang, 1980), and several economic studies have indicated the potential of dry scrubbing to compete economically with wet sulfur dioxide removal systems for low and medium sulfur coals (Burnett and O'Brien, 1980, Burnett et al., 1981 and 1981a).

In the past years a number of companies and consortia have been contracted to build commercial units. By June 1983 sixteen utility and eight industrial spray dryer system units had been sold. A few of these commercial units are now in operation and have demonstrated the capability of spray dryer systems of competing with wet scrubbing as an alternative for FGD (Gustke et al., 1984, Kaplan et al., 1983, Lewis and Gehri, 1983, Roop and Pflug, 1984, Horn and Bent, 1984, Reinauer et al., 1983, Farber, 1984).

Dry scrubbing was originally developed for low and medium sulfur coal applications, although some reports have appeared recently which deal with the adaptation of the system to utility steam generators burning high sulfur coal (Jankura et al., 1984)

2.4 Scope of Investigation

Dry systems are going to have a larger share of the FGD market in the coming years. By October 1983 spray dryer based systems constituted 4% of the total operating scrubbing capacity, but they constituted 18.6% of the scrubbing capacity under construction, and 21.4% of the planned scrubbing capacity (Melia et al., 1983). All of the spray drying systems in operation with the exception of one are lime throwaway systems. In addition to spray drying based systems, some of the other dry processes discussed may reach commercial scale in the future.

The overall reaction in a spray dryer system using lime as the active agent is:

$$Ca(OH)_2 + SO_2 \rightarrow CaSO_3 \cdot 1/2H_2O + 1/2H_2O$$

The oxygen in the flue gas oxidizes some of the sulfite to sulfate. Because of the dependence of spray dryer absorption FGD on water, the stages of the reaction are intimately linked to the drying stages of the slurry droplets. Three drying stages have been described for evaporation of slurry droplets, namely, the constant rate, the falling rate, and the pseudo-equilibrium rate periods (Getler and Furlong, 1979).

The constant rate period lasts until the droplet shrinks to the extent that the alkali particles touch each other. The length of this period will depend on droplet size, initial gas temperature, and solids concentration in the slurry. Under typical dry scrubber conditions the constant rate period would last about 0.12 seconds for a 25 micrometer droplet at 5% solids, and 0.06 seconds for a 25 micrometer droplet at 25% solids. The constant rate period for a 100 micrometer droplet will be about 1.6 times more than that for a 25 micrometer droplet (Downs et al., 1980).

During the falling rate period, the remaining moisture becomes more difficult to remove because the water needs to diffuse through the pores of the agglomerate. Diffusion through and around the particles becomes the limiting step for further moisture removal. If the droplets were evaporated to complete dryness, the time for the falling rate period could be estimated using a correlation suggested by Ranz and Marshall (1952).

The solids, however, do not dry completely but instead establish a pseudo-equilibrium with the cool and humid environment of the spray dryer. The "pseudo-equilibrium stage" or "dry stage" (Downs et al., 1980) does not occur to a major extent within the spray dryer itself but represents the properties of the spray dried solids. Due to the moisture remaining in the solids, they continue to react with SO_2 in the ducts leaving the spray dryer and in the fabric filters used for solids collection.

Reported results from pilot and demonstration spray drying plants indicate that depending on the experimental conditions 10 to 20% of the overall SO_2 removal takes place in the bag filters (Stevens, 1981, Samuel et al., 1983, Samuel et al., 1984, Bresowar et al., 1981, Blythe and Rhudy, 1984). These results are misleading because the SO_2 removal is calculated based on the SO_2 concentration entering the spray dryer. If the baghouse removal is calculated based on the SO_2 concentration entering the bag filters, it can be seen more clearly that the bag house alone is an efficient SO_2 removal device, especially at high stoichiometric ratios. At an approach to adiabatic saturation temperature of 15°F in the baghouse and lime stoichiometries (at inlet to spray dryer) from 1.0 to 1.6, SO_2 removal efficiencies between 35 and 68% have been reported for the baghouse (Robards et al., 1985). Baghouse SO_2 removal would be especially important if spray drying were to be extended to high-sulfur coal applications.

The reaction between moist lime solids and SO_2 taking place in the ducts and bag filters of a spray dryer system is the subject of the present research. This reaction also occurs during SO_2 removal using the coolside process described in Subsection 2.3.3. A better understanding of this reaction and the parameters affecting the reaction rate is crucial to optimize SO_2 removal efficiency and/or decrease sorbent stoichiometric ratios in both spray dryer and coolside processes. Most of the information available in the literature for this reaction is reported in results of SO_2 removal across the bag filters of pilot and demonstration spray dryer plants. These results are difficult to interpret, because the conditions of the flue gas entering the bag filters will be dependent on the spray absorber behavior. Any variable changes that affect the SO_2 removal across the spray absorber will change the concentration of SO_2 entering the bag filters. So, two variables will have effectively been changed in the bag filters and the contribution of each one can not be isolated.

Several bench scale studies regarding the reaction of interest have been reported (Klingspor et al., 1983, Klingspor et al., 1984, Jorgensen et al., 1986). However, the characterization of this reaction is far from complete. The bench scale studies, as well as spray drying results from pilot and demonstration plants, will be discussed in detail in the next Section.

The present study will be carried out in a bench scale fixed bed reactor, operated at conditions similar to those found in bag filters of commercial spray drying systems, and using powdered reagent grade $Ca(OH)_2$ as the sorbent. The effect of $Ca(OH)_2$ loading, temperature, SO_2 concentration, and relative humidity will be studied. Also, additives that improve the lime reactivity towards SO_2 will be identified.

Section 3

Reaction of $Ca(OH)_2$ with SO_2

3.1 Introduction

In a spray drying flue gas desulfurization system, the solids leaving the spray dryer are removed in collection equipment such as bag filters or electrostatic precipitators. Bag filters are the preferred particulate collectors, because the unreacted $Ca(OH)_2$ present in the solids reacts with SO_2 in the bag filters, thus producing additional SO_2 removal (Kelly and Dickerman, 1981, Kelly et al., 1983). As was discussed in the previous section, the contribution of bag filters to the overall SO_2 removal becomes especially important if spray drying is to be extended to high-sulfur coal (Robards et al., 1985). The study of the reaction between $Ca(OH)_2$ solids and SO_2 that takes place in the bag filters and ducts leading to the bag filters is the subject of this Section.

The study was carried out in a bench scale fixed bed reactor, the bed consisting of powdered reagent grade $Ca(OH)_2$ dispersed in silica sand. The experimental conditions were similar to those of commercial scale bag filters, the main differences being in the gas composition and type of reagent used. The gas phase used in the bench scale experiments consisted of a mixture of N_2, SO_2, and water vapor. O_2, NO_x, and CO_2, also components of flue gas, were not included. Powdered reagent grade $Ca(OH)_2$ was used in the fixed bed reactor, while commercial dry scrubbing units use slaked lime.

The effects of $Ca(OH)_2$ loading, temperature, relative humidity, and inlet SO_2 concentration were studied. Before discussing the results of the present research, a brief review of previous research done in bench scale reactors will be presented, as well as results that have been reported in the literature for SO_2 removal in the bag filters of spray drying pilot and demonstration plants.

3.2 Previous Work on the Reaction of SO_2 with $Ca(OH)_2$

3.2.1 Previous Work on Fixed Bed Reactors

Some work has been reported on the reaction of slaked lime and limestone with SO_2 at low temperature using a fixed bed reactor similar to the one used in this research (Klingspor et al., 1983, Klingspor et al., 1984, Jorgensen et al., 1986).

Klingspor and coworkers primarily studied limestone, but they found the conclusions to be applicable to lime as well. They used five different samples containing 90.0 to 93.7% $Ca(OH)_2$ with surface areas of 14.4 to 25.5 m^2/g. Some of the conclusions of their research were:

- The initial reaction rate is an exponential function of the relative humidity of the gas stream.
- The initial reaction rate is a very weak function of the temperature.
- The initial reaction rate is zero order in SO_2 for relative

humidities below 70%. For relative humidities greater than 70%, the SO_2 concentration becomes increasingly important.

- If the relative humidity is below 20%, the SO_2 does not react with the lime.
- The lime-SO_2 reaction is not controlled by gas film diffusion at relative humidities of 92% or lower.
- The chemical reaction controlled unreacted core model can be used to describe the dependence of the reaction rate on lime conversion after the conversion has reached a certain value X_B'. Before this lime conversion X_B', the rate of reaction decreases much faster than can be predicted by a simple shrinking core model. The authors attributed this decrease in reaction rate to a decrease in surface roughness of the solid reactant.

Klingspor and coworkers obtained the initial reaction rate for the reaction of slaked lime and SO_2 by extrapolating to time zero the data obtained in their fixed bed reactor. In the experiments run in the present research, it was found that the reaction rate was extremely fast initially, so an extrapolation procedure was not considered reliable.

Acurex Corporation also conducted studies of the $Ca(OH)_2$-SO_2 reaction in a bench-scale sand bed reactor (Jorgensen et al., 1986). Some of their conclusions are:

- $Ca(OH)_2$ conversion (mols SO_2 removed/mol $Ca(OH)_2$) has a very strong dependence on relative humidity.
- There is no clear indication of increasing conversion rate with increasing SO_2 concentration in the concentration range tested (500-1000 ppm) for relative humidity less than 70%.
- Conversion rate is increased moderately with temperature for a given relative humidity in the relative humidity range tested (30-75%). An Arrhenius plot for measured reaction

rates at 55% relative humidity gives an activation energy of 6000 cal/mol.

3.2.2 Results from Spray Drying Pilot Plants

The effects of process variables on SO_2 removal have been reported for a number of spray drying pilot and demonstration plants, but only a few of the reported results separate SO_2 removal in the bag filters from removal in the spray dryer (Stevens, 1981, Samuel et al., 1983, Samuel et al., 1984, Robards et al., 1985, Bresowar et al., 1981, Blythe and Rhudy, 1984) One of the most important variables affecting SO_2 removal in the bag filters is the stoichiometric ratio (or ratio of lime to SO_2 feed to the spray dryer). These results are not surprising because at low stoichiometric ratio (below 0.8) practically all the lime is consumed in the spray dryer, leaving no lime available for reaction with SO_2 in the bag filters. When the stoichiometric ratio increases, more unreacted lime leaves the spray dryer, because the SO_2 removal in the spray dryer does not increase significantly as the reagent ratio increases. This unreacted lime reacts with SO_2 in the bag filters, thus greatly increasing the bag filter contribution to the total SO_2 removal (Blythe and Rhudy, 1984).

The other variable that affects the SO_2 removal in the bag filters is the approach to the adiabatic saturation temperature at the spray dryer outlet (ΔT_{as}). Typical values of ΔT_{as} in spray drying systems range from 7 to 22 °C (13 to 40 °F), which correspond to relative humidities in the range 38 to 70%. The approach to the adiabatic saturation temperature has been reported to have a smaller impact on the bag house performance than on the spray dryer removal efficiency (Robards et al., 1985). It must be noted though, that when the approach to the adiabatic saturation temperature is very low, the absorber efficiency is also improved, and there is little residual SO_2 in the flue gas left for the bag filters to remove (Bresowar et al., 1981).

Other process variables that affect the spray dryer removal efficiency, such as SO_2 concentration in the inlet flue gas, gas temperature drop across the spray dryer, liquid-to-gas (L/G) ratio in the spray dryer, or recycle ratio of solids have been reported to have a negligible effect on SO_2 removal in the bag filters (Bresowar et al., 1981, Blythe and Rhudy, 1984).

3.3 Experimental Apparatus

The general design of the experimental apparatus is given in Figure 3-1. A simulated flue gas was synthesized by combining nitrogen and sulfur dioxide from gas cylinders. The gas flow rates were measured using rotameters (a Lab Crest Century for the nitrogen and a Gilmont micro-flow meter with a capillary valve for the sulfur dioxide). Water was added to the system by means of a syringe pump (Sage Instruments, Model 341A) and evaporated at 120°C in a stainless steel evaporation chamber before mixing with the gas stream.

The evaporation chamber was cylindrical, 5-cm diameter and 14-cm height. Heating was provided by electric wire wrapped around the chamber and insulated with asbestos tape. Heating was modulated by a voltage controller. The evaporation chamber was filled with 5-mm glass beads, to increase the contact surface. The temperature in the center of the evaporation chamber was measured using an Omega digital thermometer (Model 199) with a chromel-alumel thermocouple.

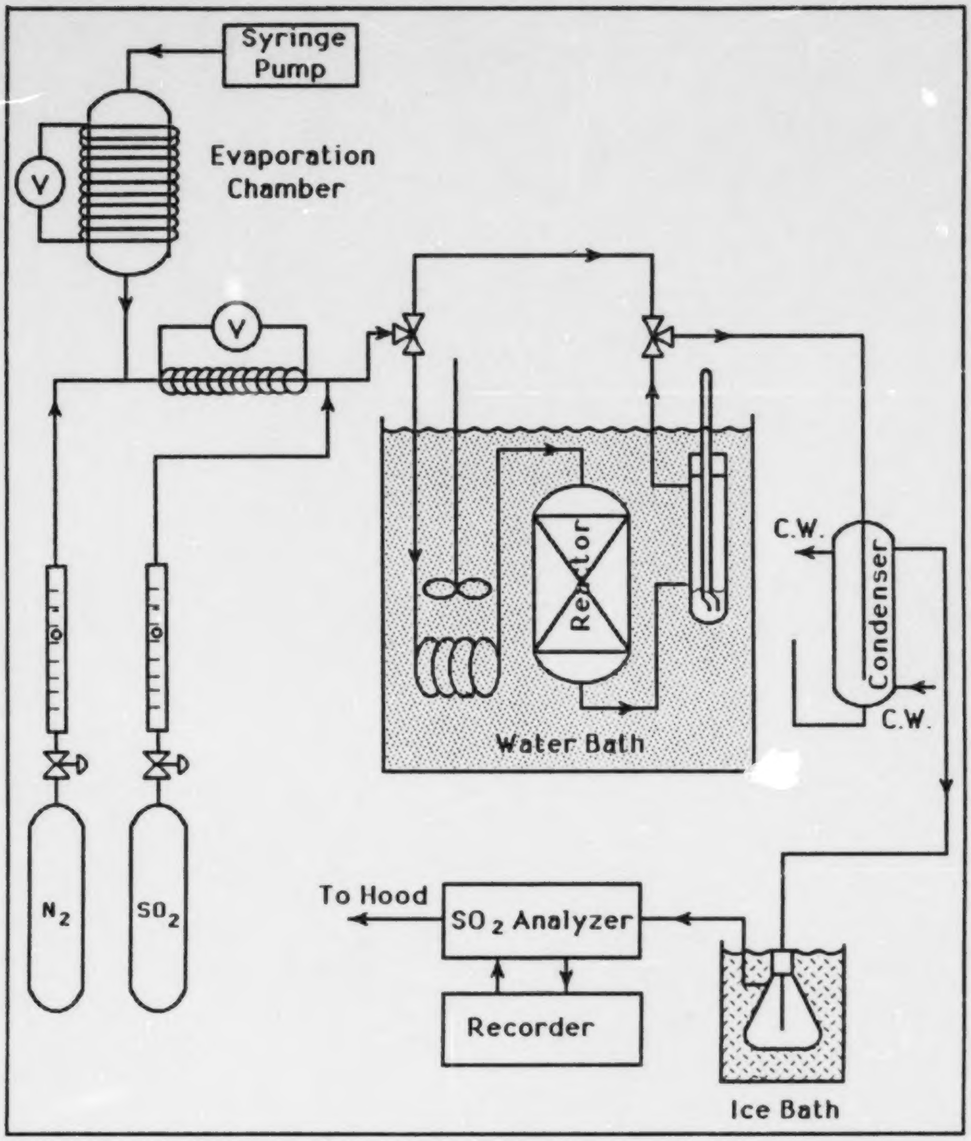
Syringe Pump
Evaporation Chamber
V
V
N2
SO2
Reactor
Water Bath
C.W.
Condenser
C.W.
To Hood
SO2 Analyzer
Recorder
Ice Bath

Figure 3-1: Experimental Apparatus

The reactor was made of glass, and it had a diameter of 4 cm and 12-cm height. The reactor was packed with a mixture of silica sand and $Ca(OH)_2$ reactant in a weight ratio of 40:1. The addition of sand is necessary to avoid channeling caused by lime agglomeration (Karlsson et al., 1983). The silica sand (between 80 and 115 mesh) was obtained from Martin-Marietta Aggregates.

The reactor was immersed in a water bath that maintained the system temperature within 0.1°C. Tubing upstream from the reactor was heated to prevent the condensation of moisture on the walls. After leaving the reactor, the wet bulb temperature of the gas was measured using a mercury thermometer with a wet cloth at the tip. The mercury thermometer was placed in a small Dewar container. Before going to analysis, the gas was cooled and the water vapor condensed by cooling water and an ice bath. The gas was analyzed for SO_2 using a pulsed fluorescent SO_2 analyzer (Thermoelectron Corporation model 40) and the concentration was continuously recorded. The SO_2 analyzer was calibrated using a calibration standard (a mixture of 2000 ppm SO_2 and N_2). The reactor was equipped with a bypass, to allow the bed to be preconditioned and to allow the gas flow to be stabilized at the desired SO_2 concentration before beginning the experimental run. Prior to each experimental run, the bed was humidified by flushing with pure nitrogen at a relative humidity of about 98% for 10 minutes then later with pure nitrogen at the relative humidity at which the experiment was to be performed for 8 minutes. This was done to simulate the moisture conditions encountered in the bag filters where the solids are originally slurry droplets.

The reaction time was normally 1 hour. The raw data from each experimental run was a curve of SO_2 concentration leaving the reactor versus time. This curve was given by the recorder of the SO_2 analyzer.

3.4 Analysis of the Experimental Data

The raw data from the experiments are SO_2 concentrations from the reactor as a function of time. By integration of the SO_2 concentration over time and a mass balance on the reactor, the average fraction of lime converted can be calculated at each time. A sample calculation can be found in Appendix D. As a backup, the reacted solids were analyzed for sulfite and hydroxide using acid/base and iodine titrations described in Appendix A.

The relative humidity of the gas stream was calculated from the amount of water injected by the syringe pump and the gas flow rate. The wet-bulb temperature measurement was not accurate enough to calculate relative humidity. Heat flow from the water bath was reduced by the use of a Dewar container but not eliminated. As a consequence, the wet-bulb temperature measured was systematically higher than the one corresponding to the relative humidity calculated from the injected water. Even with this systematic error, the wet-bulb temperature was useful to check that the relative humidity remained constant during the experiment.

3.5 Reagent Used

Most of the experimental work was done using $Ca(OH)_2$ powder reagent A.C.S. (Matheson Coleman & Bell Manufacturing Chemist) as the reactant. The $Ca(OH)_2$ has maximum impurities of 1.213 wt%, the main impurities being magnesium and alkali salts (1% expressed as sulfates).

Table 3-1: Particle Size and BET Surface Area of Reactant

Reactant	Coulter Counter Median Particle Size (μm)	BET Surface Area (m^2/g)
Reagent $Ca(OH)_2$		
Lime 0	7.4	8.2
Lime A	5.6	9.4
Lime A (slurried)	-	8.8
Pressure Hydrated Dolomitic Lime		
after hydrator	-	20.1
after ball mill	-	21.1
sieved material after ball mill (< 125 μm)	-	18.4

Two batches of $Ca(OH)_2$ that will be identified as lime 0 and lime A were used. These two batches of $Ca(OH)_2$ differ slightly in particle size and BET surface area as shown in Table 3-1. The particle size distribution was measured using a Coulter Counter Model T_{AII}, and the BET surface area by nitrogen adsorption isotherms in a Physical

Adsorption Analyzer (Accusorb Model 2100E). The complete particle size distribution of the two $Ca(OH)_2$ used, as well as details of the BET area measurement, can be found in Appendix A, Sections A.1 and A.2. Also shown in Appendix A (Section A.3) are Scanning Electron Microscope pictures of lime 0 and lime A. The use of these two different batches of $Ca(OH)_2$ was not by choice, but rather forced by the depletion of the first batch of $Ca(OH)_2$ (lime 0).

A few experimental runs were also made using high surface area, pressure-hydrated dolomitic lime as the reactant. The chemical composition of the dolomitic lime is not exactly known but analysis made using Energy Dispersive Spectrometry (EDS) and X-Ray Powder Diffraction, as well as measured alkalinity (by acid/base titration) indicate it is composed mainly of $Mg(OH)_2$ and $Ca(OH)_2$ with small amounts of unhydrated MgO and CaO. The EDS and x-ray analysis results are discussed in detail in Appendix A (Sections A.4 and A-6). For the conversion calculation the dolomitic lime was assumed to consist of 40 mole% $Mg(OH)_2$ and 60 mole% $Ca(OH)_2$. Three samples of pressure-hydrated dolomitic lime (provided by Dr John Chang, Acurex, 1984) differing in particle size and BET surface area were used. One sample was taken when the dolomitic lime left the hydrator (hydrator lime), another when the dolomitic lime left the ball mill (ball mill lime), and the last one corresponds to ball mill lime dry-sieved through a 125-μm sieve. The BET surface areas of the dolomitic limes are given in Table 3-1.

3.6 Experimental Results

The effects of relative humidity, temperature, inlet SO_2 concentration, and amount of lime in the reactor on the reaction of SO_2 with powdered reagent $Ca(OH)_2$ were studied in the sand reactor described in Section 2.3. The experimental conditions were similar to the ones encountered in the bag filters during spray drying flue gas desulfurization. Table 3-2 shows the range of experimental conditions used in the experiments.

Table 3-2: Experimental Conditions

Relative Humidity:	17 - 90%
SO_2 Inlet Concentration:	500 - 4000 ppm
Reactor Temperature:	30.5 - 95°C
Nitrogen Flow Rate:	4600 cm^3/min (0°C, 1 atm)
Amount of Lime:	1.0 - 4.0 g

3.6.1 Effect of Relative Humidity

The relative humidity was found to have a dramatic effect on the rate of reaction of SO_2 with $Ca(OH)_2$. Figure 3-2 shows lime conversion as a function of time at 19, 50 and 70% relative humidity. All three experiments were run at 2000 ppm inlet SO_2 and 66°C using 4 g of lime 0. The dashed line in the figure corresponds to the $Ca(OH)_2$ that would be converted if all the SO_2 were being removed. Figure 3-2 shows that for all relative humidities, 100% of the SO_2 is removed during the first one or two minutes of reaction, then the reaction rate decreases quickly at low relative humidities but more slowly at high relative humidities.

The same kind of behavior was observed with the other batch of $Ca(OH)_2$ (lime A) which differs slightly in particle size and BET surface area. Figure 3-3 shows the $Ca(OH)_2$ conversion versus time for 1 g of lime A at relative humidities of 54 and 74%. The inlet SO_2 concentration was 500 ppm. Some "differential experiments" were also performed at these two relative humidities. The differential experiments were run using a very small amount of $Ca(OH)_2$ in the reactor (0.125 g) so that the SO_2 concentration did not change significantly across the reactor. In these experiments, the integration of the SO_2 removed was not accurate enough to determine the lime converted, so chemical analysis of the solids at different times was used instead. Figure 3-4 shows the results of these experiments, and even though there is some scattering of the data, it is obvious that the relative humidity is strongly affecting the reaction rate.

The fact that the rate of reaction is a very strong function of the relative humidity of the gases agrees with the findings of Klingspor and coworkers (Klingspor et al., 1984), who reported the initial reaction rate to be an exponential function of the relative humidity. The Acurex results (Jorgensen et al., 1986) also show an exponential type of dependence of the reaction rate with relative humidity.

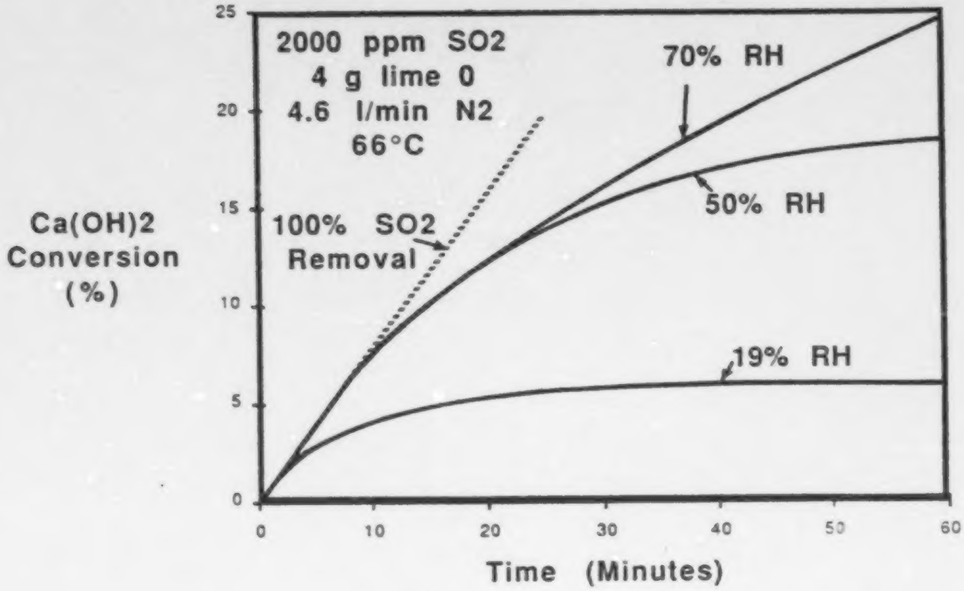

Figure 3-2: Lime 0, Effect of Relative Humidity

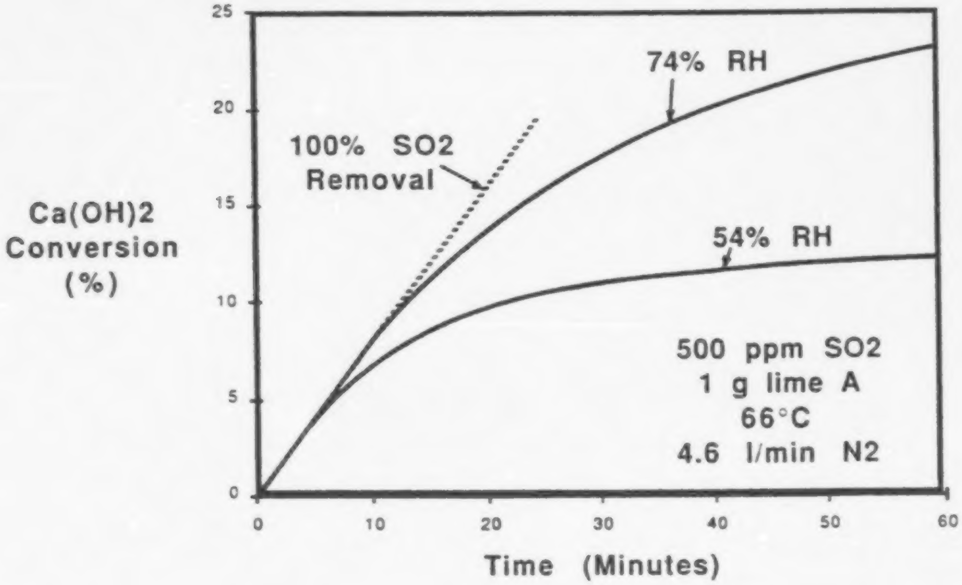

Figure 3-3: Lime A, Effect of Relative Humidity

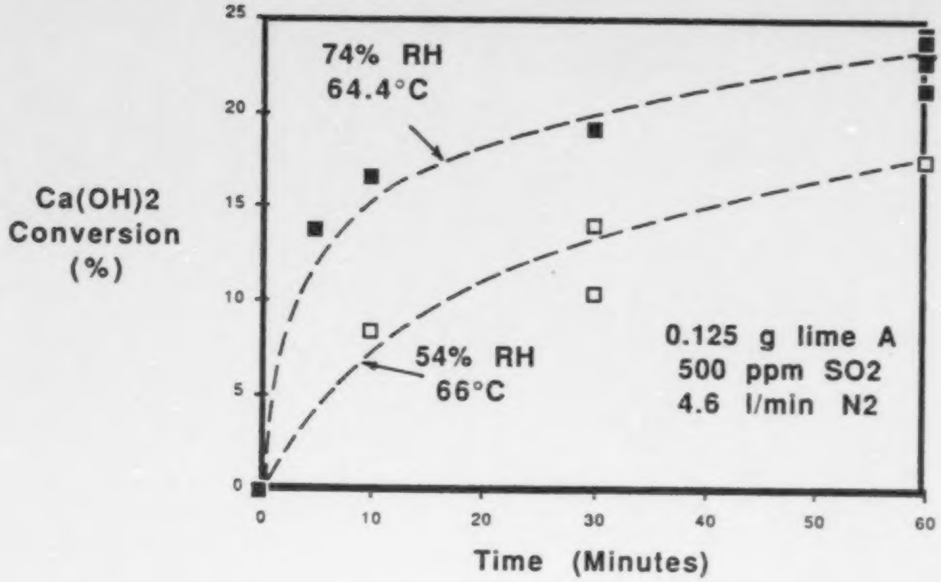

Figure 3-4: Differential Experiments, Effect of Relative Humidity

3.6.2 Effect of Inlet SO_2 Concentration

The effect of the inlet SO_2 concentration on the reaction rate was found to depend on the relative humidity. At 70% relative humidity, the $Ca(OH)_2$ conversion was practically independent of the inlet SO_2 concentration as illustrated by Figure 3-5. At lower relative humidity, the reaction rate was not affected by the SO_2 concentration if the SO_2 concentration is high. However, at lower levels of SO_2, the reaction rate was affected by the SO_2 concentration as illustrated by Figure 3-6 which shows the $Ca(OH)_2$ conversion at 50% relative humidity. These results are not in disagreement with the findings of Klingspor and coworkers (Klingspor et al., 1984) who reported the initial

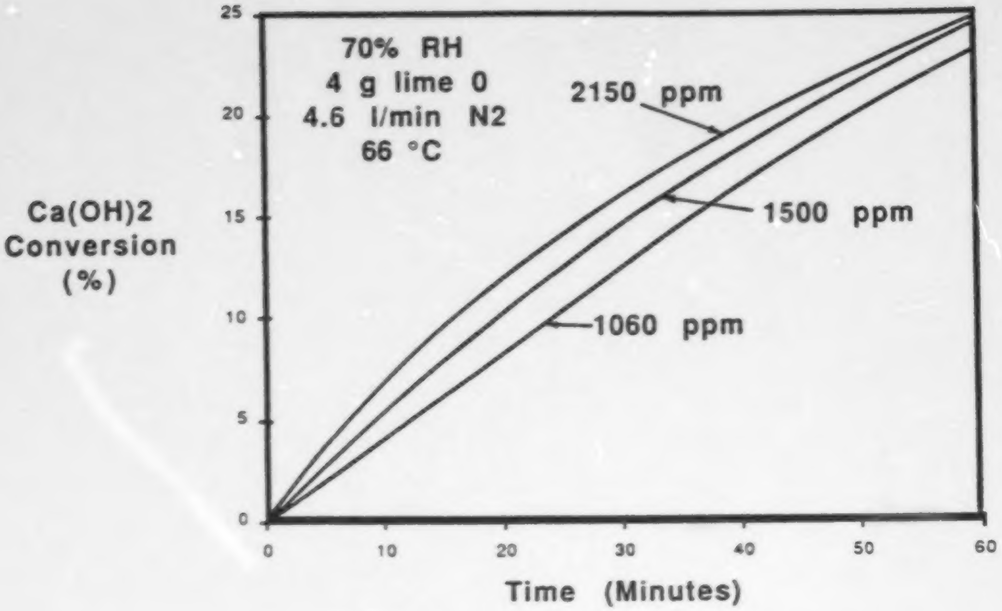

Figure 3-5: Effect of SO_2 Concentration, High Relative Humidity

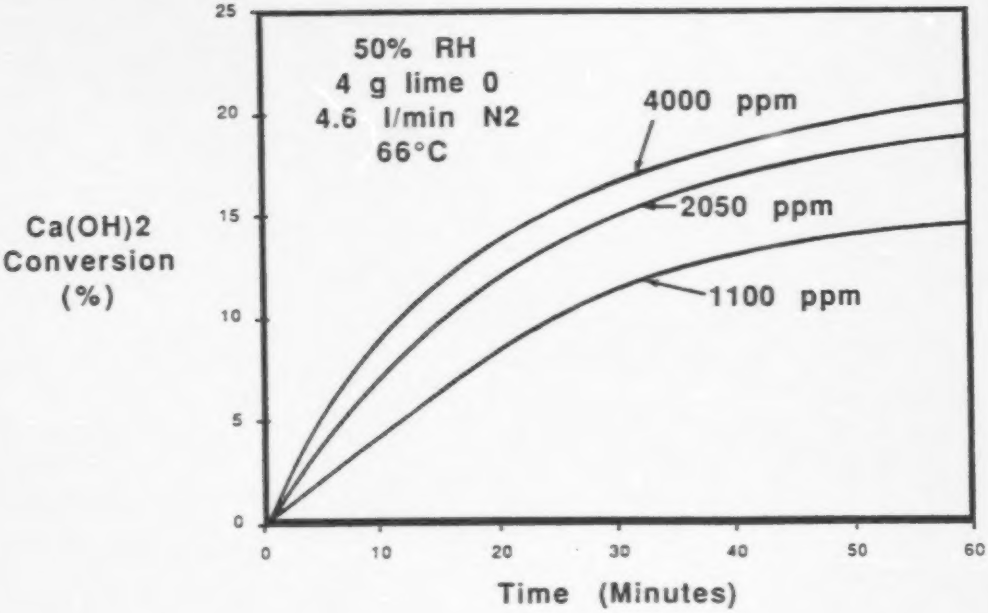

Figure 3-6: Effect of SO_2 Concentration, Moderate Relative Humidity

reaction rate to be zero order in SO_2 for relative humidities of 70% or lower. They measured initial reaction rate, that is reaction rate when no product has been formed. At this condition the reaction is kinetically controlled, because there is no diffusion through product layer or pore plugging to consider. In the present research, the reaction was carried out for 1 hour, so that a considerable amount of product was produced. Under this condition, diffusion of the SO_2 through the product layer can become important so the overall reaction rate may be dependent on the SO_2 concentration even when the kinetic rate is zero order in SO_2. The fact that at low relative humidities and low SO_2 levels the SO_2 concentration affects the reaction rate could be explained by assuming that at these conditions mass transfer becomes the controlling step instead of chemical reaction.

3.6.3 Effect of Amount of $Ca(OH)_2$ in the Reactor

The effect on the average $Ca(OH)_2$ conversion of changing the amount of $Ca(OH)_2$ in the reactor is illustrated by Figures 3-7 and 3-8 which show the $Ca(OH)_2$ conversion when the amount of lime 0 in the reactor was reduced from 4 to 1 g at SO_2 levels of 1000 and 2000 ppm respectively. The relative humidity was 50% for these two sets of experiments. From Figure 3-7 it can be seen that the amount of $Ca(OH)_2$ present in the reactor makes a difference during the first few minutes of reaction, but the effect is less marked at later times. These results are consistent with the effect of SO_2 concentration discussed in the previous subsection. When more $Ca(OH)_2$ is present in the reactor, more SO_2 is removed at the entrance of the reactor, so the $Ca(OH)_2$ present further down in the reactor "sees" a lower concentration of SO_2, and the reaction rate is slower. At later times when the SO_2 removal is lower, the amount of $Ca(OH)_2$ present will not be as important. When

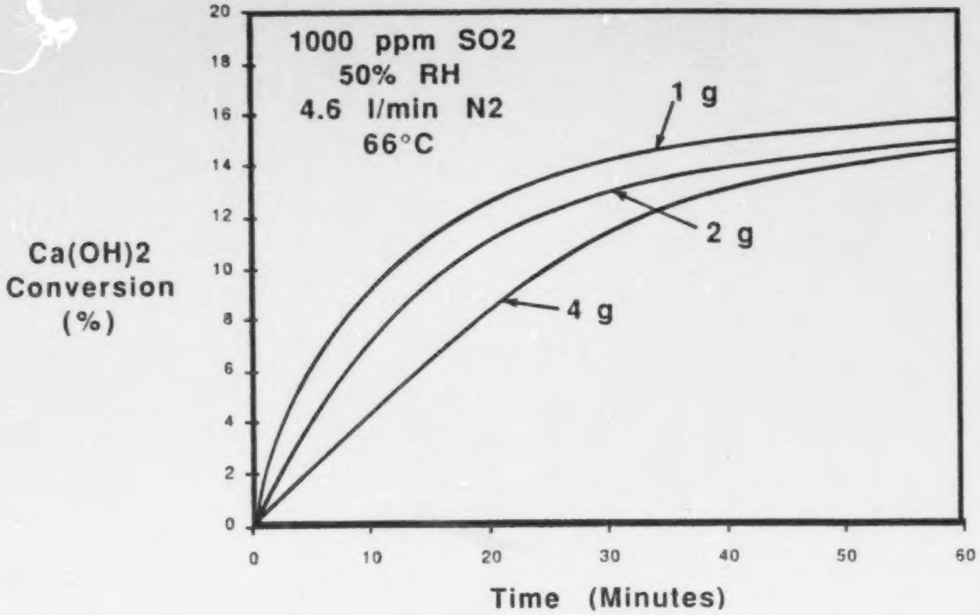

Figure 3-7: Effect of $Ca(OH)_2$ Loading, 1000 ppm SO_2

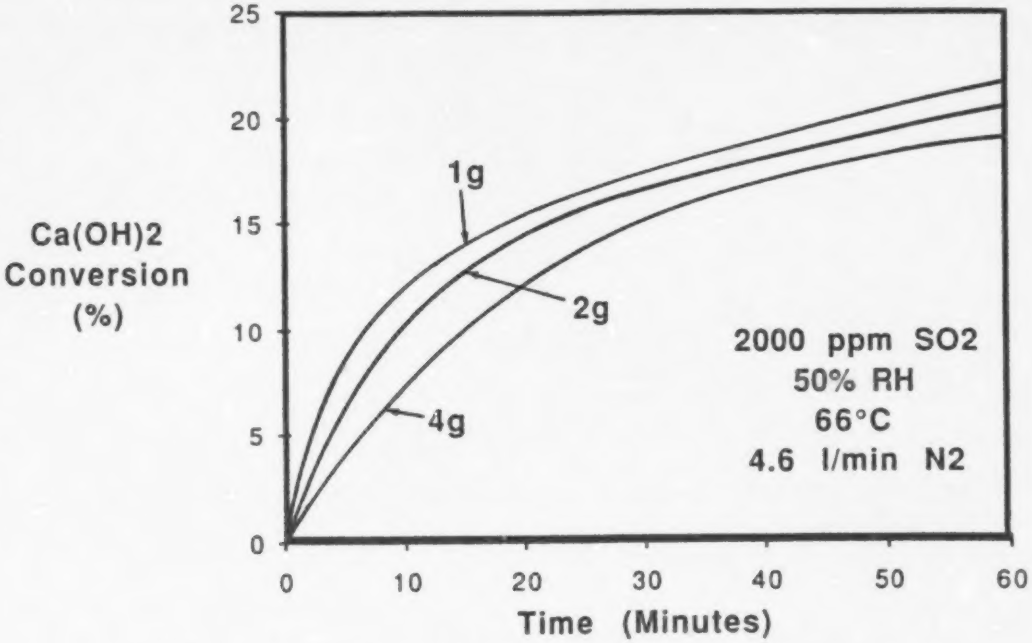

Figure 3-8: Effect of $Ca(OH)_2$ Loading, 2000 ppm SO_2

the SO_2 concentration entering the reactor is higher, lime conversion should be less dependent on the amount of $Ca(OH)_2$ present as illustrated by Figure 3-8.

3.6.4 Effect of Reactor Temperature

Reactor temperature has a very moderate effect on $Ca(OH)_2$ reactivity, as illustrated by Figure 3-9 which shows the effect on $Ca(OH)_2$ conversion when the reactor temperature was increased from 30.4 to 64.4°C while keeping all other variables constant. The relative humidity was 74%, so in this region the reaction is expected to be kinetically controlled.

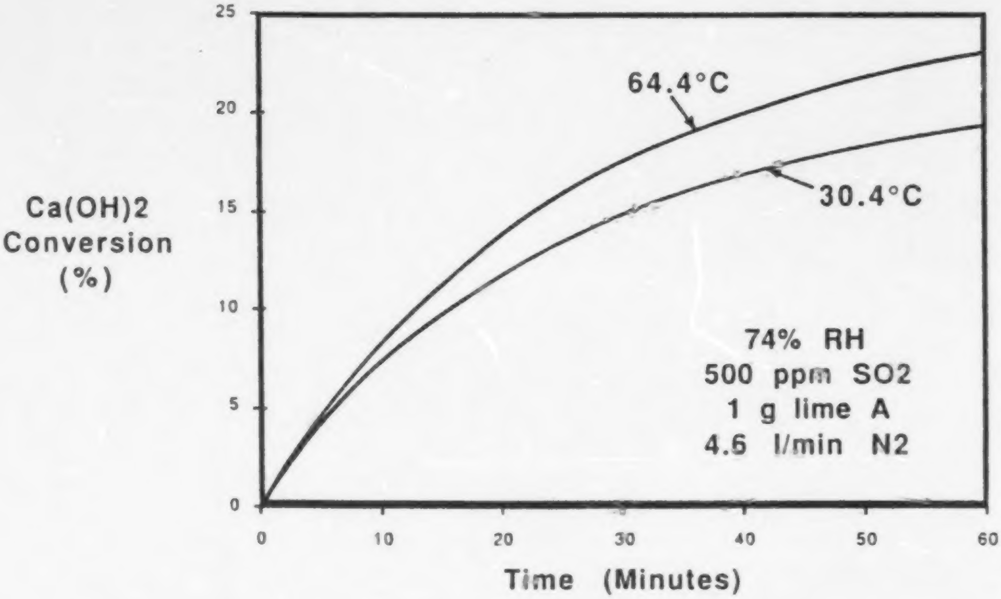

Figure 3-9: Effect of Reactor Temperature, Lime A

A very weak dependence of the reaction rate on temperature was also reported by Klingspor and coworkers (Klingspor et al., 1984) and by Acurex Corporation (Jorgensen et al., 1986).

3.6.5 Other Types of Lime

A few experimental runs were made using samples of pressure hydrated dolomitic lime. The three samples differ in particle size and BET surface area.

Table 3-3 shows the average $Ca(OH)_2$ conversion after 60 minutes of reaction for the three different samples of hydrated dolomitic lime, together with the BET surface area. Also included in the table is the conversion of pure $Ca(OH)_2$ at the same experimental conditions. The hydrator and ball mill limes are only slightly more reactive than the pure $Ca(OH)_2$ despite having a much higher surface area (about 2 times that of pure $Ca(OH)_2$). When the ball mill lime was dry sieved using a 125 μm sieve, the reactivity of the hydrated dolomitic lime increased, even when its surface area decreased slightly.

The pressure hydrated lime consisted of a few very large particles (some over 100 μm), and a majority of small particles of 1 μm in size or lower that tend to agglomerate (See Appendix A, Section A.3). The reactivity of the dolomitic lime may have improved after being sieved, because the large particles that were eliminated by sieving consisted mainly of dead-burned, unreactive or other unhydrated material (MgO and CaO) that did not contribute significantly to the SO_2 absorption.

MgO has been reported to be usually "dead-burned" in the calcining process, and therefore will not explosively slake to form the highly reactive lime slurry needed for best results in spray absorption flue gas desulfurization (Parsons et al., 1981). Acurex Corporation (Jorgensen et al., 1986) also tested some pressure hydrated dolomitic

Table 3-3: Reactivity of Pressure Hydrated Dolomitic Lime

74% R H, 64.4°C, 500 ppm SO_2, 1 g lime A

Type of Lime	Average Conversion after 60 Min (%)	BET Surface Area (m^2/g)
Pure $Ca(OH)_2$ slurried	22	8.2
Pure $Ca(OH)_2$ non-slurried	23	9.4
Hydrator Lime	24[a]	20.1
Ball Mill Lime	25[a]	21.1
Sieved Ball Mill Lime	31[a]	18.4

a Average hydroxide conversion assuming composition of dolomitic lime to be 40 mole% $Mg(OH)_2$ and 60 mole% $Ca(OH)_2$

---

limes and found them to show somewhat lower conversion with SO_2 after 1 hr of reaction in comparison with reagent grade $Ca(OH)_2$.

Section 4

Effect of Additives

4.1 Introduction

The experimental results discussed in Section 3, as well as results from other sources (Klingspor et al., 1984, Jorgensen et al., 1986), indicate that the relative humidity of the gases has the greatest impact on the rate of absorption of SO_2 by $Ca(OH)_2$. The relative humidity is in turn correlated with the moisture content of the solids. Additives that will modify the moisture content of the $Ca(OH)_2$ solids in equilibrium with a gas phase of a given relative humidity would then be expected to change the reactivity of the $Ca(OH)_2$ towards SO_2. The present research was undertaken to investigate in a systematic manner the kind of additives that could be used to improve the $Ca(OH)_2$ reactivity. The small fixed bed reactor described in Subsection 3.3 was used to collect the data. Three different kind of additives were tried: buffer acids, organic deliquescents, and inorganic deliquescents.

4.2 Previous Research

4.2.1 Bench Scale Fixed Bed Reactor

Some inorganic and organic compounds like sodium sulfite, Fe^{++} compounds, ethylene-diamine tetra-acetic acid (EDTA), and its disodium salt have been tested as additives for slaked lime during simultaneous SO_2/NO_x removal (Niro Process) (Felsvang et al., 1984) in a bench scale fixed bed reactor. The emphasis in the Niro process was to improve the NO_x removal rather than the SO_2 removal.

Acurex Corporation tested $CaCl_2$, NaCl, and NaOH as additives to improve the reactivity of hydrated lime towards SO_2 in a fixed bed reactor (Jorgensen et al., 1986). Increased reactivity was reported for $CaCl_2$, NaOH and $NaNO_3$, but in the case of NaCl a slight decrease in the conversion was observed. The additives were added to the hydrated lime samples by dry mixing.

Karlsson et al. (1983), tried a number of deliquescent salts as additives for limestone in a small fixed bed reactor. Most of the halides tried (chlorides of Zn, Sn, Pd, Ca, Al, Ru, Fe, Ti, Te, and Pt, CaBr, CaI_2, and NiBr) were successful in promoting the reaction of limestone and SO_2, the exception being the chlorides of Mg, Mn, and Ce. None of the nitrates tried (nitrates of Ca, Mn, Cu, Fe, and Al) enhanced the reaction. After economic and secondary environmental considerations, the authors selected $CaCl_2$ as the most promising candidate for use in a spray drying bag filter system. Based on their results for limestone, Karlsson et al. then tried $CaCl_2$ as an additive for $Ca(OH)_2$ in the same reactor. They found the $CaCl_2$ to have some promoting effect on the reaction of $Ca(OH)_2$ with SO_2, but not to the same degree as in the limestone case.

Stouffer et al. (1985) reported some laboratory work in a glass tube differential reactor using slaked lime with a number of water soluble inorganic and organic additives, including $CaCl_2$, $NaFeCl_4$, NaOH, NaCl, Na_2CO_3 and adipic acid. The objective of this laboratory work was to identify an active sorbent/additive system for use in the coolside desulfurization technique under development at Conoco Coal Research Division. They found NaOH and Na_2CO_3 to be the most effective additives. At 60% relative humidity, 150°F, and 1000 ppm SO_2, the sorbent utilization at 60 minutes of reaction increased from 30 to 42% and 53% with the addition of 5 and 10 mole% Na_2CO_3 respectively.

4.2.2 Spray Dryer Pilot Plants

Karlsson et al. (1983) performed tests in a 0.5 MW spray dryer with a slaked lime stoichiometry of one at 20 to 70% relative humidity. They found that the addition of 4 mole% $CaCl_2$ increased SO_2 removal by about 25% from 45-80% to 70-98%. Unfortunately, they did not indicate how much of the removal takes place in the spray dryer itself, and how much in the bag filters used for collection of the solid products. It is not then clear if the $CaCl_2$ improves the rate of absorption during the wet phase that takes place in the spray dryer, or if the improvement occurs mainly in the "dry stage" that takes place in the bag filters.

Rhudy and Blythe (1985) presented results of $CaCl_2$ addition tests conducted at the Arapahoe EPRI spray dryer/bag filter pilot scale test facility (21/2 MW). The tests were conducted at high SO_2 levels (2000 and 3000 ppm), 11.1 °C (20°F) approach to the adiabatic saturation temperature at the spray dryer outlet (60% relative humidity), and with chloride levels of 0.4 and 0.8 wt% in the fabric filter solids collected. With 2000 ppm inlet SO_2 and a reagent stoichiometric ratio of around 1.1 the overall SO_2 removal increased from 85 to 92% with the addition of 0.4 wt% of $CaCl_2$ and from 85 to 98% when 0.8% $CaCl_2$ was added. With 3000 ppm SO_2, the SO_2 removal increased from 85 to 92% when 0.8 wt% $CaCl_2$ was added. At a reagent ratio of 1.1, the improvement in SO_2 removal was evenly split between the spray dryer and the fabric filters. When the reagent ratio was higher (1.3 to 1.4), the benefit appears to lie entirely in the spray dryer. This observation is misleading, though, because overall removal levels of essentially 100% were observed. So, even when the bag filter contribution to the overall removal is not increased, the bag filter is removing 100% of the SO_2 reaching the bags.

Blythe et al. (1984a, 1985), reported results of chloride addition in a full scale (100 MW) utility spray dryer baghouse dry FGD system located at the Northern States Power Company's Riverside Station. Addition of chlorides at levels which resulted in a chloride content of 1 percent in the fabric filter solids reduced the lime reagent ratio requirements to achieve 90% SO_2 removal by about 25%. Thus, $CaCl_2$ addition appears to result in improved lime utilization and/or increased SO_2 removal capabilities in high sulfur operations.

However, some potentially negative impacts on the operation and maintenance of the spray dryer bag filter system were also reported (Rhudy and Blythe, 1985). There was an increase in the pressure drop across the bag filters following the $CaCl_2$ addition, some chloride related stress corrosion cracking was detected on the 300 series stainless steel bag clamps, and changes occurred in the solid waste disposal properties (the unconfined compressibility values for wetted, compacted and cured samples of waste solid decreased when $CaCl_2$ was added). These potential problems need to be further investigated before $CaCl_2$ can be implemented on a commercial (full scale) system.

Adipic acid has also been tested as an additive in spray dryer pilot plants, but the results were not very conclusive. When the spray dryer system was operated without solids recycle, the adipic acid did not show a significant effect on the SO_2 removal efficiency (Parsons et al., 981a, Yeh et al., 1983). Some improvement of the removal efficiency was reported when the system was operated with solids recycle and 3000 ppm of adipic acid in the feed (Parsons et al., 981a). Because of the recycle the total concentration of adipic acid in the system increases due to recovery of residual adipic acid in the waste product. The results were reported as overall SO_2 removal, so it is not clear if the SO_2 removal in the bag filters was affected or not.

Some patents have been issued that involve the use of salt additives to improve the reactivity of $Ca(OH)_2$ towards SO_2 in spray drying bag filter systems. Lindau and Ahman (1980) patented the use of $FeCl_2$, $Fe(NO_3)_2$, $Fe(NO_3)_3$, $Al(NO_3)_3$ $Ca(NO_3)_2$, $Mg(ClO_3)_2$, $MnCl_2$, KSO_4, $NaAl(SO_4)_2$, NaClO, Na_3PO_4, Na_2SiO_3, $NaSO_4$, and $Zn(NO_3)_2$. Niro Atomizer included a claim involving the use of NaCl to improve the reactivity of slaked lime in their spray drying system with solids and fly ash recycle (Felsvang, Hansen and Rasmussen, 1981).

4.3 Experimental Apparatus

The experimental apparatus used in the additive experiments was the same as that used in the experiments with no additives, and it is described in Section 3, Subsection 3.3.

4.4 Reactants

Most of the experiments with additives were run using reagent grade $Ca(OH)_2$ (Lime A). Lime A has a BET surface area of 9.4 m^2/g and a median particle size of 5.6 μm (determined by Coulter Counter). One experimental run was also made using pressure hydrated dolomitic lime (sieved ball mill lime) with a BET surface area of 18.4 m^2/g and an approximate composition of 40 mole% $Mg(OH)_2$ and 60 mole% $Ca(OH)_2$. More details about size and surface area of these two limes along with scanning electron microscope pictures of the $Ca(OH)_2$ and dolomitic lime particles can be found in Appendix A.

4.5 Preparation of the Samples with Additives

An aqueous solution containing the desired additive was prepared. Five ml of this solution were then added to 1 g of $Ca(OH)_2$ and slurried and ambient temperature for 2 minutes. The sample was placed in a oven to dry at 75°C for about 14 hours, and then later sieved to separate the individual $Ca(OH)_2$ particles prior to mixing with the silica sand and being placed in the reactor.

4.6 Organic Acids as Additives

Organic acids have been successfully used as additives to enhance lime and limestone scrubbing (Rochelle and King, 1977, Burbank et al., 1984, Rochelle et al., 1982, Chang and Rochelle, 1982, Burke et al., 1985, Glover et al., 1985). Organic acids buffer the pH in the lime/limestone SO_2 absorbers and improve the SO_2 removal efficiency. The buffering action limits the drop in pH at the gas/liquid interface during SO_2 absorption, and the resultant higher concentration of SO_2 at the interface accelerates the liquid-phase mass transfer.

Two organic acids were selected as test additives for the reaction of $Ca(OH)_2$ with SO_2: adipic acid because of its extensive use in wet scrubbing, and glycolic acid, because of its deliquescent properties.

Both of these acids proved to be detrimental to the reaction of $Ca(OH)_2$ with SO_2, as can be seen from Table 4-1. At 74% relative humidity, the average $Ca(OH)_2$ conversion in the reactor after 1 hour of reaction decreased from 22 to 11% when 5 wt% of glycolic acid was added to the $Ca(OH)_2$, and from 22 to 20% when 1 wt% adipic acid was used as an additive.

4.7 Organic Deliquescents as Additives

Ethylene glycol (EG), tri-ethylene glycol (TEG), and monoethanolamine (MEA) were selected to be tested as additives to the $Ca(OH)_2$ due to their deliquescent or hygroscopic properties. Because of their high hygroscopicity, ethylene glycol and tri-ethylene glycol are commonly used as desiccants for natural gas (NGPSA, 1966). Ethylene

Table 4-1: Effect of Organic Acids and Organic Deliquescents on $Ca(OH)_2$ Reactivity

500 ppm SO_2, 1.0 g lime A, 74% RH, 64.4°C, 4.6 l/min N_2

Additive	Average $Ca(OH)_2$ conversion after 1 hour (%)
None	22.4
ORGANIC ACIDS	
5 wt% Glycolic Acid	11.3
1 wt% Adipic Acid	20.3
ORGANIC DELIQUESCENTS	
5 wt% Monoethanolamine	19.6
5 wt% Ethylene Glycol	20.3
5 wt% Tri-ethylene Glycol	20.5

glycol is also used as an antifreeze and as a refrigerant (Perry and Chilton, 1973, Kirk-Othmer, 1980). Monoethanolamine is used in scrubbing H_2S and CO_2 from petroleum gas streams (NGPSA, 1966).

The experimental results of runs made adding 5 wt% of ethylene glycol, TEG, or MEA to the $Ca(OH)_2$ are presented in Table 4-1. At a relative humidity of 74%, all three additives slightly decreased the average $Ca(OH)_2$ conversion after 1 hour of reaction, when compared with the conversion of pure $Ca(OH)_2$ at the same experimental conditions.

4.8 Inorganic Deliquescents as Additives

A number of deliquescent salts were tested as additives to improve the $Ca(OH)_2$ reactivity towards SO_2. These inorganic salts were selected according to their deliquescent properties, or lowering of the water vapor pressure over their saturated solutions. The salts were added to the $Ca(OH)_2$ by the slurrying and drying process described in Subsection 4.5. X-ray analysis of the samples showed that most of the salts tried remained unchanged after this mixing procedure. However, with $CaCl_2$ and $Ca(NO_3)_2$, the less deliquescent solid phases, $Ca(OH)_2 \cdot CaCl_2 \cdot H_2O$ and $Ca_2N_2O_7 \cdot 2H_2O$ were formed. The presence of $Ca(OH)_2 \cdot CaCl_2 \cdot H_2O$ was confirmed by x-ray powder diffraction analysis of the sample. The presence of $Ca_2N_2O_7 \cdot 2H_2O$ could not be confirmed by x-ray analysis as the diffraction pattern of this solid phase was not available, but it was confirmed that neither $Ca(NO_2)_2$ nor any of its hydrates was present. Details of the x-ray diffraction work can be found in Appendix A, Section A.6.

The results of experimental runs using salts as additives are presented in Table 4-2 as average $Ca(OH)_2$ conversion after 1 hour of reaction. Runs were made at 54 and 74% relative humidity. As can be seen from Table 4-2, all of the salts tried were successful in increasing the $Ca(OH)_2$ reactivity, but their effectiveness depended on the amount of additive added, the type of salt, and the relative humidity at which the experiment was performed. The prehumidification of the bed prior to each experimental run also affected the results.

Table 4-2: Effect of Deliquescent Salts in $Ca(OH)_2$ Reactivity and Deliquescent Properties of the Salts

500 ppm SO_2, 1.0 g lime A, 4.6 l/min (0°C,1 atm) N_2

	$Ca(OH)_2$ Conversion at 60 minutes (%)		Water Activity over Saturated Solutions	
Additive (Mole%)	74% RH 64.4°C	54% RH 66°C	at 25°C	at 70°C
None	22.4	11.8	-	-
5% Na_2SO_4	28.3	-	.93[f]	.887[c]
5% Na_2SO_3	29.8	16.1	.95[f]	-
5% $CaCl_2$[b]	34.6	16.4	.850[c]	.686[c]
10% NaCl	38.5	27.0	.753[d]	.751[e]
5% $Ca(NO_3)_2$[b]	39.4	12.3	-	.553[a,c]
5% $Co(NO_3)_2$		13.2		
10% $NaNO_2$	40.0	-	.66[f]	.593[e]
10% $NaNO_3$	41.5	27.2	.738[d]	.657[e]
5% $BaCl_2$	-	19.4	.902[d]	.876[c]
5% $Na_2S_2O_3$	-	21.6	.78[e]	.298[c]
10% KCl	-	37.3	.842[d]	.80[e]
10% NaBr	-	42.0	.577[d]	.507[e]
10% LiCl	-	43.9	.112[d]	.099[c]
100% SO_2 Removal	48.2	48.2		

a Data at 100°C.

b Solid phases were $CaCl_2 \cdot Ca(OH)_2 \cdot H_2O$ and $Ca_2N_2O_7 \cdot 2H_2O$ respectively.

c Source (National Research Council, 1930)

d Source (Stokes and Robinson, 1949)

e Source (Lange, 1961)

f Source (Lange, 1961) data at 20 °C.

4.8.1 Effect of Amount of Additive

Figure 4-1 illustrates the effect of the amount of additive added on $Ca(OH)_2$ reactivity. $Ca(OH)_2$ conversion increases as the NaCl or $NaNO_3$ concentration increases from 0 to 10 mole%. Further increase of the amount of additive to 15 mole% does not improve $Ca(OH)_2$ reactivity.

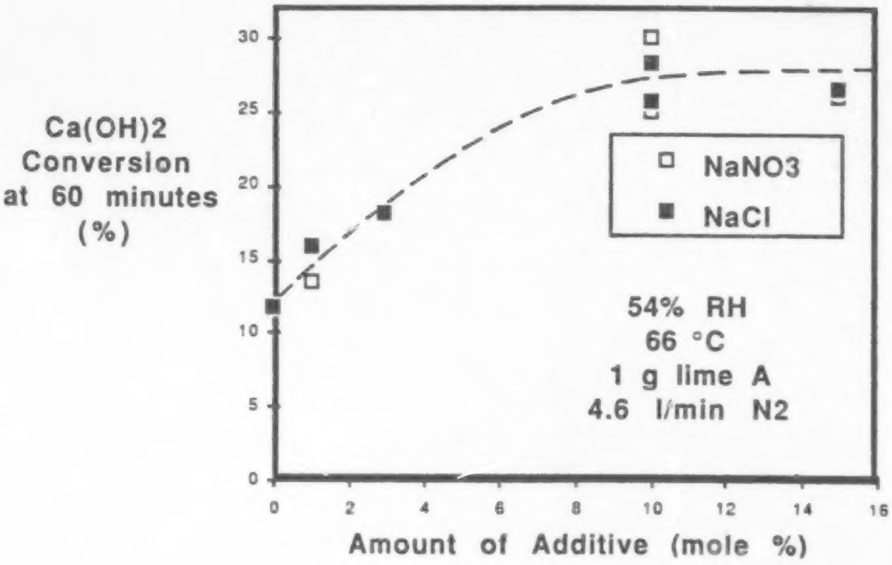

Figure 4-1: Effect of Amount of Additive on $Ca(OH)_2$ Reactivity

The optimal amount of additive appears to be about 10 mole% for 1:1 electrolytes such as NaCl and $NaNO_3$, and that was the concentration used in the experiments. For 2:1 and 1:2 salts, 5 mole% was used because it gives about the same level of deliquescence.

4.8.2 Effect of Type of Deliquescent Salt

Also presented in Table 4-2 are the deliquescent properties of the salts expressed as water activity in saturated solutions of the salt at 25 and 70°C and 1 atm. The water activity is approximately equal to the relative humidity of the gas phase in equilibrium with the saturated solution.

If one of these deliquescent salts is contacted with a gas phase of relative humidity greater than the water activity, the salt will capture water from the gas phase and become a solution. This tendency to capture water has been extensively documented in the literature by studies of the growth of salt containing aerosols as a function of the atmospheric relative humidity (Winkler, 1973, Ferron, 1977, Tang, 1976, Tang et al., 1977, Tang and Munkelwitz, 1977, Tang et al., 1978). A sharp increase in the diameter of the aerosol particle occurs when the relative humidity becomes greater than the water activity of the saturated solution of the salt.

From the data presented in Table 4-2, it is clear that the effectiveness of a salt in promoting SO_2 removal is related to its deliquescent properties. A very deliquescent salt will be a good additive to $Ca(OH)_2$. Nevertheless, deliquescence alone can not explain the beneficial effect of some salts. For example KCl is the least deliquescent of all the salts tried but it is one of the most effective at 54% relative humidity.

For an additive to be effective, it is necessary that the hydroxide of the cation be very soluble; otherwise, the cation will precipitate as the hydroxide and the anion will form the Ca salt. For example $Co(NO_3)_2$ is a very deliquescent salt, and the addition of Co^{+2} salts have been reported to increase dramatically the reactivity of limestone towards SO_2 (Bjerle et al., 1983). However, when added to $Ca(OH)_2$, Co precipitates as the insoluble $Co(OH)_2$, and adding $Co(NO_3)_2$ is equivalent to adding $Ca(NO_3)_2$, as can be seen from Table 4-2.

The effectiveness of a certain salt also depends on the relative humidity at which the experiment is performed. This could be expected because when the relative humidity of the gaseous phase is lower than the water activity in a saturated solution of the salt, the salt should not absorb water and as a consequence should not be expected to increase $Ca(OH)_2$ reactivity in any appreciable degree. When examining the data in Table 4-2, it can be seen that the salts do not behave as would be expected from deliquescence considerations alone. $NaNO_3$ and all the chlorides tried, with the exception of LiCl, should not work at a relative humidity of 54%. Nevertheless, the $Ca(OH)_2$ reactivity was improved by the presence of these salts at that relative humidity. A possible explanation for this phenomenon is hysteresis, and this will be discussed in the next subsection.

4.8.3 Effect of Prehumidification at 98% RH

As was mentioned in the Experimental Apparatus Subsection (Subsection 3.3), prior to each experimental run the fixed bed (consisting of $Ca(OH)_2$ dispersed in silica sand) was prehumidified by flushing with pure nitrogen at a relativity humidity of about 98% for 10 minutes before flushing with nitrogen at the relative humidity at which the experiment was to be performed for 8 minutes. This prehumidification was done to simulate the moisture conditions encountered in the bag filters during spray drying, where the solids are originally slurry droplets.

This prehumidification step could be the reason why some of the salts are still effective at a relative humidity lower than the one predicted from equilibrium considerations. Due to hysteresis it is possible that when the relative humidity was lowered to the experimental conditions after the prehumidification, some excess water remains in the solids. Strong hysteresis effects have been reported in NaCl aerosols (Tang and Munkelwitz, 1977).

To check if hysteresis was responsible for the beneficial effect of some salts at low relative humidities, experimental runs were made omitting this step. Table 4-3 shows the results obtained at 54 and 17.4% relative humidity with and without prehumidification of the bed at 98% relative humidity. The additives used were NaCl, $NaNO_3$ and KCl.

At 54% relative humidity and although some decrease of the lime conversion was found without prehumidification, the results are still far superior to the pure lime case. Hysteresis, then, cannot explain all of the improvement observed at 54% relative humidity. An alternate explanation would be that the chlorides and $NaNO_3$ modify the properties of the product $CaSO_3 \cdot 1/2H_2O$ layer that is formed as the reaction takes place thereby facilitating the access of the SO_2 to the unreacted $Ca(OH)_2$ which remains in the interior of the particle. NaCl and $CaCl_2$ have been reported to enhance the sulfur dioxide reactivity of limestones in fluidized bed combustion by affecting the pore structure of

Table 4-3: Effect of Prehumidification of the Bed at 98% RH on $Ca(OH)_2$ Reactivity

500 ppm SO_2, 1.0 g lime A, 4.6 l/min (0°C,1 atm) N_2

	Average $Ca(OH)_2$ Conversion after 1 hour (%)			
	54% RH		17.4% RH	
	66°C		95°C	
Additive	Prehumidified		Prehumidified	
(Mole%)	Yes	No	Yes	No
None	11.2	-	4.0	-
10% NaCl	27.0[a]	23.2	9.7	4.0
10% $NaNO_3$	27.2[a]	23.7	11.9	-
10% KCl	37.3	19.3	3.4	-

a Average of two experimental runs.

the lime during calcination, which then increases the extent of sulfation of the limestone (Chopra et al., 1980).

At 17.4% relative humidity, all the beneficial effect in the case of the NaCl appears to be due to the prehumidification of the bed, i.e. due to a hysteresis phenomena.

4.8.4 Effect of Nitrogen Purity

When experiments using NaCl as an additive were performed, it was found that the lime conversion given by chemical analysis of the reacted solids was consistently lower than the lime conversion calculated by integration of SO_2 removal over time. The disappearence of sulfite could be explained by: 1) a disproportionation reaction of sulfite to produce thiosulfate and sulfate or 2) the oxidation of the sulfite product by oxygen present as impurity in the nitrogen. The first explanation was discarded after chemical analysis showed no traces of thiosulfate in the reacted solids. The more likely explanation is then partial oxidation of the sulfite produced in the reaction by the oxygen present as an impurity in the nitrogen. To test this possibility, some experiments were run using oxygen-free nitrogen (purity of 99.998%) instead of the nitrogen previously used that had a purity of 99.5%. Table 4-4 shows the comparison of two experiments run at the same experimental conditions but using the two different types of nitrogen. A much better agreement was found between the lime conversion obtained by chemical analysis and the one obtained by integrating SO_2 removal when oxygen-free nitrogen was used.

Table 4-4: Effect of Nitrogen Purity on Lime Reactivity

500 ppm SO_2, 54% RH, 10 mole% NaCl, 1.0 g lime A, 4.6 l/min N_2

	Average $Ca(OH)_2$ Conversion after 1 hour (%)	
Type of Nitrogen	By Integrating SO_2 Curves	By Chemical Analysis
Common (99.5% purity)	27.0	19.7
O_2 Free (99.998% purity)	27.0	25.1

The lime conversion estimated by integration of SO_2 removal was the same in both experiments, indicating that the rate of SO_2 removal is not affected by the nitrogen purity even when some oxidation of the sulfite appears to be taking place when the less pure nitrogen was used. Differential scanning calorimetry (DSC) and X-ray powder diffraction results indicate that any sulfate produced in the reactor will be present in solid solution with $CaSO_3 \cdot 1/2H_2O$ and not as a separate gypsum or $CaSO_4 \cdot 1/2H_2O$ phase. Details of the DSC and X-ray work are given in Appendix A, Sections A.5 and A.6.

4.9 Other Experimental Runs

4.9.1 Effect of Relative Humidity

Several experiments were run keeping the absolute humidity of the gases constant but modifying the relative humidity by increasing the reactor temperature. The experiments were run using $Ca(OH)_2$ with NaCl or $NaNO_3$ as additives. Figure 4-2 shows the results of experimental runs made at 66, 77.5 and 95°C, which correspond to relative humidities of 54, 35 and 17%, using 10 mole% NaCl as additive. $Ca(OH)_2$ conversion decreases dramatically when the relative humidity decreases even when the reactor temperature is higher. Figure 4-3 shows the same results with 10 mole% $NaNO_3$. Both additives behaved in an almost identical way.

4.9.2 $CaCl_2$ and Adipic Acid as Additives

As has been discussed, the addition of an organic acid like adipic acid proved to be detrimental to the reaction of $Ca(OH)_2$ with SO_2, while $CaCl_2$ increased the reactivity of the $Ca(OH)_2$. When adipic acid and $CaCl_2$ were simultaneously added to the $Ca(OH)_2$, the detrimental effect of adipic acid nullified the beneficial effect of the salt, and the combined result was a conversion that was very close to the $Ca(OH)_2$ with no additives. This is illustrated by Table 4-5 which shows

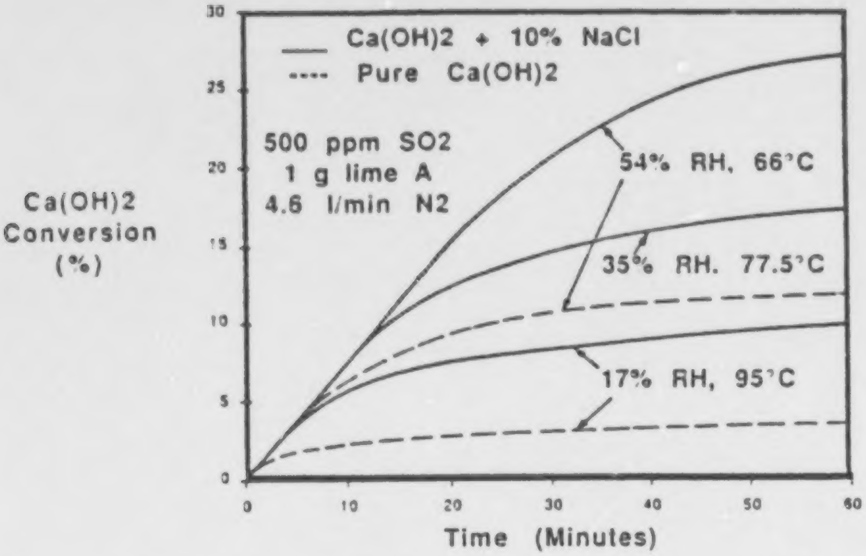

Figure 4-2: Effect on $Ca(OH)_2$ Conversion of Decreasing Relative Humidity by Increasing Temperature, With and Without 10 mole% NaCl

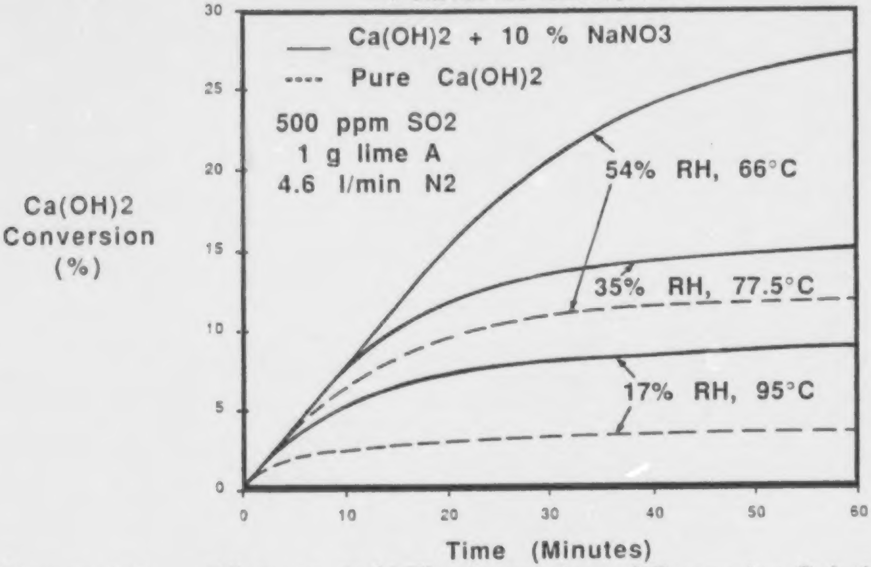

Figure 4-3: Effect on $Ca(OH)_2$ Conversion of Decreasing Relative Humidity by Increasing Temperature, With and Without 10 mole% $NaNO_3$

the average $Ca(OH)_2$ conversion after a hour of reaction for $Ca(OH)_2$ with no additives, using adipic acid and $CaCl_2$ alone and together.

Table 4-5: Effect of Adipic acid and $CaCl_2$ as Additives for $Ca(OH)_2$

500 ppm SO_2, 64.4°C, 74% RH, 1.0 g lime A, 4.6 l/min N_2

Additives	Average Conversion after 1 hr (%)
None	22.4
5 mole% $CaCl_2$	34.6
1 wt% Adipic Acid	20.3
1 wt% Adipic Acid + 5 mole% $CaCl_2$	23.5

4.9.3 Differential Experiments

Differential experiments were also performed using pure $Ca(OH)_2$ and $Ca(OH)_2$ with NaCl. Differential experiments were run with a very small amount of lime in the reactor (0.125 g), so that the SO_2 concentration across the reactor did not change significantly. In these experiments, the integration of SO_2 removal was not accurate enough to determine the $Ca(OH)_2$ conversion, so the conversion was determined by chemical analysis of the reacted solids at different reaction times. All of the differential experiments were run using oxygen-free nitrogen to prevent oxidation of the sulfite in the reactor. Figures 4-4 and 4-5 show the results of these differential experiments for pure $Ca(OH)_2$ and $Ca(OH)_2$ with 10 mole% NaCl and 5 mole% $CaCl_2$. The rate of reaction decreased much more slowly during the first few minutes of reaction when NaCl is present.

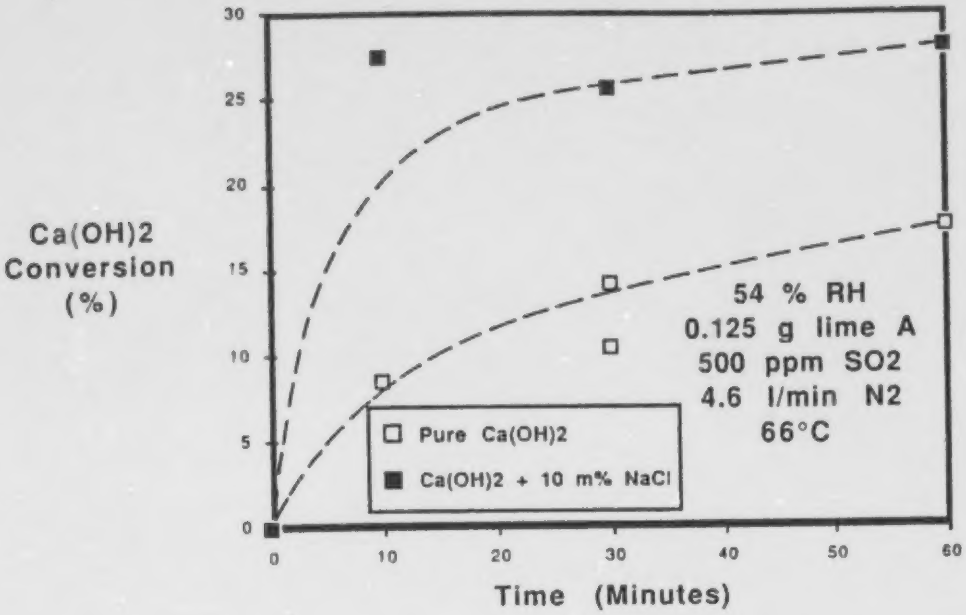

Figure 4-4: Differential Experiments, Effect of NaCl on $Ca(OH)_2$ Conversion

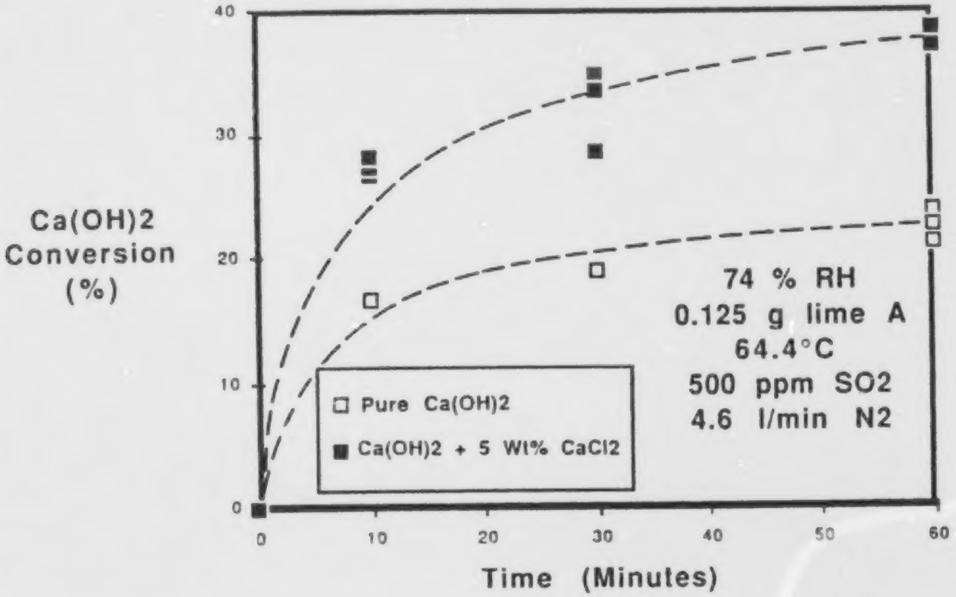

Figure 4-5: Differential Experiments, Effect of $CaCl_2$ on $Ca(OH)_2$ Conversion

4.9.4 Effect of NaCl in the Reactivity of Dolomitic Lime

An experimental run was also made to see how the addition of NaCl affected the reactivity of pressure hydrated dolomitic lime towards SO_2. The sample of dolomitic lime used was provided by Dr. John Chang (Acurex), and corresponds to dolomitic lime collected after the ball mill. The lime sample was dry sieved through a 125-μm sieve to eliminate the bigger particles. Table 4-6 shows the average lime conversion after 1 hour of reaction for dolomitic lime without additive and with 10 mole% NaCl. To calculate the conversion, the composition of the dolomitic lime was assumed to be 40 mole% $Mg(OH)_2$ and 60 mole% $Ca(OH)_2$. The average conversion at 74% relative humidity and 64.4 °C increased from 31.2 to 39.3% with the addition of the NaCl.

Table 4-6: Effect of NaCl on the Reactivity of Pressure Hydrated Dolomitic Lime

500 ppm SO_2 74% RH 64.4°C 1.0 g lime A 4.6 l/min N_2

Type of Sample	Average Lime Conversion after 1 hr (%)
Sieved Ball Mill Lime (< 125 μm)	31.2
Sieved Ball Mill Lime + 10 Mole% NaCl	39.3

Section 5

Modelling of the Reaction of SO_2 with $Ca(OH)_2$

5.1 Summary

A shrinking core model with zero order kinetics in SO_2 was used to model experimental data on the reaction of SO_2 with $Ca(OH)_2$ solids in a fixed bed reactor at 30.4 to 66°C and 19 to 74% relative humidity. An empirical correlation was included in the model to account for shape and surface roughness of the $Ca(OH)_2$ particles. The diffusion coefficient of the SO_2 through the product layer increases linearly with relative humidity, and the kinetic rate constant increases exponentially with relative humidity. With a few exceptions the model was able to predict the experimental data within the margin of experimental error (± 10%). At high relative humidity and/or high SO_2 concentration, reaction kinetics control the rate, while at low relative humidity and/or low SO_2 concentration, SO_2 diffusion through the $CaSO_3 \cdot 1/2H_2O$ product layer controls the rate. Diffusion coefficient values ranging from 0.75E-9 to 1.20E-6 (cm^2/sec) and kinetic constant values ranging from 1.0E-9 to 8.23E-9 (cm^4/gmol s) simulated the experimental results. An activation energy of 2.9 kcal/gmol was estimated for the reaction. Deliquescent salt additives increase the SO_2 diffusion coefficient and the kinetic rate constant in the same manner as relative humidity. Depending on the amount or type of deliquescent salt, the rate can be kinetically or diffusion controlled.

5.2 Introduction

A bench scale study of the reaction of SO_2 with $Ca(OH)_2$ with and without deliquescent salt additives was reported in Sections 3 and 4. The study was done at experimental conditions similar to the ones found in the bag filters following the spray dryer during flue gas desulfurization. This section presents the modelling of those experimental results using a modified shrinking core model with kinetics of zero order in SO_2.

The shrinking core model originally developed by Yagi and Kunii (1961) for the isothermal reaction of spherical solid particles assumes that the solid reactant has a low porosity and is practically impervious to the gaseous reactant. Under these conditions the reaction is narrowly confined to the surface of the solid particle, or to the interface between unreacted solid and the porous product layer. After the reaction has progressed, the solid will consist of an unreacted core surrounded by an envelope of reacted material. The reactant fluid must then diffuse through the reacted solid region to reach the inner-core and react. The original shrinking core model of Yagi and Kunii was extended to nonisothermal cases by several researchers (Hills, 1968, Shen and Smith, 1965, Wen and Wei, 1971). The shrinking core model has been extensively used to interpret experimental results of a number of gas-solid reactions (McKewan, 1962, St. Clair, 1966, Lu and Bistsianes, 1966, Spitzer et al., 1966, Yagi and Kunii, 1961, Hellinckx, 1954, Narsimhan, 1961, Samuel and Lapp, 1980, Samuel et al., 1984).

Klingspor et al. (1983, 1984) used an integral shrinking core model with kinetics as the controlling step to explain the dependence of reaction rate on lime conversion for the reaction of SO_2 with different types of slaked limes in a fixed bed reactor. They found the model did not fit their experimental data at the beginning of the reaction, and it only applied after a certain lime conversion had been reached. They attributed the sharp decrease in reaction rate to a decrease in surface roughness of the solid particles.

In the present work, the reaction of SO_2 with $Ca(OH)_2$ was modelled by a differential shrinking core model with zero order kinetics in SO_2. The model includes SO_2 diffusion through the gas film surrounding the solid particle, diffusion of SO_2 through the product layer, and chemical reaction. An empirical correlation to account for the non-sphericity and surface roughness of the $Ca(OH)_2$ particles was also included in the model.

5.3 Experimental

The experimental data being modelled were obtained in a bench scale fixed bed reactor, the bed consisting of a mixture of silica sand and reagent grade $Ca(OH)_2$. The gaseous phase consisted of a mixture of N_2, SO_2 and water vapor. Details of the experimental apparatus and procedure have been given in Subsection 3.3, Section 3. Two batches of reagent grade $Ca(OH)_2$, differing slightly in particle size distribution and BET surface area (namely lime 0 and lime A), were used in the experiments. The particle size distribution of these two batches of $Ca(OH)_2$ was measured by a Coulter Counter IIA (See Section A-1 of Appendix A). The BET surface area, measured by nitrogen adsorption isotherms, was 8.2 m^2/g for lime 0 and 9.4 m^2/g for lime A. Direct observation of the $Ca(OH)_2$ particles using a scanning electron microscope showed them to be of irregular shape and considerable surface roughness. No pores were visible under the microscope. Scanning electron microscope pictures of reacted and unreacted samples of limes 0 and A are shown in Appendix A, Section A-2.

The deliquescent salts tested as additives were added to the $Ca(OH)_2$ by a slurrying and drying procedure.

5.4 Model

The equations that describe the absorption of a component from a moving gas stream by a fixed solid in a packed bed consist of two partial differential equations obtained from material balances in the gaseous and solid phases.

Schematically:

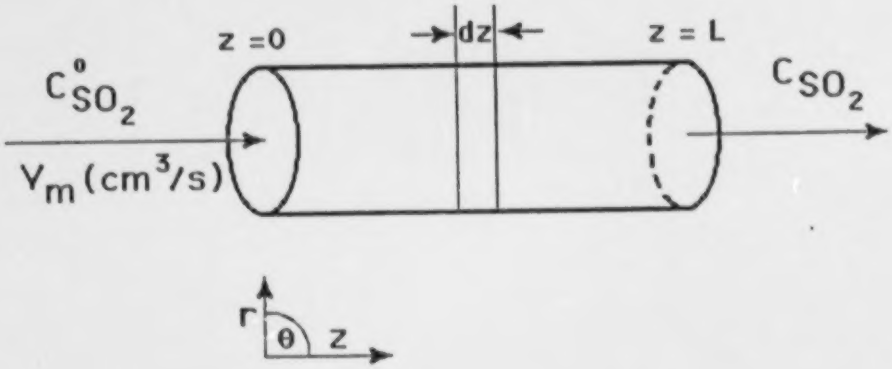

Assuming uniform SO_2 and $Ca(OH)_2$ concentrations in the r and θ directions, and neglecting SO_2 diffusion and dispersion in the z direction with respect to convective flow, the following equations are obtained:

$$\frac{\partial C_{SO_2}}{\partial t} + \frac{v_m}{A}\frac{\partial C_{SO_2}}{\partial z} = r_{SO_2} \qquad (5.1)$$

$$\frac{dC_{lime}}{dt} = r_{SO_2} \tag{5.2}$$

Where:

C_{SO_2} = concentration of SO_2 in the gas phase ($gmol/cm^3$)

t = time (sec)

v_m = volumetric flow rate of gas (cm^3/sec)

A = cross sectional area of the reactor (cm^2)

z = length of the reactor (cm)

r_{SO_2} = rate of disappearence of SO_2 ($gmol/cm^3$ sec)

C_{lime} = $Ca(OH)_2$ concentration ($gmol/cm^3$)

For most cases the concentration of SO_2 in the gas phase does not change rapidly with time at a given point (von Rosenberg et al., 1977), thus the time derivative of the SO_2 concentration in Equation (5.1) is much smaller than the spatial derivative. Neglecting the time derivative in Equation (5.1), the set of differential equations reduces to:

$$\frac{v_m\, dC_{SO_2}}{A\, dz} = r_{SO_2} \tag{5.3}$$

$$\frac{dC_{lime}}{dt} = r_{SO_2}$$

with boundary and initial conditions:

$$\text{At } z = 0 \qquad C_{SO_2} = C^{o}_{SO_2} \tag{5.4}$$

$$\text{At } t = 0 \qquad C_{lime} = C^{o}_{lime}$$

The rate expression r_{SO_2} will depend on the model selected to represent the kinetics of the reaction.

The shrinking core model for spherical particles of constant radius with kinetics of zero order in SO_2 was chosen to fit the experimental data. Because the $Ca(OH)_2$ particles are non-spherical and have a rough surface, their surface area is much higher than that of spherical particles of the same volume. An empirical expression was introduced to account for the decrease in roughness as the reaction progresses.

The shrinking core model or unreacted core model assumes that the reaction takes place at the exterior surface of the particle. As the reaction proceeds, the surface of reaction will move into the interior of the solid leaving behind a layer of inert product. The external radius of the particle remains the same, assuming no shrinkage or swelling of the product layer. Schematically, at any given time t the model is:

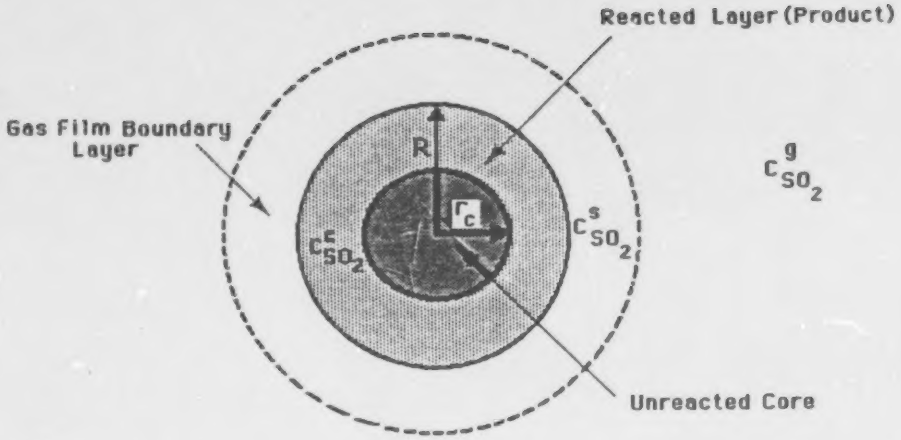
Reacted Layer (Product)
Gas Film Boundary Layer
R
$C^{g}_{SO_2}$
r_c
$C^{s}_{SO_2}$
$C^{c}_{SO_2}$
Unreacted Core

Shrinking Core Model

Where:

R $=$ Radius of the spherical particle (cm)

r_c $=$ Radius of the unreacted core (cm)

$C^{g}_{SO_2}$ $=$ SO_2 concentration in the gas bulk (gmol/cm^3)

$C^{s}_{SO_2}$ $=$ SO_2 concentration at the surface of the particle (gmol/cm^3)

$C^{c}_{SO_2}$ $=$ SO_2 concentration at the surface of the core (gmol/cm^3)

In order for the gaseous reactant to reach the surface of the unreacted core, it must diffuse through the gas film surrounding the particle and through the inert product layer. Once the SO_2 reaches the surface of the $Ca(OH)_2$ core, the chemical reaction takes place.

Assuming that the chemical reaction at the surface of the core is zero order in SO_2 and irreversible, the rate of disappearance of SO_2 with time is given by:

$$r_{SO_2} = \frac{1}{V} 4\pi R^2 k_g N (C^g_{SO_2} - C^s_{SO_2}) \quad \text{Gas film diffusion} \tag{5.5}$$

$$r_{SO_2} = \frac{1}{V} \frac{4\pi R r_c D_e N (C^s_{SO_2} - C^c_{SO_2})}{R - r_c} \quad \text{Product diffusion} \tag{5.6}$$

$$r_{SO_2} = \frac{1}{V} 4\pi r_c{}^2 N k_s \rho_{lime} \quad \text{Chemical reaction} \tag{5.7}$$

where:

V = volume of reactor (cm^3)

k_g = mass transfer coefficient (cm/sec)

N = number of $Ca(OH)_2$ particles

D_e = diffusivity of SO_2 through product (cm^2/sec)

k_s = kinetic rate constant (cm/sec)

ρ_{lime} = $Ca(OH)_2$ molar density (gmol/cm^3)

If the chemical reaction is slow, the rate of disappearance of SO_2 will be given by equation (5.7). If the chemical reaction is fast, all of the SO_2 that reaches the surface of the core will be immediately consumed and the concentration of the SO_2 at the surface of the unreacted core will become zero. At these conditions the rate of diffusion of the SO_2 through the gas film and product layer will become the limiting steps. In this case equations (5.5) and (5.6) can be combined to give:

$$r_{SO_2} = \frac{1}{V} \frac{C^g_{SO_2}}{\dfrac{R - r_c}{4\pi D_e N R r_c} + \dfrac{1}{4\pi R^2 N k_g}} \tag{5.8}$$

Using the relationship:

$$r_c = X_{lime}^{1/3} R \tag{5.9}$$

Where X_{lime} is the fraction of lime unreacted, Equations (5.7) and (5.8) become :

$$r_{SO_2} = \frac{1}{V} 4\pi R^2 N \rho_{lime} k_s X_{lime}^{2/3} \tag{5.10}$$

$$r_{SO_2} = \frac{1}{V} \frac{C^g_{SO_2}}{\dfrac{X_{lime}^{-1/3} - 1}{4\pi D_e N R} + \dfrac{1}{4\pi R^2 k_g N}} \tag{5.11}$$

Of Equations (5.10) and (5.11), the one that gives the smallest rate of disappearance of SO_2 will determine the overall reaction rate.

To account for the nonsphericity of the lime particles and their surface roughness, a dimensionless roughness parameter was defined as:

$$\sigma = \frac{A}{A_\phi} \tag{5.12}$$

Where:

A = actual surface area of the lime (m^2/g)

A_ϕ = surface area of spherical particles of equal mass (m^2/g)

When the lime is unreacted, σ can be estimated as the ratio of the BET surface area of the lime and the surface area calculated from the Coulter Counter particle size distribution assuming spherical particles. As the reaction progresses, σ should decrease and approach the limit σ = 1.0 when all the lime has reacted. This roughness parameter should decrease very rapidly at the beginning of the reaction and more slowly as the particles approach spherical shape.

An empirical expression of the form:

$$\sigma = 1.0 + \exp(a\,X_{lime} + b) \tag{5.13}$$

was used to describe the change of roughness with the fraction of $Ca(OH)_2$ unreacted. Equation (5.13) must satisfy the condition:

$$\text{at } X_{lime} = 1.0 \qquad \sigma = \sigma_o = \text{BET area}/A_\phi \tag{5.14}$$

To force σ to decrease more rapidly at high values of X_{lime} and to simulate the experimental results, an additional condition was imposed:

$$\text{at } X_{lime} = 0.8 \qquad \sigma = 2.0 \tag{5.15}$$

For the two batches of $Ca(OH)_2$ used in the experiments, namely lime 0 and lime A which differ slightly in surface area and particle size, the constants a and b in equation (5.13) took slightly different values.

For lime 0:

$$\sigma = 1 + \exp(12.878\,X_{lime} - 10.302) \qquad (5.16)$$

For lime A:

$$\sigma = 1 + \exp(13.428\,X_{lime} - 10.742) \qquad (5.17)$$

After introducing the roughness parameter σ, Equations (5.10) and (5.11) become:

$$r'_{SO_2} = \frac{1}{V}\, 4\pi R^2 N \sigma \rho_{lime} k_s X_{lime}^{2/3} \qquad (5.18)$$

$$r'_{SO_2} = \frac{1}{V} \frac{C^g_{SO_2}}{\dfrac{X_{lime}^{-1/3} - 1}{4\pi D_e N R (\sigma\sigma_o)^{1/2}} + \dfrac{1}{4\pi R^2 k_g N \sigma_o}} \qquad (5.19)$$

Of equations (5.18) and (5.19), the one that gives the lowest rate of SO_2 disappearance will determine the overall kinetic rate. The parameters of the model are k_g, D_e, and k_s. The integration assumed an average particle size which gave the same surface area as the measured particle size distribution assuming spherical particles. The mass transfer coefficient, k_g, was not used as an adjustable parameter because at the conditions at which the experiments were performed gas film diffusion is not likely to be important. The only effect of gas film diffusion is that it provides a limit to the rate expression (5.19) at the beginning of the reaction where product layer resistance is zero as there is no product. The value of k_g was estimated using a Sherwood number of 2 (Sherwood et al., 1975):

$$\frac{k_g d_p}{D_e} = 2.0 \tag{5.20}$$

corresponding to mass transfer from spherical particles in an stagnant fluid. In fact, mass transfer coefficients several orders of magnitude smaller than the value given by this correlation (k_g = 544 cm/sec) can be used in the model without affecting the results, which confirms the fact that gas phase diffusion is not likely to become a limiting factor during the reaction of $Ca(OH)_2$ with SO_2.

Thus D_e and k_s were the only parameters used to fit the experimental data. As will discussed in the next subsection, which presents the results of fitting the experimental data, depending on whether mass transfer or chemical reaction is the controlling step, only one of these parameters may be important.

A computer program with variable step size in time and in distance along the reactor was written to model the reaction. This computer program uses the IMSL integration routine DGEAR to carry out the integration, and the IMSL interpolation routine ICSCCU to provide interpolated values of lime conversion needed for each time integration step. A listing of the computer program is given in Appendix C.

5.5 Modelling Results

Figures 5-1 to 5-7 show the results of correlating with the model the experimental data obtained by reacting pure $Ca(OH)_2$ with SO_2. The adjustable parameters of the model are the diffusion coefficient of SO_2 through the product layer (D_e in cm^2/sec), and the kinetic constant (k_s in cm/sec).

Figure 5-1 shows several sets of experiments performed using 4 g of lime 0, 66°C, and 2000 ppm SO_2 at different relative humidities. At high relative humidity the chemical reaction is the controlling step, and k_s is the parameter that determines the rate of reaction. Any value of D_e greater than 8.0E-8 cm^2/sec will give essentially the same result. SO_2 diffusion through the product layer becomes more important as the relative humidity decreases. At 19% relative humidity,, D_e is the parameter that determines the rate of adsorption of SO_2. At 19% relative humidity, any value of k_s greater than 1.0E-9 cm/sec will give essentially the same results. Both D_e and k_s are affected by the relative humidity, but in the range of relative humidities studied, k_s increases approximately linearly while D_e increases exponentially (see Figure 5-2). Because the SO_2 diffusion coefficient (D_e) changes more rapidly than the kinetic constant (k_s), a change in the controlling mechanism occurs when the relative humidity is increased.

The same values of D_e and k_s were used to model the results obtained using a 1 g of lime A and 500 ppm SO_2, as illustrated by Figure 5-3. Because the SO_2 concentration in these experiments is much lower than in the experiments presented in Figure 5-1, SO_2 diffusion through the product layer becomes the controlling step at a much higher relative humidity (54%).

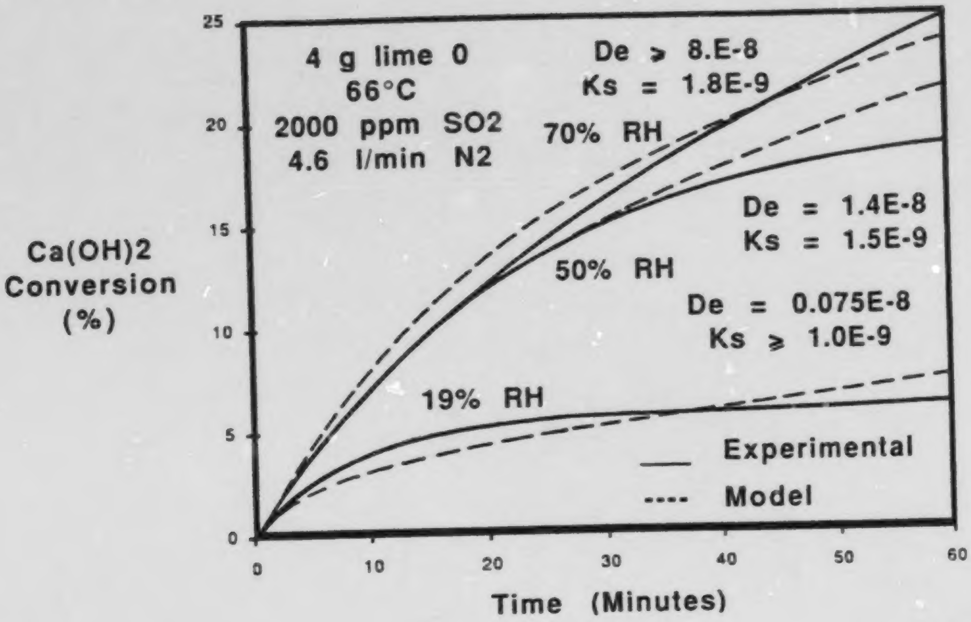

Figure 5-1: Effect of Relative Humidity on Reaction Rate, Lime 0

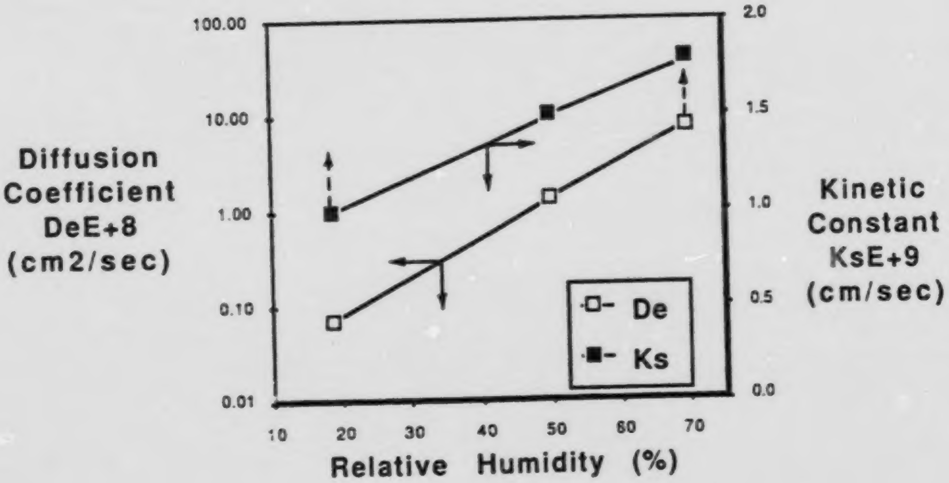

Figure 5-2: Effect of Relative Humidity on Model Parameters

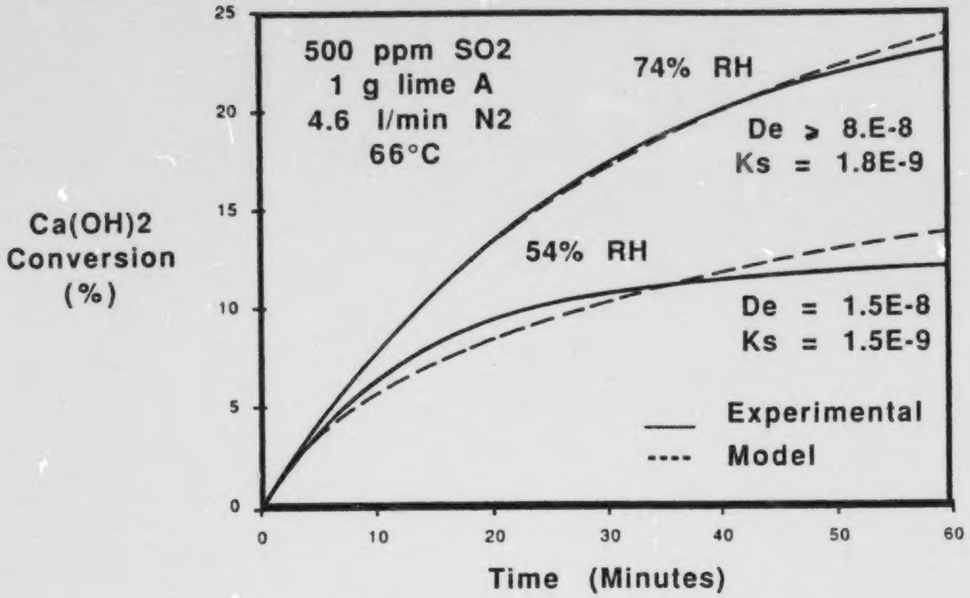

Figure 5-3: Effect of Relative Humidity on Reaction Rate, Lime A

The effect of SO_2 concentration on lime conversion at high relative humidity is illustrated in Figure 5-4. These experiments were run at 70% relative humidity, and 4 g lime 0 loaded in the reactor. At high relative humidity and high SO_2 levels, the reaction rate is kinetically controlled, so changing the SO_2 concentration from 1060 to 2150 ppm has little effect on the reaction rate. At lower relative humidity (50%) and high SO_2 concentrations, reaction kinetics are still controlling, so the reaction rate is practically independent of SO_2 concentration as illustrated by Figure 5-5. When the SO_2 concentration is reduced to 1100 ppm, mass transfer of the SO_2 through the product layer becomes important, and the reaction rate is dependent on the SO_2 level. As can be seen from Figures 5-4 and 5-5, the model is able to predict the SO_2 effect with reasonable accuracy.

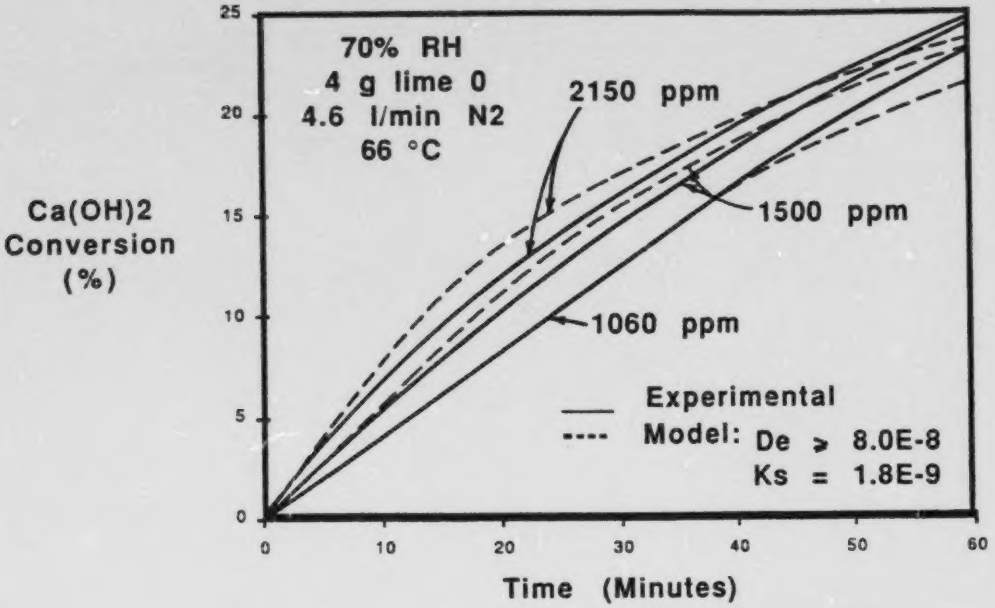

Figure 5-4: Effect of SO_2 Concentration, 70% Relative Humidity

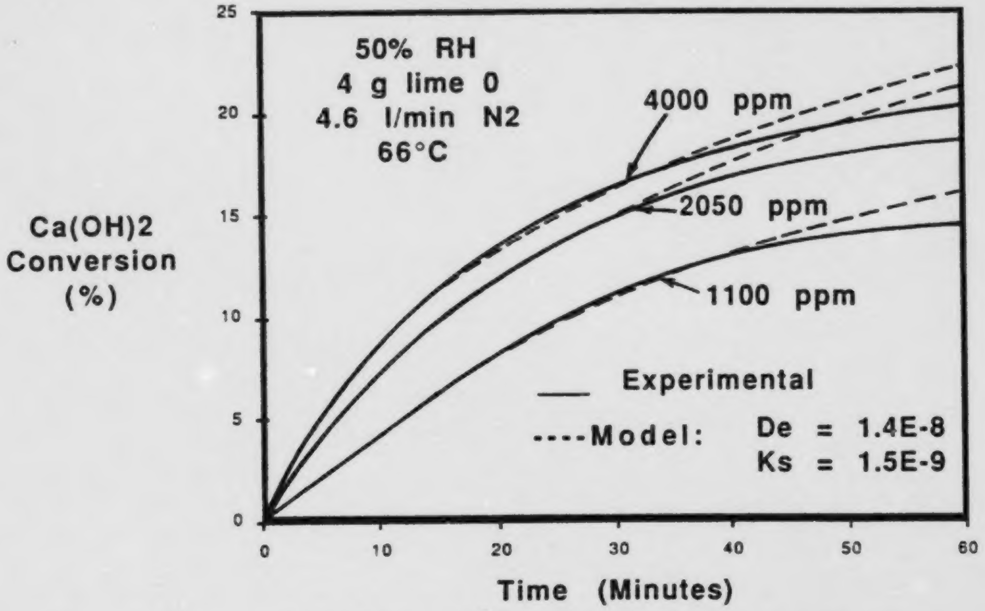

Figure 5-5: Effect of SO_2 Concentration, 50% Relative Humidity

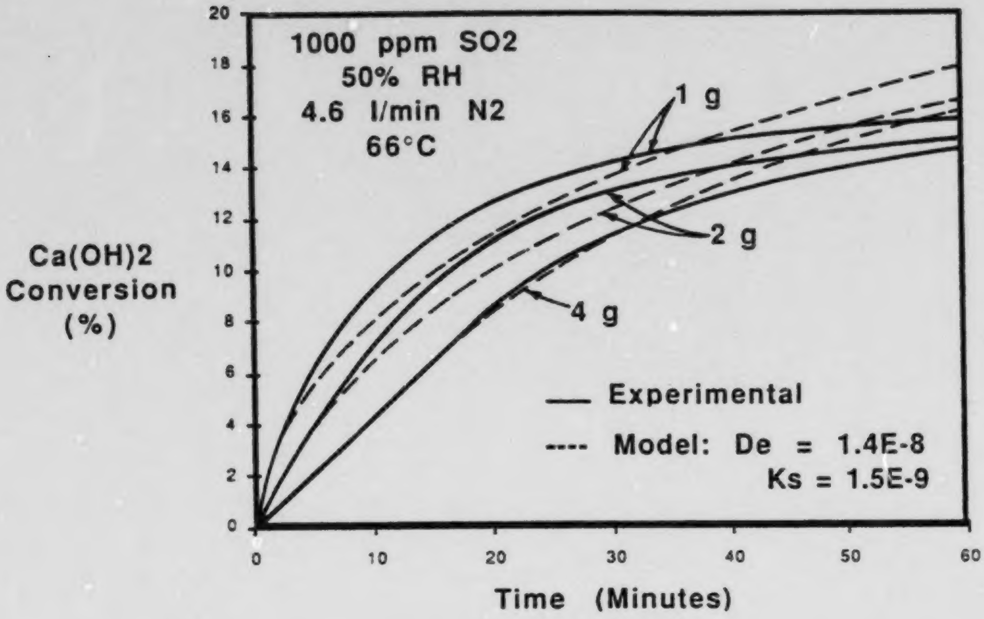

Figure 5-6: Effect of $Ca(OH)_2$ Load on Reaction Rate

The ability of the model to predict the effect of changing the lime 0 load in the reactor is illustrated by Figure 5-6 for experiments run at 50% relative humidity and 1000 ppm SO_2. During the first 20 or 30 minutes of reaction, the SO_2 removal in the reactor is high and the amount of lime present in the reactor affects the reaction rate because the lime at the end of the reactor "sees" different levels of SO_2. At later times, when the SO_2 removal is lower, the SO_2 level inside the reactor is practically the same regardless of how much lime is present, and the reaction rates are essentially the same in all three cases.

Figure 5-7 shows the effect of temperature on the kinetic constant k_s. At the conditions at which the experiments were performed,

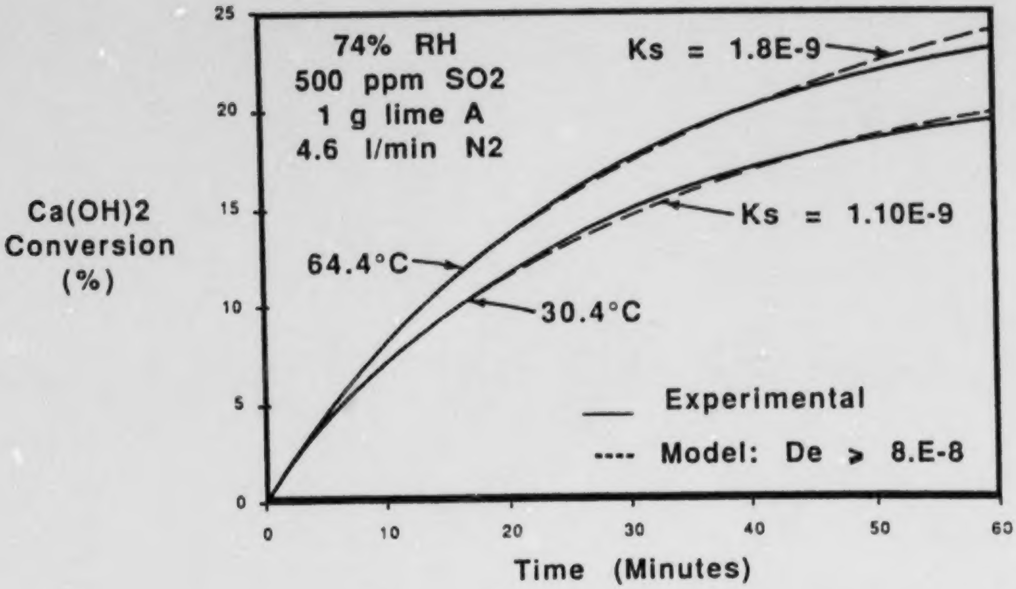

Figure 5-7: Effect of Temperature on Reaction Rate

the reaction rate is kinetically controlled, so k_s is the only important adjustable parameter in the model. By using the values of k_s given by the model, an apparent activation energy of 2.9 kcal/gmol can be estimated for $Ca(OH)_2$. This value of activation energy is somewhat lower than the value of 6 kcal/gmol reported by other sources for this reaction (Jorgensen et al., 1986).

Experiments using lime with a number of deliquescent salt additives can also be simulated using the modified shrinking core model. The results obtained for the modelling of experiments run at 74 and 54% relative humidity are presented in Tables 5-1 and 5-2. A reasonably good agreement was found between the predictions of the model and the experimental results. The standard deviation was calculated using the experimental and predicted values of percentage of $Ca(OH)_2$ converted at

Table 5-1: Modelling Experiments with Salt Additives at High Relative Humidity

74% RH, 64.4 °C, 1 g lime A, 4.6 l/min N_2, 500 ppm SO_2

Exp No	Additive (Mole%)	Conversion at 60 min (%)	Model Constants		Std. Dev.[a]	Max. Diff. (%)
			D_eE+8 (cm^2/sec)	k_sE+9 (cm/sec)		
77	None	23	$\geq$ 8.0	1.8	0.39	3.8
127	10% NaOH	39	$\geq$ 90.0	6.2	0.42	2.6
128	5% Na_2SO_3	30	$\geq$ 17.0	2.6	1.17	7.7
129	5% Na_2SO_4	28	$\geq$ 18.0	2.7	0.43	3.1
130	10% NaCl	39	$\geq$ 85.0	6.1	0.37	3.0
131	10% $NaNO_3$	42	$\geq$ 95.0	7.6	0.49	2.9
132	10% $NaNO_2$	40	$\geq$ 80.0	7.0	1.23	7.5
133	5% $Ca(NO_3)_2$	39	$\geq$ 85.0	7.0	0.40	2.7
98	5% $CaCl_2$	37	$\geq$ 73.0	5.4	0.29	2.6

a The standard deviation (Std. Dev.) was calculated using the experimental and predicted values of % lime converted every 5 minutes of reaction time.

Table 5-2: Modelling Experiments with Salt Additives at Moderate Relative Humidity

54% RH, 66°C, 1 g lime A, 4.6 l/min N_2, 500 ppm SO_2

Exp No	Additive (Mole%)	Conversion at 60 min (%)	Model Constants		Std. Dev.[a]	Max. Diff. (%)
			D_eE+8 (cm^2/sec)	k_sE+9 (cm/sec)		
136	None	12	1.5	≥ 1.50	1.08	14.9
140	10% NaCl	27	≥ 18	2.75	0.73	5.8
162	10% NaCl (O_2 free N_2)	27	≥ 18	2.75	0.82	5.3
150	3% NaCl	18	4.1	≥ 1.85	0.88	9.5
191	3% NaCl	16[b]	4.1	≥ 1.85	0.89	10.5
149	1% NaCl	16	2.8	≥ 1.60	0.78	9.1
134	10% $NaNO_3$	27	≥ 18	2.75	0.56	4.7
143	3% $NaNO_3$	18	4.1	≥ 1.85	1.30	13.6
135	5% $Ca(NO_3)_2$	12	1.6	≥ 1.50	1.39	19.4
139	10% NaOH	17	3.9	≥ 1.80	1.27	13.6
141	5% Na_2SO_3	16	3.3	≥ 1.70	1.50	17.0
142	5% $Na_2S_2O_3$	22	6.6	2.15	0.90	7.8
176	5% $BaCl_2$	19	4.5	≥ 1.90	0.70	6.8
177	5% $Co(NO_3)_2$	13	1.9	≥ 1.50	1.29	17.0
178	10% NaBr	42	≥ 90	7.70	0.48	3.2
179	10% KCl	35	≥ 80	4.80	0.54	2.5
180	10% LiCl	43	≥ 120	8.23	0.20	2.8
183	5% $CaCl_2$	17	2.9	≥ 1.60	1.38	15.7

a The standard deviation (Std. Dev.) was calculated using the experimental and predicted values of % lime converted every 5 minutes of reaction time.

b 330 ppm SO_2

intervals of 5 minutes of reaction time. The maximum percentage of difference between the experimental data and predicted values is also presented in the tables. For most cases the maximum differences are below 10% with a few exceptions where they are below 20%.

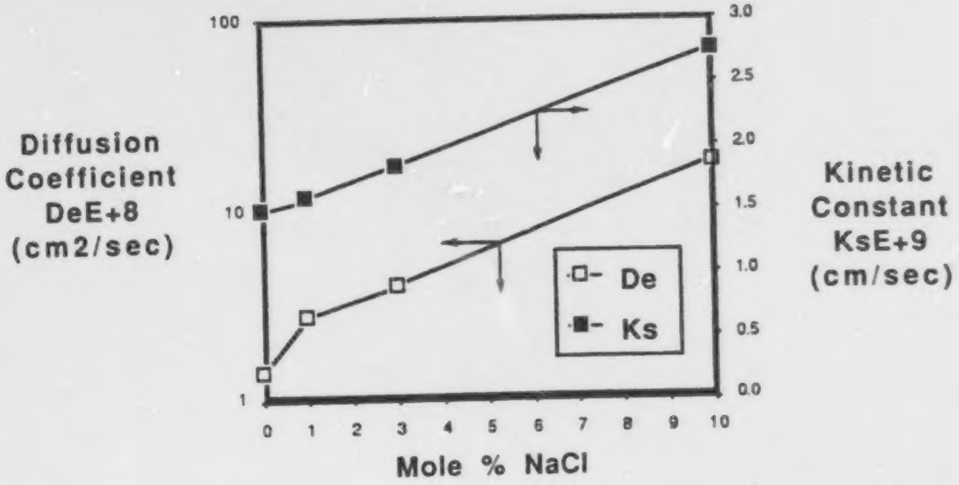

Figure 5-8: Effect of NaCl on the Model Parameters

The deliquescent salts affected the model parameters in a similar way to the relative humidity, the diffusion coefficient increasing more rapidly than the kinetic constant. D_e values ranging from 1.5E-8 to 120E-8 (cm^2/s) and k_s values from 1.5E-9 to 8.23E-9 ($cm^4/gmol\ s$) were used in the simulation of the salt experiments. Depending on the amount and type of salt added, chemical reaction or SO_2 diffusion can become the controlling step. Figure 5-8 illustrates the effect of NaCl on the model parameters. The kinetic constant increased linearly when NaCl concentration was increased from 0 to 10 mole%, while the diffusion coefficient increased exponentially after a sharp increase from 0 to 1 mole% NaCl.

5.6 Discussion

The only previous modelling effort for this reaction was the work of Klingspor et al. (1983, 1984). Their work used an integral shrinking core model with only reaction kinetics to explain the dependence of reaction rate on lime conversion. Their experimental data fit their integral shrinking core model only after a certain lime conversion had been reached. They attributed the sharp decrease in reaction rate observed at the beginning of the reaction to a decrease in surface roughness, but did not attempt to correlate this decrease in surface roughness with lime conversion. Their model neglects the effects of SO_2 diffusion through the product layer, and it also neglected the SO_2 concentration and lime concentration profiles in the fixed bed reactor. All of these factors will be more important at the start of the reaction, when the SO_2 removal is higher, thus it is not surprising that they were able to fit their model to the experimental data only at later times.

The simple model presented in this paper seems able to predict with reasonable accuracy the effect of all the process variables tested and explain the trends observed in the experimental data. The experimental data are estimated to have 11% experimental error (see Appendix E for details). Consequently the predictions of the model are well within the range of experimental error in most cases. The values of the diffusion coefficient used in the modelling (from 0.75E-9 to 1.20E-6 cm^2/sec) seem reasonable for diffusion of SO_2 in a solid, as they are of the same order of magnitude of the diffusivities of gases in polymers (Vieth and Amini, 1974, Brzozowski and Kumins, 1974, MacDonald and Haung, 1981, McBride et al., 1979, Minoura et al., 1981).

5.7 Conclusions

The modified shrinking core model presented in this subsection proved to be a very helpful in interpreting experimental data obtained in the fixed bed reactor. The most important process variable for the reaction is the relative humidity of the gas, which affects both the diffusion coefficient of SO_2 and the kinetic constant. In the range of relative humidity studied (19 to 74%), the kinetic constant increased linearly with relative humidity while the diffusion coefficient increased exponentially. This dependence of the parameters on the relative humidity leads to a change in controlling mechanism for SO_2 capture as the relative humidity decreases. At high relative humidity and/or high SO_2 concentration, the reaction rate is kinetically controlled and the reaction rate is independent of the SO_2 level. At low relative humidity and/or low SO_2 concentration the controlling step is the diffusion of the SO_2 through the $CaSO_3 \cdot 1/2H_2O$ product layer. At these conditions the overall reaction rate depends on the SO_2 concentration which is the driving force for diffusion.

The addition of deliquescent salts increases the diffusion coefficient and the kinetic constant in a similar way to the relative humidity, the diffusion coefficient increasing more rapidly than the rate constant. When increasing amounts of the same salt (NaCl) were added, k_s increased linearly and D_e increased nearly exponentially. Depending on the amount and type of salt additive, chemical reaction or gas diffusion can be the controlling mechanism.

The kinetic constant was a very weak function of temperature. The estimated activation energy was 2.9 kcal/gmol.

Section 6

Conclusions and Recommendations

6.1 Conclusions

- Relative humidity is the most important variable affecting the reaction of SO_2 and $Ca(OH)_2$. At 500 ppm SO_2, increasing the relative humidity from 54 to 74% increased $Ca(OH)_2$ conversion after 1 hour of reaction from 12 to 23%.

- The chemical reaction taking place at the surface of the unreacted $Ca(OH)_2$ solids has zero order kinetics in SO_2.

- At high relative humidity and/or high SO_2 concentration, the chemical reaction at the surface of the unreacted $Ca(OH)_2$ solids controls the overall reaction rate.

- At low relative humidity and/or low SO_2 levels, diffusion of SO_2 through the solid product layer becomes the controlling step.

- Deliquescent salt additives increase the reaction rate of SO_2 with $Ca(OH)_2$. The extent of the increase depends on the type and concentration of the salt and on the relative humidity.

- Deliquescence alone cannot explain the observed effect of the salt additives. Some of the salts show beneficial effect at relative humidities well below the values predicted by their deliquescent properties.

- A shrinking core model with an empirical correlation to account for the decrease in the surface roughness of the $Ca(OH)_2$ particles due to reaction can be used to simulate the observed reaction rates with reasonable accuracy.

- The parameters of the model are the SO_2 diffusion coefficient through the product layer (D_e) and the kinetic constant (k_s). Diffusion coefficient values ranging from 0.75E-9 to 1.20E-6 (cm^2/s) and kinetic constant values ranging from 1.0 to 8.23E-9 (cm/s) can be used to simulate all the experimental results.

- Relative humidity and the presence of deliquescent salts affect both the kinetic constant and the SO_2 diffusion coefficient.

- The diffusion coefficient increases exponentially with relative humidity and amount of salt added, while the kinetic constant increases linearly.

- The reaction rate has a weak temperature dependence. The estimated activation energy of the SO_2-$Ca(OH)_2$ reaction is 2.9 kcal/gmol.

- The product of the SO_2-$Ca(OH)_2$ reaction is mainly

$CaSO_3 \cdot 1/2H_2O$. The oxygen present as impurity in the nitrogen oxidizes some of the sulfite to sulfate. X-ray and differential scanning calorimeter results indicate that the sulfate produced is present in solid solution with the $CaSO_3 \cdot 1/2H_2O$.

- The presence of small amounts of oxygen (< than 0.5%) as impurity of the nitrogen does not affect the reaction rate of $Ca(OH)_2$ with SO_2.
- Organic acid additives, such as adipic and glycolic acid, decrease the $Ca(OH)_2$ reactivity towards SO_2.
- Organic deliquescents such as monoethanolamine, ethylene glycol, and tri-ethylene glycol do not affect $Ca(OH)_2$ reactivity towards SO_2.

6.2 Recommendations

- Additional experiments should be done using real flue gas. The present research was performed using as the gas phase a mixture of SO_2 and N_2. Gases like CO_2 , NO_x, and O_2 are important components of flue gas, and their effect on the reaction rate of SO_2 with $Ca(OH)_2$ should be investigated. Some oxygen was present in our gas mixture as an impurity of the nitrogen and showed no effect on the SO_2 absorption, but higher O_2 levels may affect the reaction.
- Additional sources of $Ca(OH)_2$ should be tested. Most of the

experiments in this research were made using powder reagent $Ca(OH)_2$ as the solid reactant. Only a couple of experiments were made using pressure hydrated dolomitic lime. It would also be interesting to investigate the behavior of industrial samples of spray dryer solids.

- Additional research should be done on the effect of salt additives. It would be useful to further study the correlation between relative humidity and water retention of the solids in the presence and absence of additives.

Appendix A.

Solids Characterization

A.1 Coulter Counter Particle Size Distribution

The particle size distribution of the $Ca(OH)_2$ powder reagent used in the experiments was determined using a Coulter Counter, model T_{AII}. The Coulter Counter determines the number and size of particles suspended in a conductive liquid by forcing the suspension to flow through a small aperture. Electrodes are immersed in the conductive fluid on opposite sides of the aperture. As a particle passes through the aperture, it changes the resistance between the electrodes. This produces a current pulse of short duration having a magnitude proportional to the particle volume. The series of pulses is electronically classified by size and counted.

The Coulter Counter method has been extensively used in limestone dissolution studies (Chan, 1981, Chan and Rochelle, 1982, Toprac, 1981) and $CaSO_3$ crystallization studies (Tseng, 1984). It has proved to be efficient, reliable, and reproducible in measuring particle size distribution in micrometer size ranges. The particle size distributions of the two batches of $Ca(OH)_2$ used in the experiments, namely lime 0 and lime A, are presented in Table A-1. The median of the particle size distribution (particle diameter larger than 50% of the distribution and smaller than the other 50%) is 7.4 μm for lime 0 and 5.6 μm for lime A. The electrolyte used was 4 wt% $CaCl_2$, saturated with $Ca(OH)_2$ (to minimize lime dissolution). A nonionic dispersant agent (Coulter Type IA) was also added to the electrolyte solution to prevent agglomeration of the lime particles.

The particle size distribution of lime 0 was measured using a single 140 μm aperture tube, but a multi-aperture analysis was needed to cover the complete size range of lime A. The particle size distribution

Table A-1: $Ca(OH)_2$ Particle Size Distributions

Effective Diameter (μm)	Volume% between the two diameters	
	Lime 0	Lime A
1.00	-	1.0
1.26	-	2.1
1.59	-	2.9
2.00	1.4	4.5
2.52	3.0	6.3
3.17	1.6	7.6
4.00	3.4	8.8
5.04	7.8	10.8
6.35	16.7	13.5
8.00	22.7	13.9
10.08	18.9	12.2
12.7	8.5	7.8
16.0	4.9	4.2
20.2	3.1	1.8
25.4	2.2	1.2
32.0	3.3	0.5
40.3	2.5	0.9
50.8	0	0
Median of Distribution	7.4 μm	5.6 μm

was measured with the 140 μm aperture tube. Part of the sample was then "scalped" by wet sieving through a 20 μm sieve, and the size distribution of this subsieved suspension measured with a 50 μm aperture tube. The overlap between the size distributions measured with each tube was used to normalize the distribution using the volume percent method described in the Coulter Counter Operator's Manual (Coulter, 1980).

$Ca(OH)_2$ powder reagent was used in most of the experiments, but three samples of pressure hydrated dolomitic lime (probably Corson Miracle Lime), provided by John Chang of Acurex, were also tested for their reactivity towards SO_2. The particle size distributions of these samples of dolomitic lime could not be determined using the Coulter Counter method. As will be discussed in the Scanning Electron Microscope section, these dolomitic limes consist mostly of agglomerates of very small particles (of the order of 1 μm or below) that are below the size range that can be measured using the Coulter Counter. The smallest tube available for the Coulter Counter has an aperture of 50 μm, and it can measure particles greater than 1 μm.

A.2 BET Surface Area Measurement

The standard method for measuring surface area of porous solids is the Brunauer-Emmett-Teller (BET) method (Brunauer et al., 1938). The BET method is based on the physical adsorption of a gas, normally nitrogen at its normal boiling point (- 195.8 K), on the surface of the solid. The method involves measuring the amount of nitrogen adsorbed (v) over a range of nitrogen pressures (p) below 1 atm.

The BET equation can be written as:

$$\frac{p}{v(p_o - p)} = \frac{1}{v_m C} + \frac{(C - 1) p}{C v_m p_o} \qquad (A.1)$$

p_o is the saturation pressure, C is a constant for the particular temperature and gas-solid system, and v_m is the volume of gas required to form a complete unimolecular adsorbed layer. A plot of $p/[v(p_o - p)]$ versus p/p_o will give a straight line. Extrapolating this straight line to $p/p_o = 0$ gives the intercept I. The intercept together with the slope S of the line gives v_m as:

$$v_m = \frac{1}{I + S} \qquad (A.2)$$

Once v_m is known, the surface area of the solid can be calculated as:

$$S_g = \frac{v_m N_o}{V} \alpha \qquad (A.3)$$

Where:

N_o = Avogadro's Number

V = molar volume of the gas at the conditions of v_m

α = surface area of one adsorbed molecule
= 16.2 A^{o2} for nitrogen (Mc Clellan and Harnsberger, 1967)

The BET approach is essentially an extension of the Langmuir approach to multimolecular layers. It assumes that the rate of condensation of the gas on the bare surface of the solid is equal to the rate of evaporation from the first layer, and that the heat of adsorption in layers other than the first is equal to the heat of liquefaction of the adsorbate material [ie, Van der Waals forces of the adsorbent are transmitted only to the first layer (Brunauer et al., 1938, Hill, 1977)].

The surface area given by the BET method may not correspond exactly to the surface area of the solid, but the procedure is standardized and the results are reproducible (Smith, 1981, Rase, 1977).

The BET surface area of $Ca(OH)_2$ and $Ca(OH)_2$ with salt additives was measured in the laboratory using an Accusorb Model 2100E Physical Adsorption Analyzer. The adsorbent used was nitrogen at its normal boiling point. The results obtained are listed in Table A-2. The surface areas of limes 0 and A were 8.2 and 9.4 m^2/g respectively. Repeated measurements of surface area agreed within 1.5%. The surface area of samples of lime A with different salt additives was found to be in the range 7.0 to 9.6 m^2/g. In most cases a small decrease of the surface area occurred with the addition of the deliquescent salt. The surface area of pure lime A after being slurried with distilled water and dried in the same way as when salt additives were added showed a slight decrease of surface area to 8.8 m^2/g. Measurement of surface area of reacted $Ca(OH)_2$ solids showed a decrease in surface area with conversion. Pure reacted $Ca(OH)_2$ (25% conversion) has a surface area of 6.5 m^2/g, while reacted $Ca(OH)_2$ with NaCl as additive (46% conversion) has a surface area of 5.9 m^2/g.

Finally, the surface area of three samples of pressure hydrated dolomitic lime were measured. The samples correspond to dolomitic lime collected after the lime leaves the hydrator (hydrator lime), dolomitic lime collected after the lime leaves the ball mill (ball mill lime), and a sample of ball mill lime sieved through a 125 μm sieve (sieved ball mill lime). The surface area of these dolomitic lime samples ranged from 18.4 to 21.1 m^2/g.

Table A-2: BET Surface Area of the Solids

Sample	BET Surface Area (m^2/g)
Reagent Grade Calcium Hydroxide	
Lime 0 (non-slurried)	8.2
Lime A (non-slurried)	9.4
Lime A (slurried)	8.8
Lime A + 5 mole% $CaCl_2 \cdot 2H_2O$	7.7
Lime A + 10 mole% NaCl	8.1
Lime A + 10 mole% $NaNO_3$	7.0
Lime A + 10 mole% KCl	9.3
Lime A + 10 mole% NaBr	8.6
Lime A + 10 mole% LiCl	9.6
Lime A + 5 mole% $Co(NO_3)_2$	7.2
Lime A + 5 mole% $BaCl_2 \cdot 2H_2O$	7.2
Reacted Lime A (25% conversion)	6.5
Reacted Lime A + 10 mole% NaCl (46% conversion)	5.9
Pressure-Hydrated Dolomitic Lime	
after hydrator	20.1
after ball mill	21.1
sieved material after ball mill (< 125 μm)	18.4

A.3 Scanning Electron Microscope (SEM)

The Scanning Electron Microscope (SEM) is one of the most versatile instruments available for the examination and analysis of the microestructural characteristics of solids (Goldstein et al., 1975). It is a surface examination tool in which the surface to be examined is irradiated with a finely focused electron beam. When the electron beam impinges on a specimen surface, different types of signals are produced: secondary electrons, backscattered electrons, characteristic x-rays, Auger electrons, and photons of various energies. In the SEM the primary signal of interest is the variation in secondary electron emissions that takes place as the electron beam is swept in a raster across the surface of a specimen due to differences in surface topography. The secondary electron yield is confined near the beam impact area, which permits images to be obtained at relatively high resolutions. The three dimensional appearance of the images is due to the large depth of focus of the SEM.

A SEM JEOL, model JSM-3C, was used to examine the $Ca(OH)_2$ and hydrated lime samples along with reaction products. The powdery samples were sprinkled over a thin film of graphite glue previously spread on a SEM stage. After the glue dried, a thin layer of conductive element (Al or Au-Pd alloy) was applied to the sample by vacuum evaporation at high temperature. The conductive applied layer must be as thin as possible so that it does not obscure fine details of the sample under observation, but it must be continuous in order to provide a conductive path to ground.

The SEM micrographs of the two batches of $Ca(OH)_2$ (lime 0 and lime A) used in most of the experiments are shown in Figures A-1 to A-4. Figures A-1 and A-3 correspond to 400 magnification, and Figures A-2 and A-4 to 4000 magnification. The figures confirm that the $Ca(OH)_2$ particles are in the micrometer size range. The particles are of irregular shape and have a lot of surface irregularities and roughness. No pores were visible.

SEM micrographs of the $Ca(OH)_2$ with different salt additives showed no significant difference in size or shape from the pure $Ca(OH)_2$ particles. This is illustrated by Figure A-5 that shows the SEM micrograph of a sample of $Ca(OH)_2$ with 10 mole% NaCl at 10000 magnification.

Observation of reacted samples of $Ca(OH)_2$ showed that the surface of the particles is more globular. This is illustrated by Figure A-6 which shows a micrograph of reacted $Ca(OH)_2$ with 10 mole% NaCl with a conversion of 46% (determined by chemical analysis).

Finally, Figures A-7 to A-10 show SEM micrographs of pressure hydrated dolomitic lime at 400 and 4000 magnification. These dolomitic limes have some very large particles of 40 to over 100 μm diameter, but most of the particles are very small, below 2 μm, and tend to form agglomerates.

A.4 Energy Dispersive Spectroscopy (EDS)

As was mentioned in the section dealing with the SEM, when a electron beam impinges on the surface of a sample, characteristic x-rays are produced together with other types of signals. Energy dispersive spectroscopy uses a x-ray detector that separates the x-ray spectrum by energy rather than by wavelength. This energy dispersive detector is

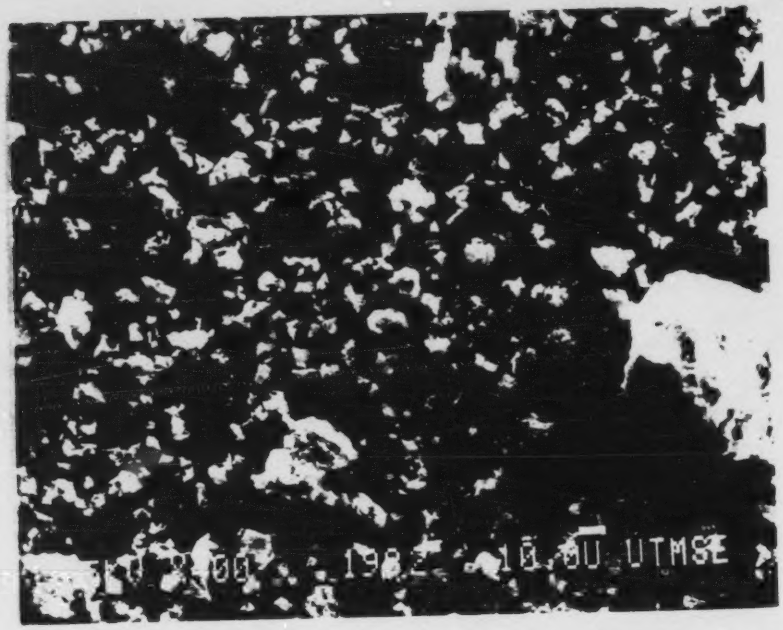
KV X400 1982 10.0U UTMSE

Figure A-1: SEM Micrograph Lime 0, 400 Magnification

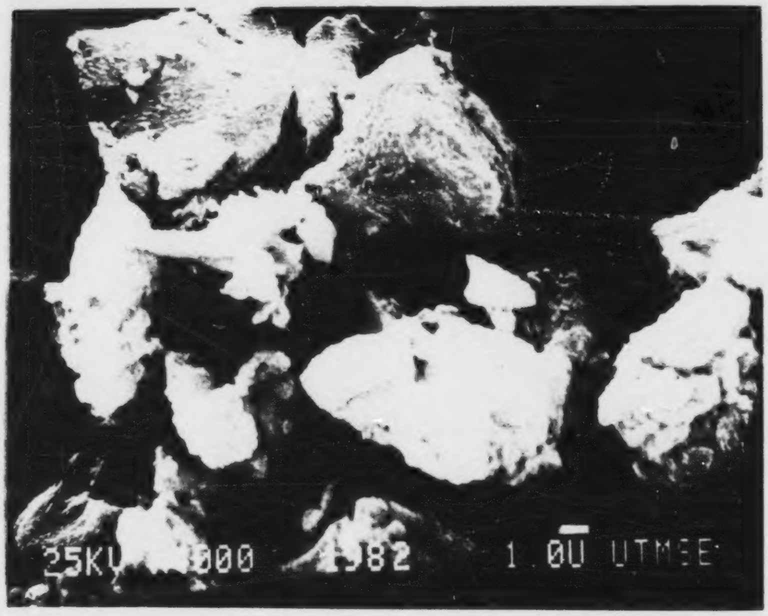
25KV 1982 1.0U UTMSE

Figure A-2: SEM Micrograph Lime 0, 4000 Magnification

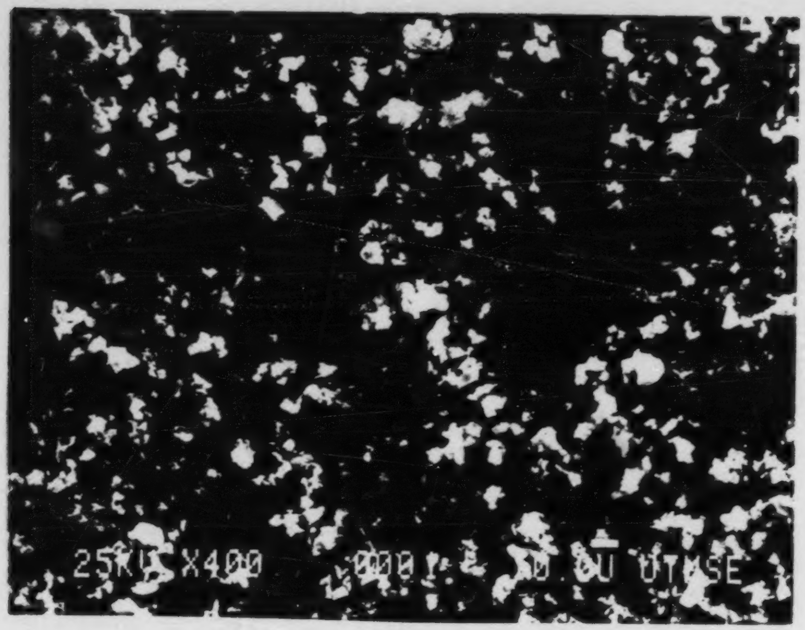
25KV X400 0001 10.0U UTMSE

Figure A-3: SEM Micrograph Lime A, 400 Magnification

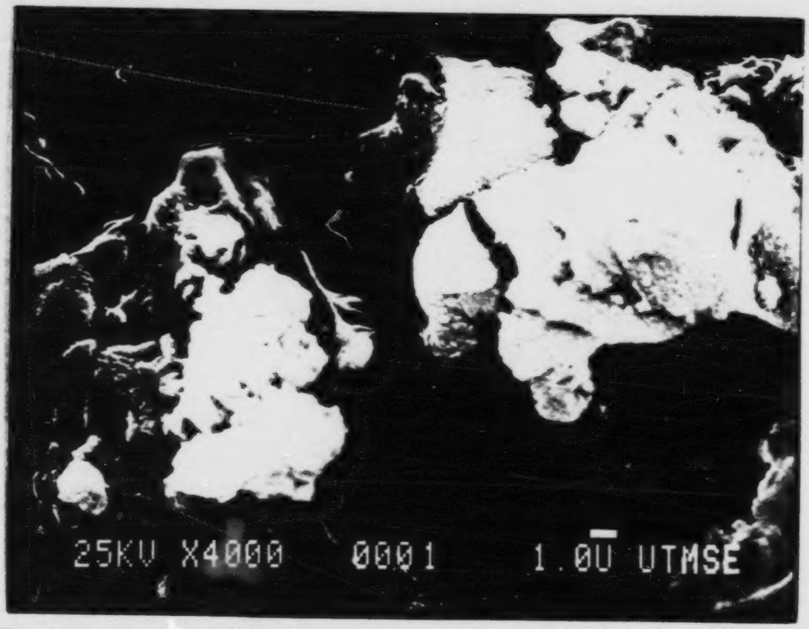
25KV X4000 0001 1.0U UTMSE

Figure A-4: SEM Micrograph Lime A, 4000 Magnification

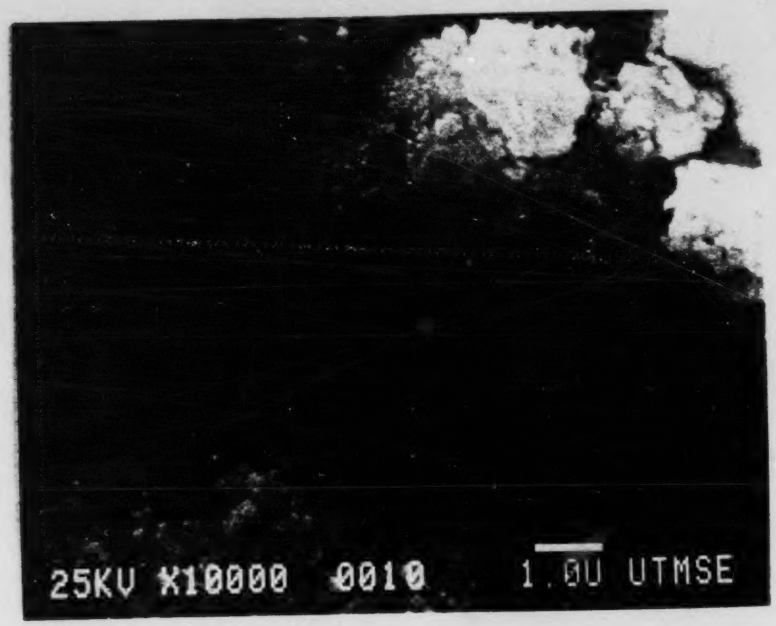
25KV X10000 0010 1.00U UTMSE

Figure A-5: SEM Micrograph $Ca(OH)_2$ + 10 mole% NaCl, 10000 Magnification

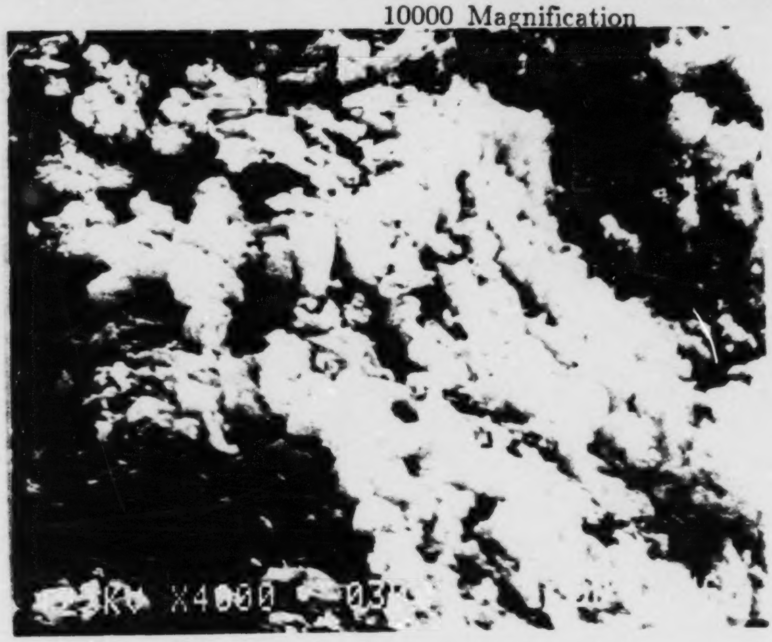

Figure A-6: SEM Micrograph Reacted Lime A + 10 mole% NaCl, 4000 Magnification, 74% RH, 500 ppm SO_2, 64.4°C, 2 hr Reaction Time, Conversion 46%

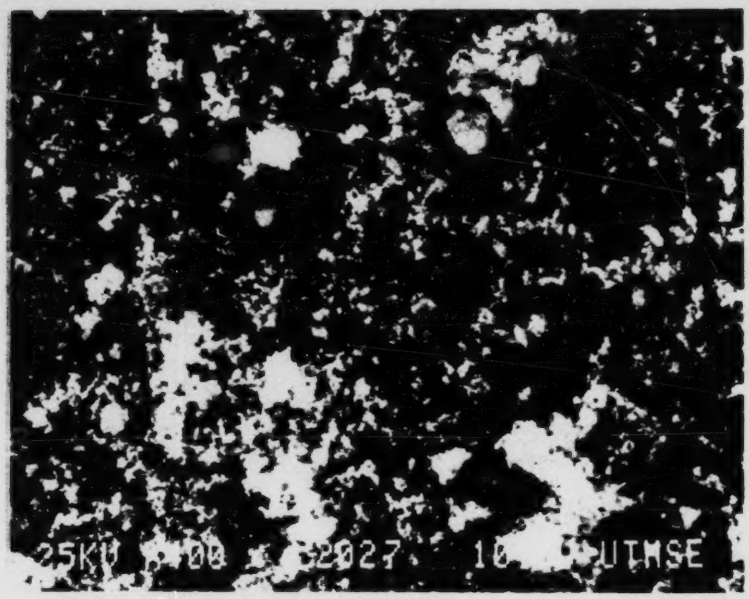
25KV
2027
UTMSE

Figure A-7: SEM Micrograph Ball Mill Hydrated Dolomitic Lime, 400 Magnification

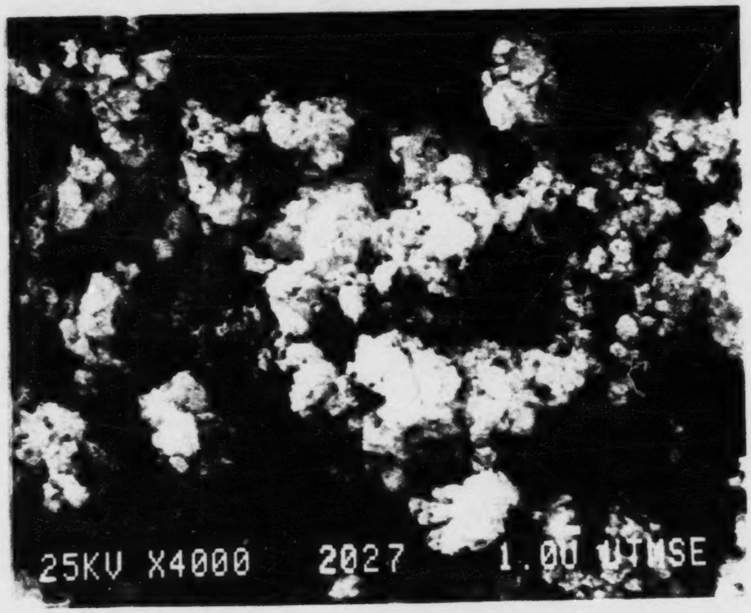
25KV X4000 2027 1.00 UTMSE

Figure A-8: SEM Micrograph Ball Mill Hydrated Dolomitic Lime, 4000 Magnification

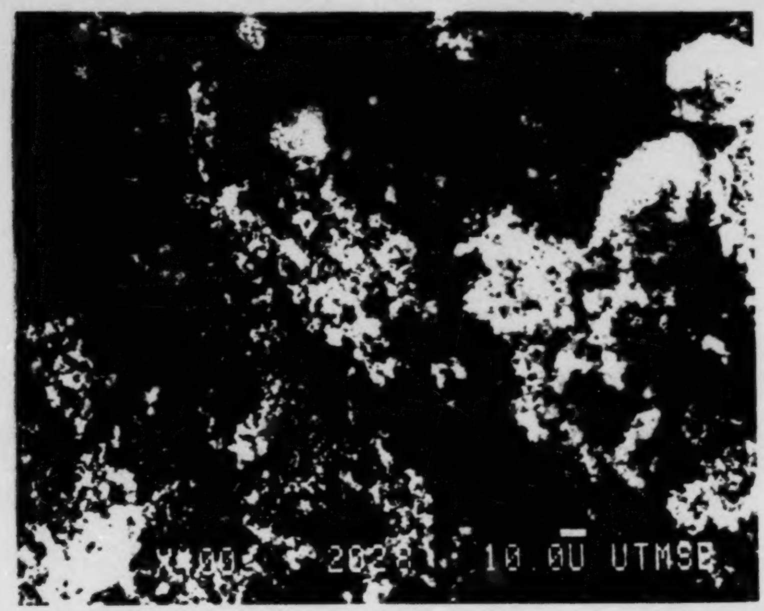
X400 2028 10.0U UTMSB

Figure A-9: SEM Micrograph Hydrator Hydrated Dolomitic Lime, 400 Magnification

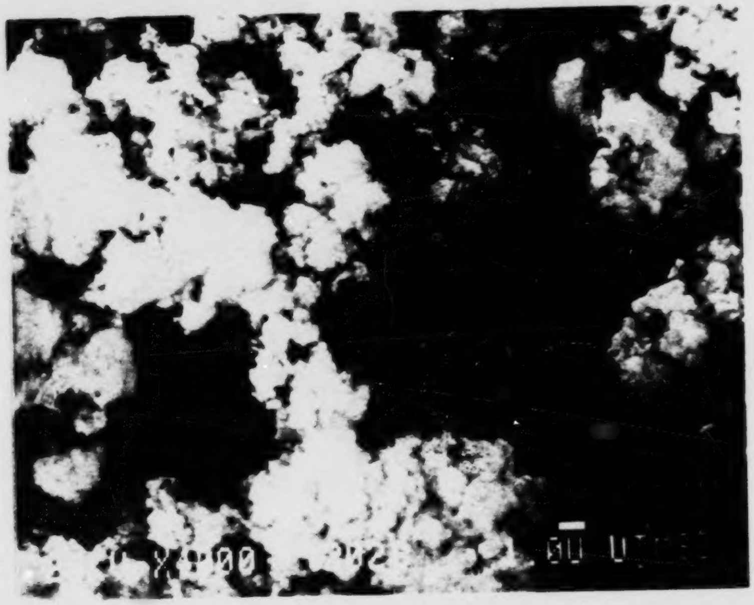

Figure A-10: SEM Micrograph Hydrator Hydrated Dolomitic Lime, 4000 Magnification incorporated within the SEM and possesses enough sensitivity to provide x-ray spectral data at the low SEM beam current. Quantitative analysis using EDS involves accurately measuring the intensity of spectral lines corresponding to preselected elements for both sample and standards under identical operating conditions. The intensity ratio (relative x-ray intensity ratio between the elements of interest in the sample and the same elements in the standards) is calculated, and from the intensity ratio, the weight fractions of the elements of interest in the sample are estimated. A limitation of the EDS is that it can not identify elements of molecular weight below sodium (molecular weigth 22.9898).

EDS was used to estimate the elemental analysis of reacted and unreacted samples of $Ca(OH)_2$ with salt additives. An example of this type of analysis is given in Table A-3 which shows the weight percent of Cl and S in a reacted sample of lime with NaCl as additive. The conversion of this sample (given by chemical analysis) was 30%. The analysis was done for a great number of particles (bulk) and for individual particles. From the results presented in Table A-3, it can be concluded that the additive (in this case NaCl) is more or less uniformly distributed on the lime particles. The lime conversion was very uniform in the particles analyzed. For comparison purposes, the concentrations of Cl and S obtained by chemical analysis are also presented in the table.

EDS was also used to analyze a sample of pressure hydrated dolomitic lime. The analysis showed the dolomitic lime to contain 40.7 mole% Mg and 59.3 mole% Ca. Oxygen and hydrogen can not be analyzed.

Table A-3: Elemental Analysis using EDS

Sample: Converted Lime A + 10 mole% NaCl

54% RH, 66°C, 500 ppm SO_2, 1 hr Reaction Time, 30% Conversion

	Wt% Cl	Wt% S
Bulk	4	17
Individual Particle	9	17
" "	4	14
" "	5	18
" "	3	17
" "	5	17
From Chemical Analysis	7	18

A.5 Differential Scanning Calorimetry (DSC)

The scanning differential calorimeter determines the enthalpy change of a sample as a function of temperature. The enthalpy change is determined by measuring the differential heat flow required to maintain the sample and an inert reference at the same temperature (Mortimer, 1984). The temperature is programmed to increase linearly at a predetermined rate. Phase changes will be marked by rapid changes in enthalpy with time or, in other words rapid changes in the constant pressure heat capacity.

Peaks should appear in the dH/dt versus temperature curve in the temperature ranges of 120 - 140°C for gypsum, 150 - 170°C for calcium sulfate hemihydrate, and 350 - 430°C for calcium sulfite hemihydrate (Jones et al., 1976, Tseng, 1984). These heat capacity changes correspond to the loss of hydrated water in the solids.

A Perkin-Elmer Differential Scanning Calorimeter (Model DSC-2) was used to characterize reacted samples of $Ca(OH)_2$ with and without salt additives. Some of these samples were obtained using nitrogen of 99.5% purity as the carrier for SO_2 and others using oxygen free nitrogen (99.998% purity) as the carrier. Figure A-11 shows a typical DSC curve of a sample of reacted $Ca(OH)_2$ with 10 mole% NaCl as additive. This sample was obtained by using oxygen of 99.5% purity. The change in heat capacity occurs at 652 K (378.9°C), which corresponds to the endothermic dehydration of $(CaSO_3)_x(CaSO_4)_{1-x} \cdot 1/2H_2O$ solid solutions. No peak was found in the 120-140°C range which indicates that no gypsum phase is present. Also no peak was detected in the 150-170°C range which means that no $CaSO_4 \cdot 1/2H_2O$ phase is present. Any sulfate produced in the reactor will then be present in solid solution with $CaSO_3 \cdot 1/2H_2O$, and not as separate phases of $CaSO_4 \cdot 2H_2O$ or $CaSO_4 \cdot 1/2H_2O$.

The DSC curves of reacted $Ca(OH)_2$ with and without NaCl additive for oxygen free nitrogen (99.998% purity) are shown in Figures A-12 and A-13 respectively. Again, only one peak is present in the DSC curves, in the 638 to 652 K range, which corresponds to the endothermic dehydration of $(CaSO_3)_x(CaSO_4)_{1-x} \cdot 1/2H_2O$.

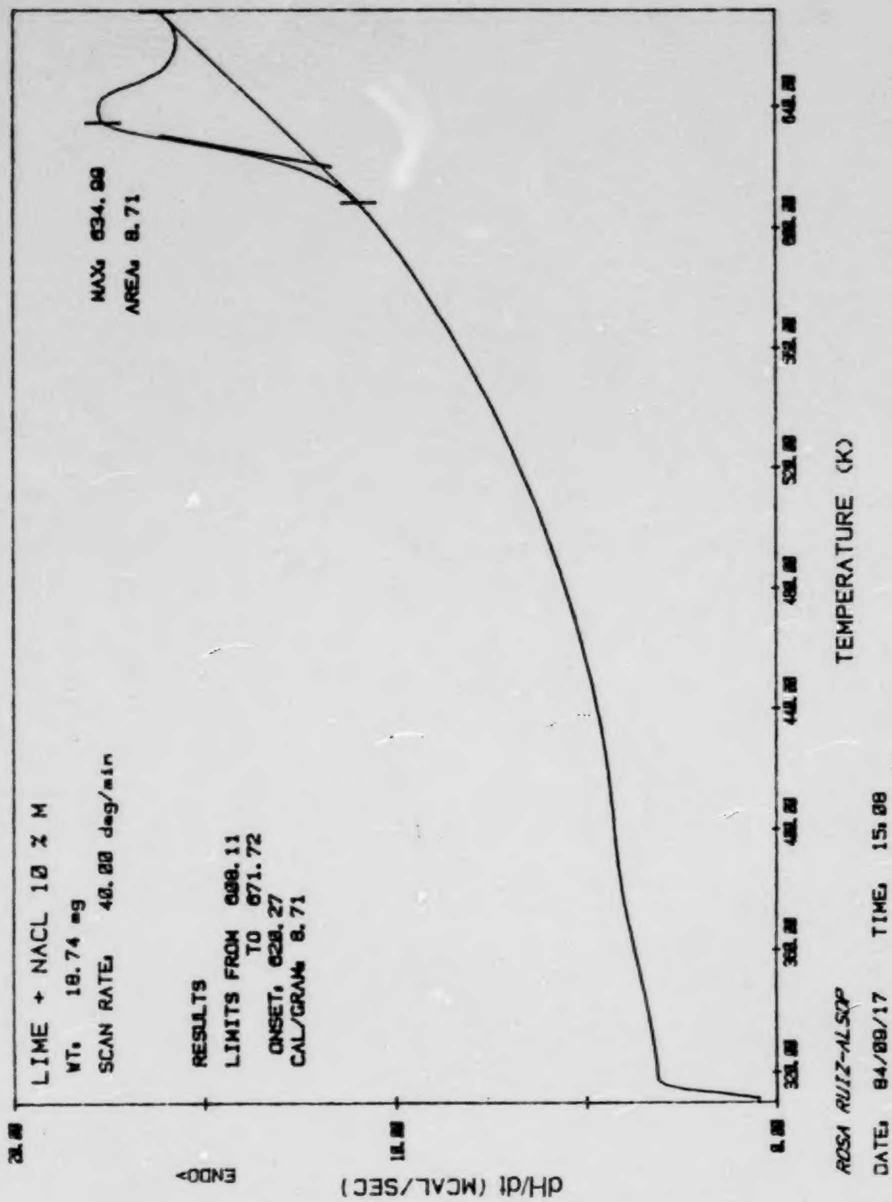

Figure A-11: DSC Curve for Reacted $Ca(OH)_2$ + 10 mole% NaCl, N_2 of 99.5% purity, 54% RH, 66°C, 500 ppm SO_2, 1 hr Reaction Time, Conversion 30%

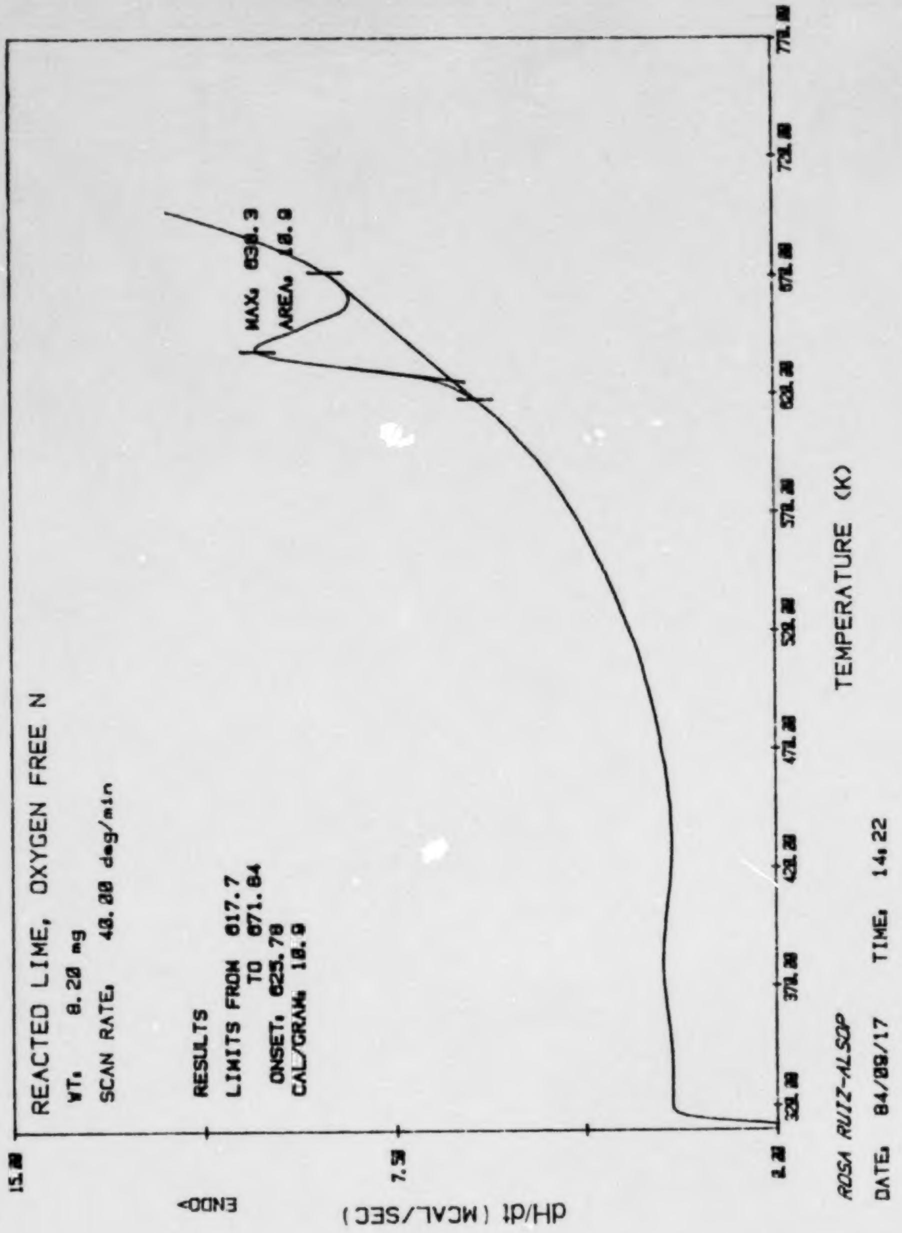

Figure A-12: DSC Curve for Reacted $Ca(OH)_2$, O_2 Free N_2, 74% RH, 64.4°C, 500 ppm SO_2, 1 hr Reaction Time, Conversion 24.5%

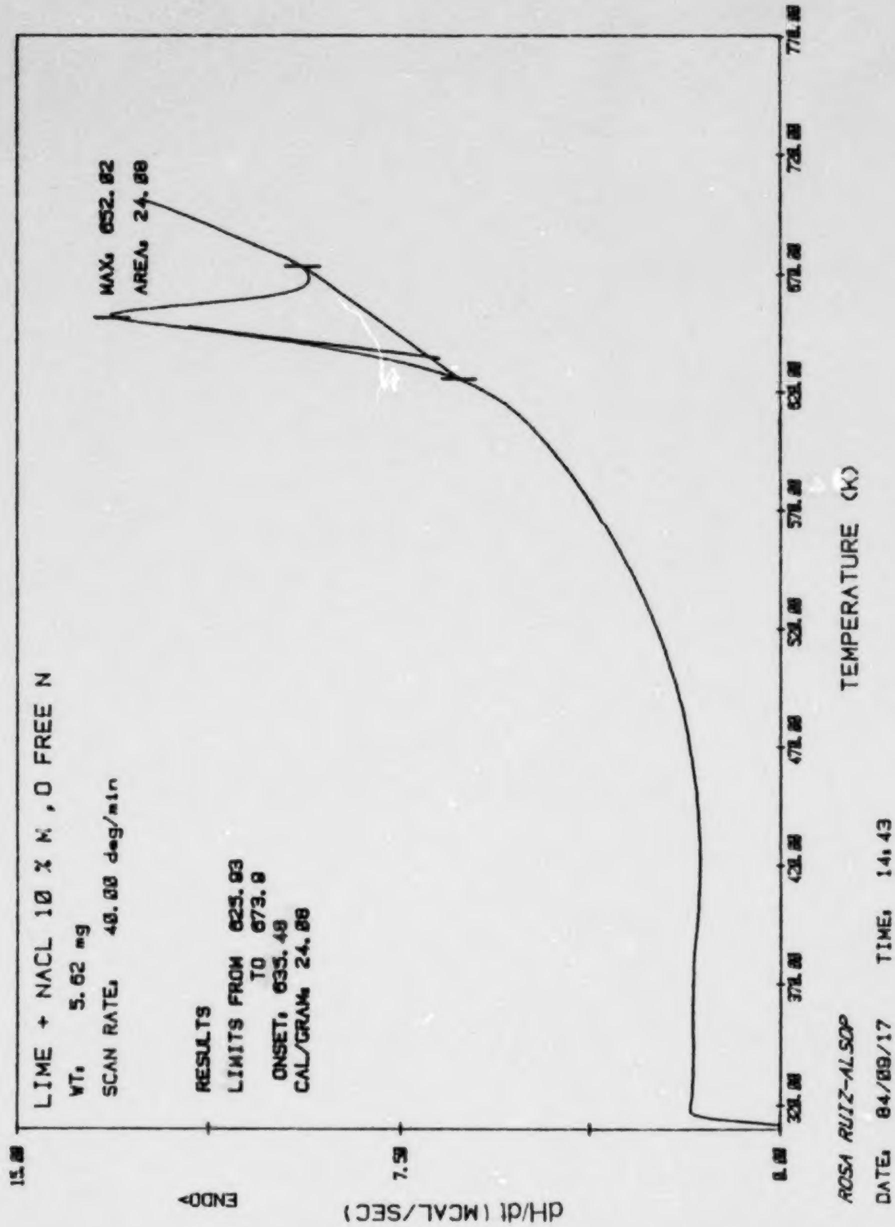

Figure A-13: DSC Curve for Reacted $Ca(OH)_2$ + 10 mole% NaCl, O_2 Free N_2, 74% RH, 64.4°C, 500 ppm SO_2, 2 hr Reaction Time, Conversion 46%

A.6 X-Ray Diffraction

X-ray powder diffraction was used to characterize the reactants and products. The x-ray diffraction method is based on the scattering of x-rays by the crystals, the scattering being caused by the electron atmosphere of the atom. When certain geometrical conditions as expressed by the Bragg law are satisfied, a diffraction pattern is produced by the scattering.

Bragg's law states:

$$\lambda = 2 \, d \sin \theta \tag{A.4}$$

Where:

λ = wavelength of x-rays

d = lattice spacing

θ = diffraction angle

The diffraction pattern produced can be used to identify molecules and to determine their atomic and molecular structure (Olsen, 1975).

The x-ray diffraction pattern of $Ca(OH)_2$ and $Ca(OH)_2$ with different salt additives are shown in Figures A-14 to A-21. The x-ray diffraction pattern gives intensity versus 2θ . $Ca(OH)_2$ has eight major peaks in its x-ray diffraction pattern (JCPDS, 1984). The d-spacing of these major peaks is 4.90, 3.11, 2.63, 1.93, 1.80, 1.69, 1.48, and 1.45 A°, which correspond to diffraction angles of 9.03, 14.33, 16.85, 23.55, 25.3, 27.11, 31.27, and 32.11 degrees respectively. These peaks appear in the $Ca(OH)_2$ diffraction pattern shown in Figure A-14.

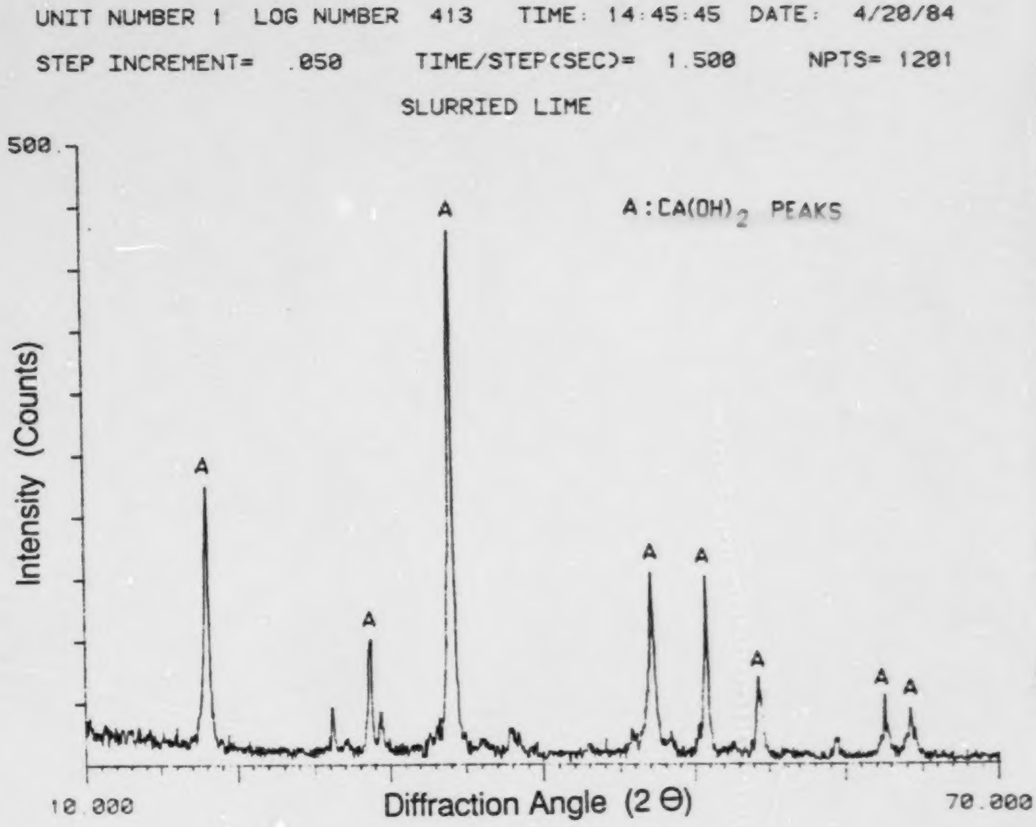

Figure A-14: X-ray Diffraction Pattern: Slurried $Ca(OH)_2$

Figure A-15 shows the x-ray diffraction pattern of $Ca(OH)_2$ with 20 mole% $CaCl_2 \cdot 2H_2O$ as additive. Neither anhydrous $CaCl_2$ nor any of the calcium chloride hydrates was detected, but the x-ray diffraction pattern shows the presence of the mixed salt $CaCl_2 \cdot Ca(OH)_2 \cdot H_2O$. The five major peaks of $CaCl_2 \cdot Ca(OH)_2 \cdot H_2O$ (JCPDS, 1984) are indicated in Figure A-15.

Figures A-16 to A-21 show the x-ray diffraction patterns of $Ca(OH)_2$ with NaCl, $NaNO_3$, LiCl, KCl, $BaCl_2 \cdot 2H_2O$, and NaBr as additives. The peaks corresponding to the solid phase detected in each sample are labeled in the figures. Table A-4 is a summary of the x-ray diffraction work showing the additive added to the lime in its original form and the solid phase detected by x-ray diffraction analysis.

In most cases the additive remains unchanged after being added to the lime by the slurrying and drying process mentioned in Subsection 3.1 and precipitates in a separate phase. In some cases the hydration state of the additive changes, but in most cases it remains unaltered. The exception is $CaCl_2$ where the mixed salt $CaCl_2 \cdot Ca(OH)_2 \cdot H_2O$ is formed. This finding agrees with data reported in the literature for the equilibrium of the $Ca(OH)_2 \cdot CaCl_2 \cdot H_2O$ system (Seidell and Linke, 1958). In the case of $Ca(NO_3)_2$ additive, the formation of the solid phase $Ca_2N_2O_7 \cdot 2H_2O$ has been reported in the literature (Seidell and Linke, 1958). The presence of this solid phase could not be confirmed by x-ray diffraction analysis as the diffraction pattern of $Ca_2N_2O_7 \cdot 2H_2O$ was not available.

When reacted samples of $Ca(OH)_2$ with and without NaCl were analyzed using x-ray diffraction, the presence of calcium sulfite

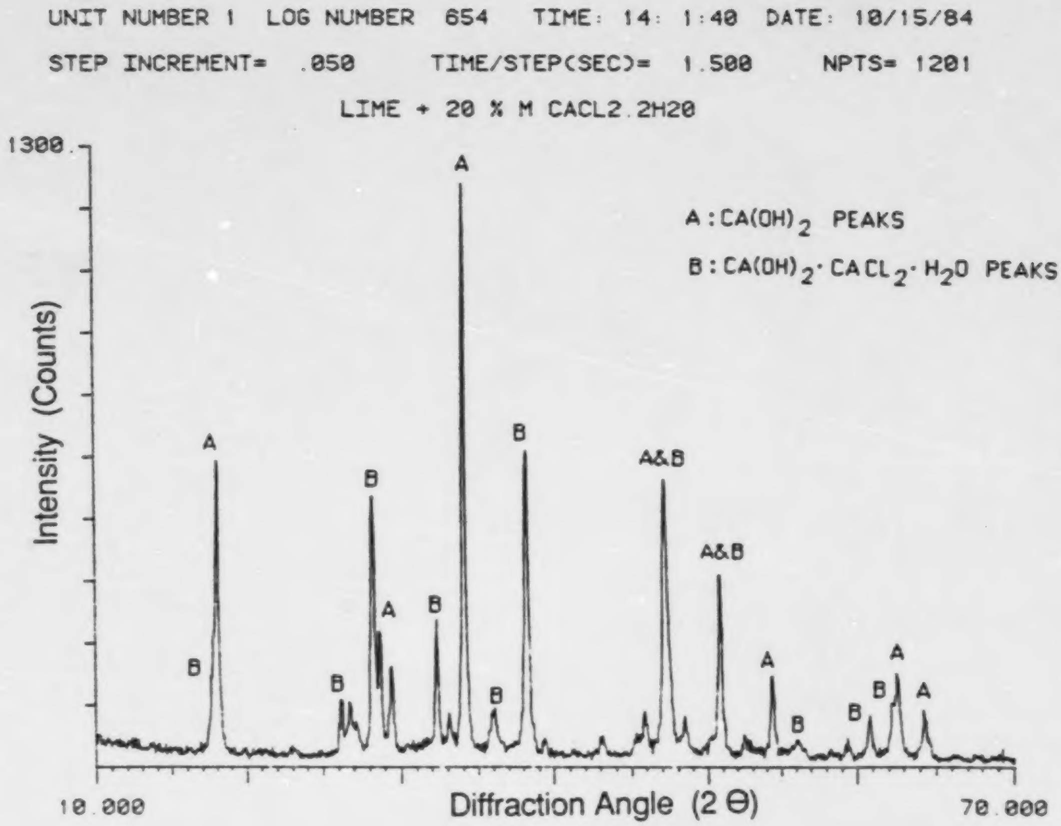

Figure A-15: X-Ray Diffraction Pattern: $Ca(OH)_2$ with 20 mole% $CaCl_2 \cdot 2H_2O$

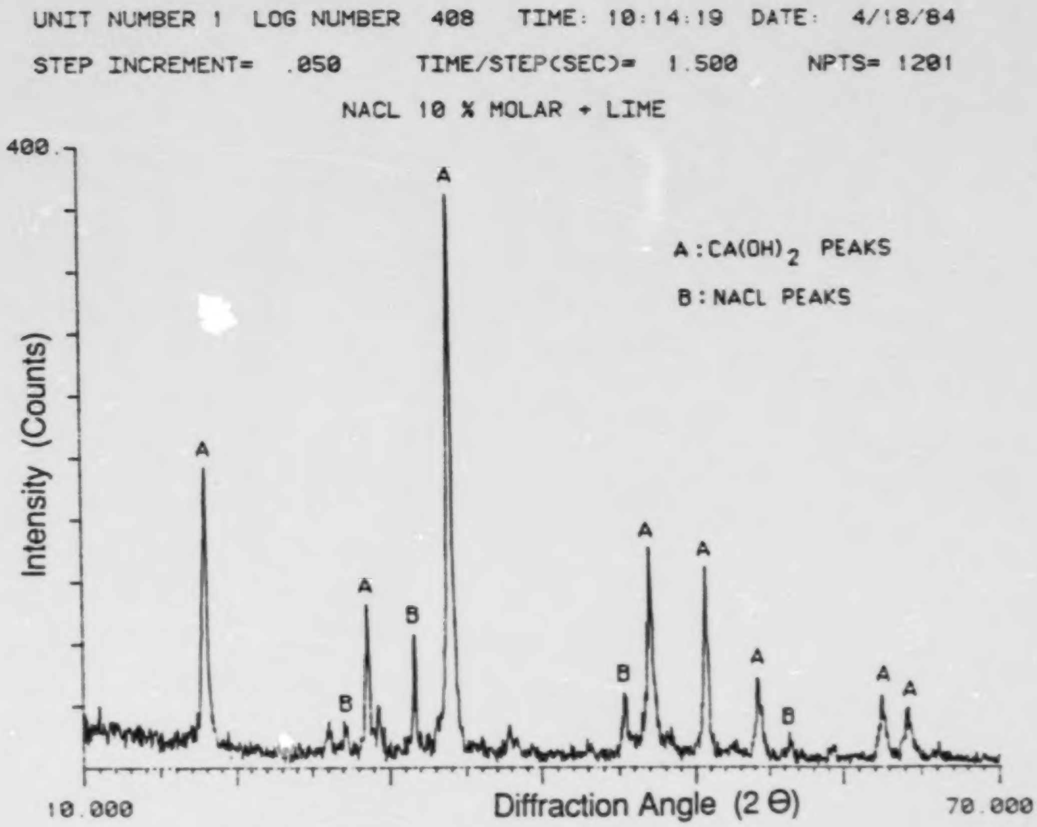

Figure A-16: X-ray Diffraction Pattern: $Ca(OH)_2$ with 10 mole% NaCl

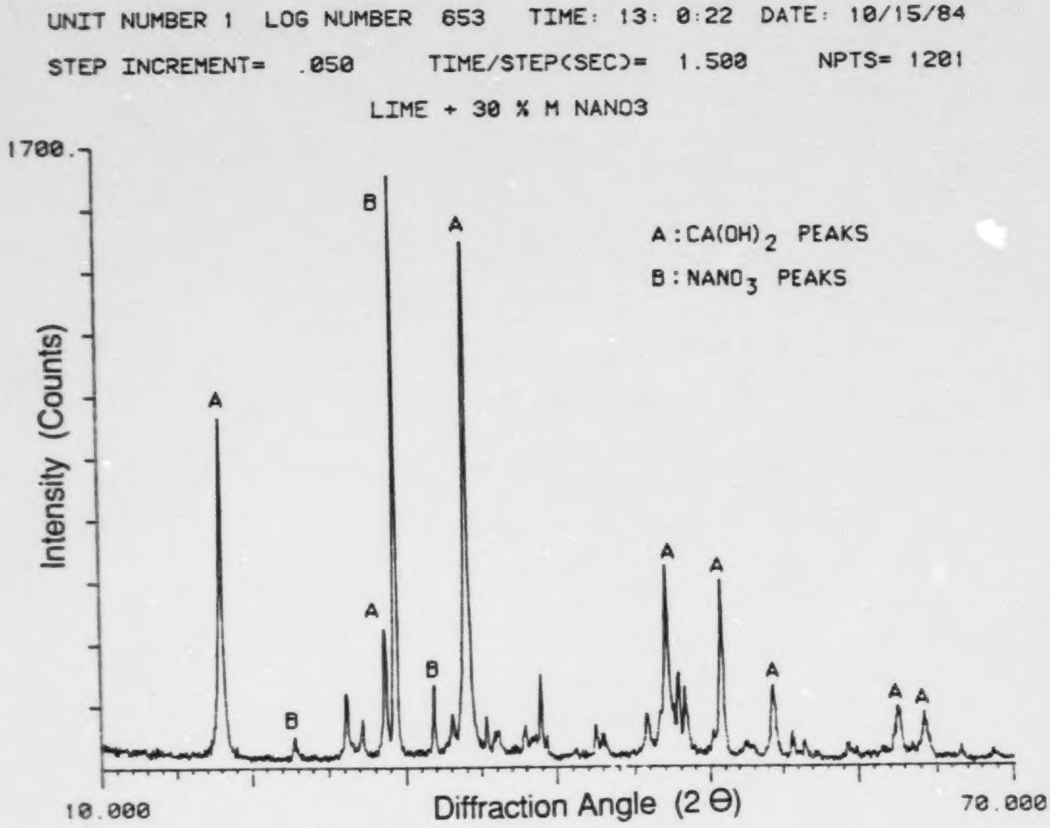

Figure A-17: X-ray Diffraction Pattern: $Ca(OH)_2$ with 30 mole% $NaNO_3$

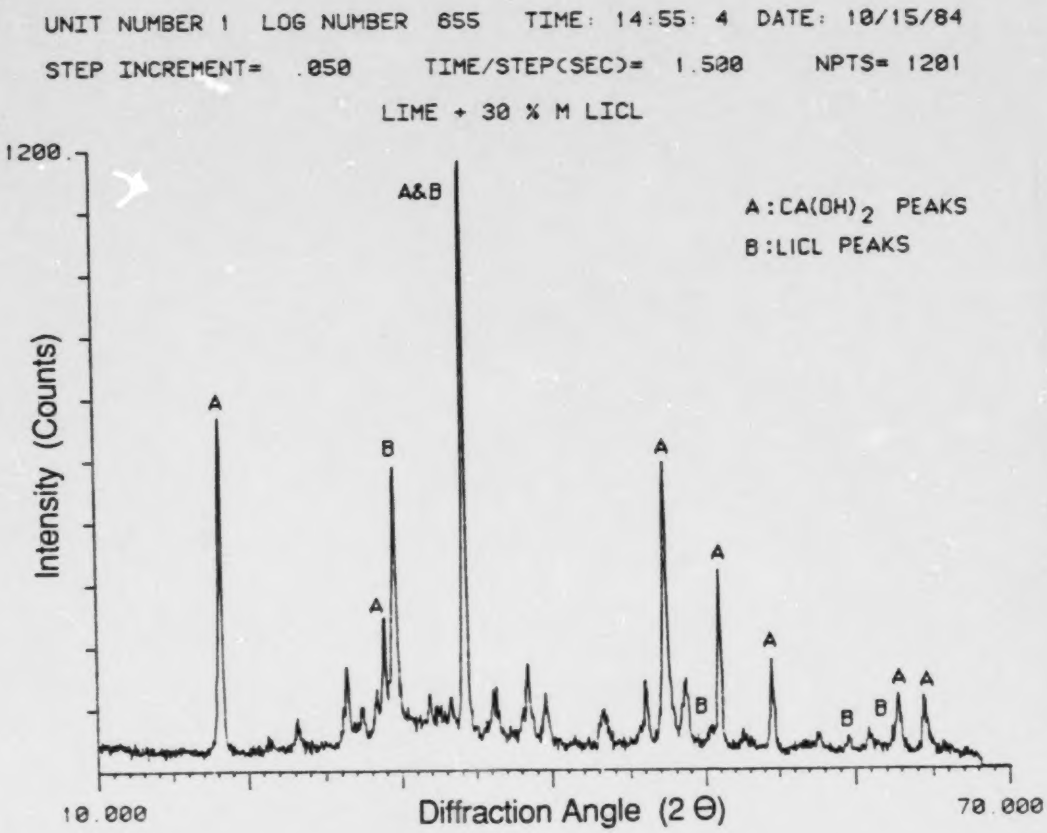

Figure A-18: X-ray Diffraction Pattern: $Ca(OH)_2$ with 30 mole% LiCl

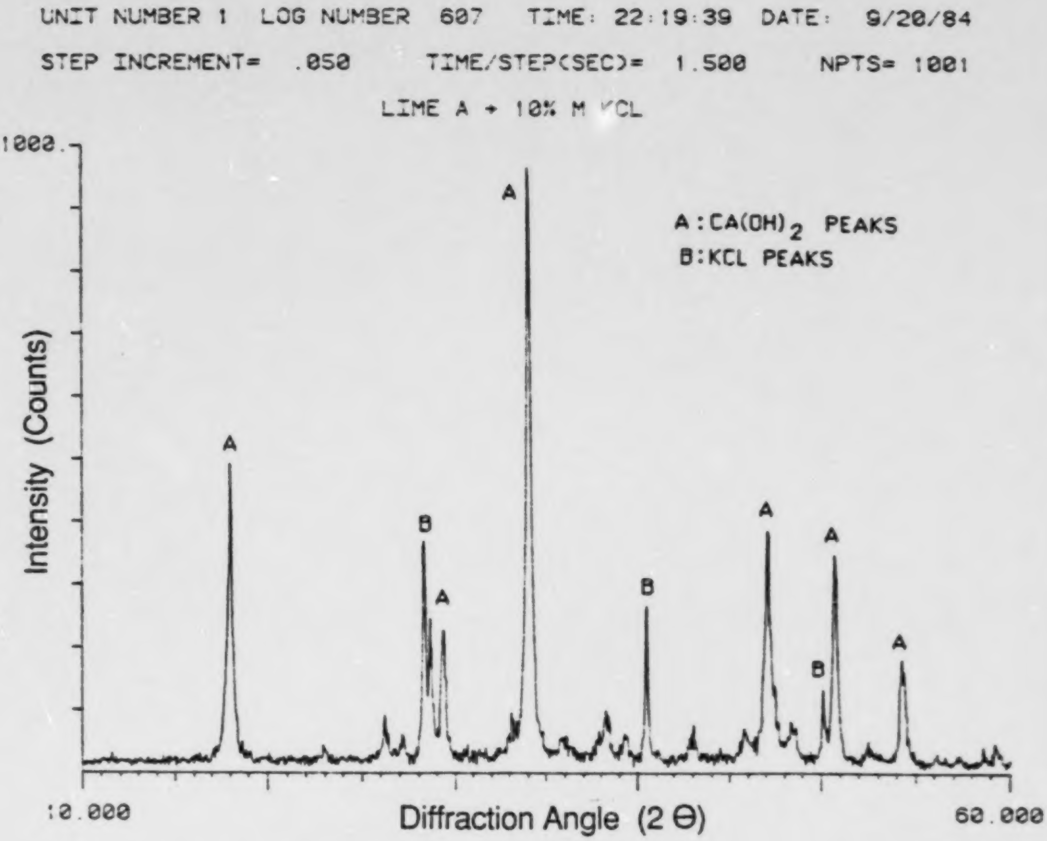

```
UNIT NUMBER 1  LOG NUMBER  607   TIME: 22:19:39  DATE:  9/20/84
STEP INCREMENT=  .050     TIME/STEP(SEC)=  1.500     NPTS= 1001
                     LIME A + 10% M KCL
```

Figure A-19: X-ray Diffraction Pattern: $Ca(OH)_2$ with 10 mole% KCl

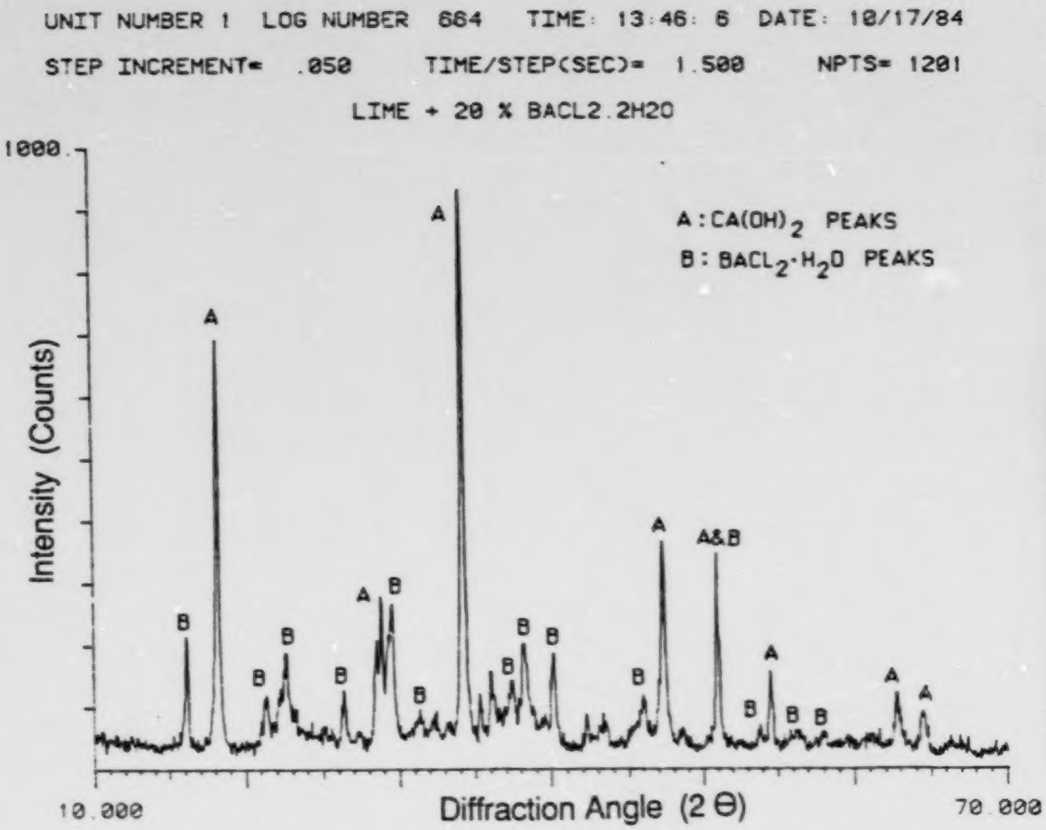

Figure A-20: X-ray Diffraction Pattern: $Ca(OH)_2$ with 20 mole% $BaCl_2{\cdot}2H_2O$

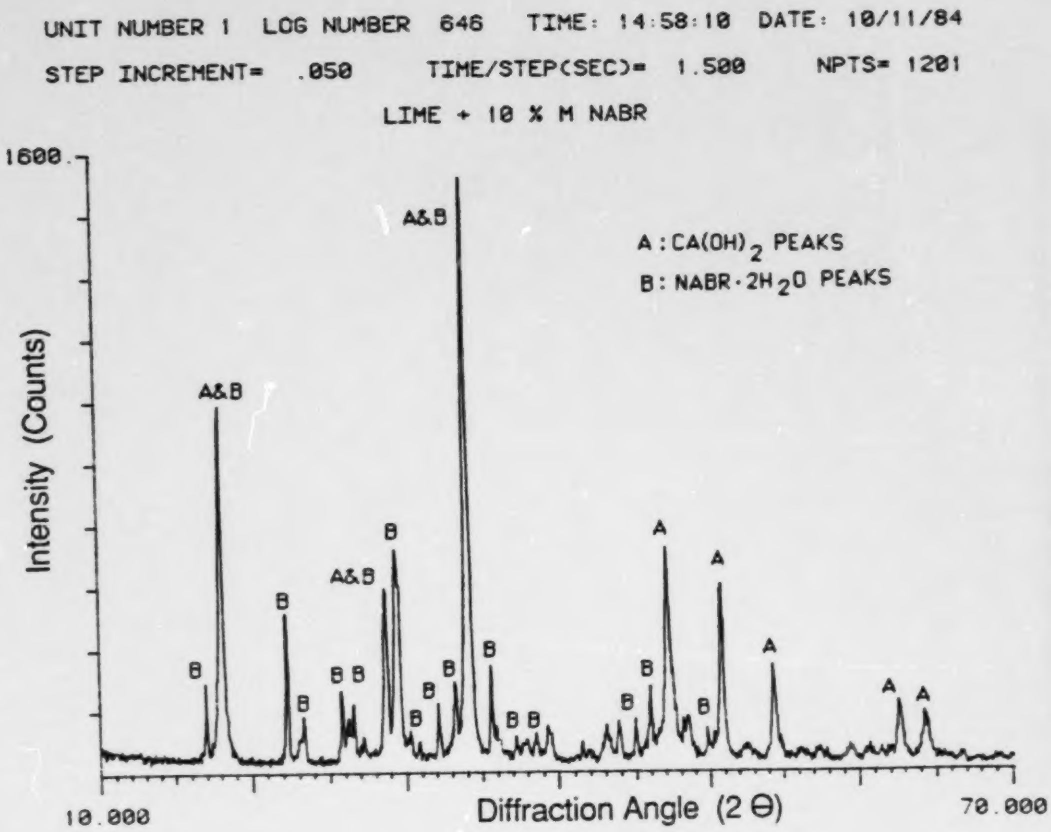

Figure A-21: X-ray Diffraction Pattern: $Ca(OH)_2$ with 10 mole% NaBr

Table A-4: X-Ray Powder Diffraction Results

Additive	Solid Phase Detected Besides $Ca(OH)_2$
NaCl	NaCl
$NaNO_3$	$NaNO_3$
$CaCl_2 \cdot 2H_2O$	$CaCl_2 \cdot Ca(OH)_2 \cdot H_2O$
LiCl	LiCl
KCl	KCl
$BaCl_2 \cdot 2H_2O$	$BaCl_2 \cdot H_2O$
NaBr	$NaBr \cdot 2H_2O$
Reacted $Ca(OH)_2$	$CaSO_3 \cdot 1/2H_2O$
Pressure Hydrated Dolomitic Lime	$Mg(OH)_2$, MgO

hemihydrate was detected. Figures A-22 and A-23 show the diffraction pattern of reacted solids. No gypsum or any other sulfate phase was detected, further supporting the hypothesis that any sulfate produced in the reactor will be present in solid solution with the $CaSO_3 \cdot 1/2H_2O$. As has been reported in the literature (Setoyama and Takahashi, 1978, Jones et al., 1976), the x-ray diffraction pattern of the solid solution is indistinguishable from the patterns of the pure $CaSO_3 \cdot 1/2H_2O$.

The x-ray analysis of pressure hydrated dolomitic lime (Figure A-24) showed the presence of $Mg(OH)_2$,$Ca(OH)_2$, CaO and MgO. This indicates that the sample was not completely hydrated.

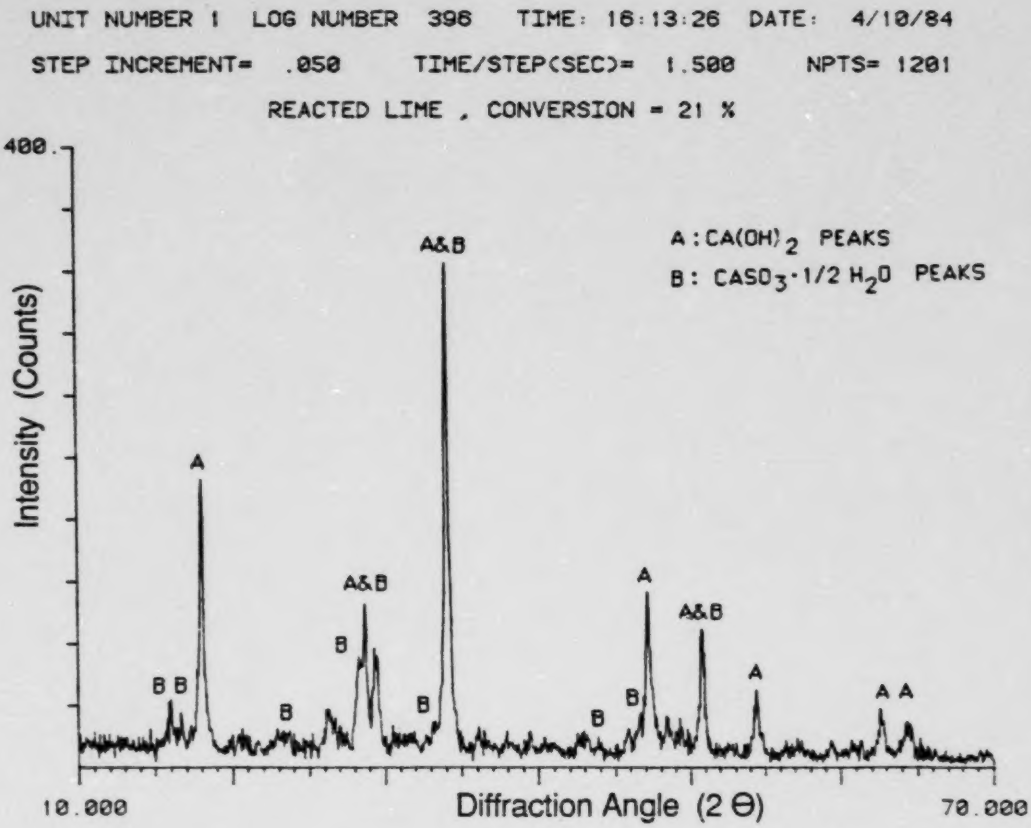

Figure A-22: X-ray Diffraction Pattern: Reacted $Ca(OH)_2$, 21% Conversion, 500 ppm SO_2, 74% R H, 64.4°C, 1 hr reaction

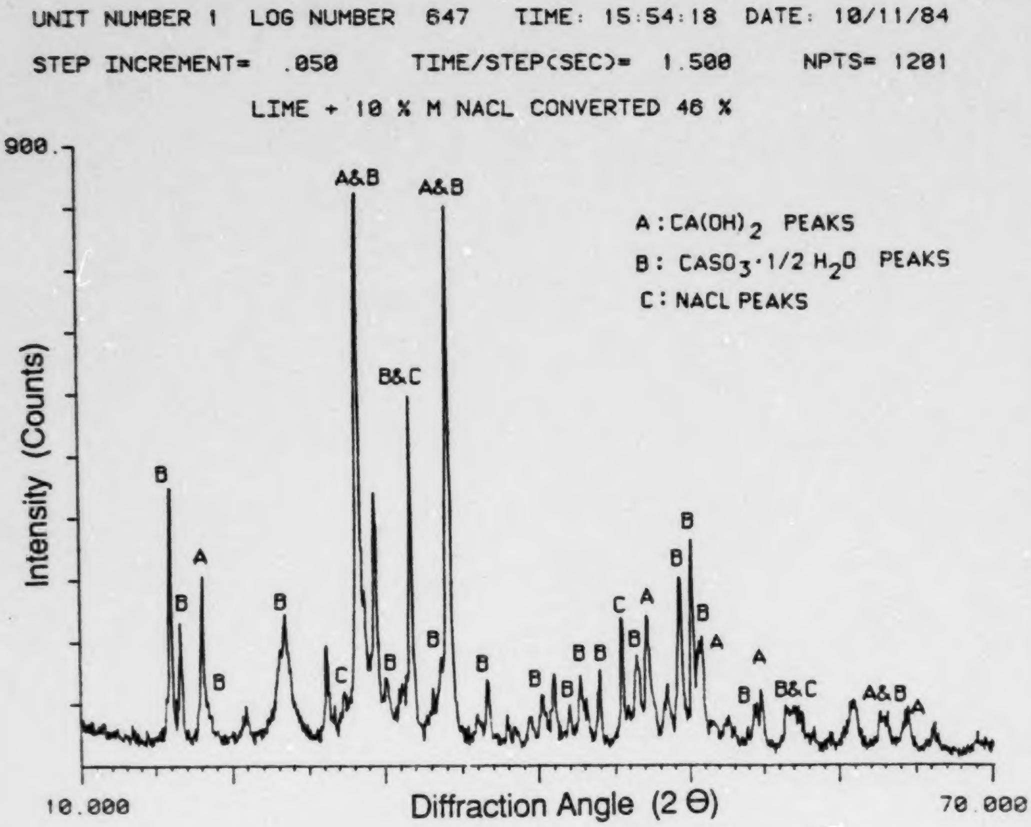

Figure A-23: X-ray Diffraction Pattern: Reacted $Ca(OH)_2$ with 10 mole% NaCl, 74% R H, 64.4°C, 500 ppm SO_2, 2 hr Reaction, 46% Conversion

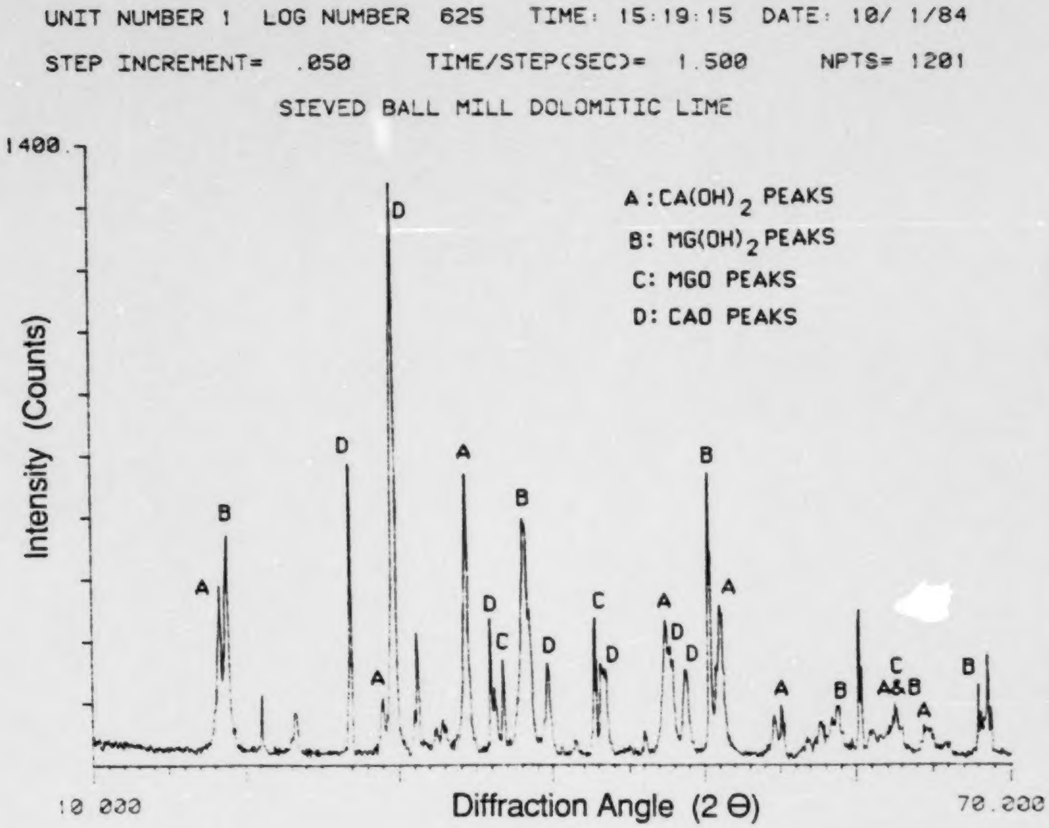

```
UNIT NUMBER 1  LOG NUMBER  625   TIME: 15:19:15  DATE: 10/ 1/84
STEP INCREMENT=  .050     TIME/STEP(SEC)=  1.500     NPTS= 1201
```

Figure A-24: X-ray Diffraction Pattern: Pressure Hydrated Dolomitic Lime

A.7 Acid/Base and Iodometric Titration

Acid/base and iodometric titration were used to analyze the reacted solids for sulfite and hydroxide. The analysis consisted of dissolving the solid sample in about 30 cc of distilled water, adding known excess of HCl and iodine solutions, and back-titrating with NaOH solution to pH 6, and then with sodium thiosulfate solution to the starch end point.

The chemistry involved in the analysis is given by:

$$Ca(OH)_2 + 2HCl \rightarrow Ca^{++} + 2H_2O + 2Cl^- \tag{A.5}$$

$$CaSO_3 + I_2 + H_2O \rightarrow Ca^{++} + SO_4^{=} + 2I^- + 2H^+ \tag{A.6}$$

$$H^+ + NaOH \rightarrow H_2O + Na^+ \tag{A.7}$$

$$I_2 + 2S_2O_3^{=} \rightarrow S_4O_6^{=} + 2I^- \tag{A.8}$$

Because the reaction of iodine with sulfite produces H^+ ions, the analyses of sulfite and hydroxide are interrelated.

Given:

x = concentration of HCl solution (Eq/l)

a = amount of HCl solution (ml)

y = concentration of I_2 solution (Eq/l)

b = amount of I_2 solution (ml)

z = concentration of NaOH solution (Eq/l)

c = amount of NaOH solution (ml)

w = concentration of $Na_2S_2O_3$ solution (Eq/l) d = amount of $Na_2S_2O_3$ solution (ml)

The amount of $CaSO_3$ and $Ca(OH)_2$ are given by:

$$n_{CaSO_3} = \frac{by - dw}{2000}, \text{ gmol } CaSO_3 \tag{A.9}$$

$$n_{Ca(OH)_2} = \frac{ax + by - cz - dw}{2000}, \text{ gmol } Ca(OH)_2 \tag{A.10}$$

$$\text{lime conversion} = \frac{by - dw}{ax + 2by - cz - 2dw}, \frac{\text{gmol } CaSO_3}{\text{gmol } Ca(OH)_2} \tag{A.11}$$

In calculating the lime conversion, it is assumed that the product is sulfite. Any oxidation of sulfite to sulfate taking place in the reactor will cause the apparent lime conversion given by chemical analysis to be lower than the actual value.

Some side reactions have been reported to occur at high pH (Dick, 1973). These side reactions are:

$$I_2 + OH^- \rightarrow HOI + I^- \tag{A.12}$$

$$3HOI + 3OH^- \rightarrow 2I^- + IO_3^- + 3H_2O \tag{A.13}$$

The hydrolysis of the iodine becomes significant at a pH of about 8, with the reaction of thiosulfate and hypoiodite being:

$$4HOI + S_2O_3^{=} + H_2O \rightarrow 2SO_4^{=} + 4I^- + 6H^+ \tag{A.14}$$

This reaction would produce a departure from the expected stoichiometry for the iodine-thiosulfate reaction. Because during the analysis the pH was lower or equal to 6, these side reactions are not likely to represent a problem.

There is another reaction that occurs at low pH that could be important in the analysis. This reaction is the oxidation of iodide by air.

$$4I^- + 4H^+ + O_2 \rightarrow 2I_2 + 2H_2O \qquad (A.15)$$

In order to minimize the amount of iodine consumed by this reaction, the analysis time was kept as short as possible. When tested with known mixtures of $CaSO_3$ and $Ca(OH)_2$, the chemical analysis was able to predict the amounts of sulfite and hydroxide with less than 2% error. This indicates that oxidation of iodide by air is not occurring in any appreciable degree during the analysis.

Appendix B.

Experimental Data from Sand Bed Reactor

Table B-1: Experimental Data, Lime 0

4.6 l/min N_2, 66°C, Lime 0, 80 g silica sand

Percentage of $Ca(OH)_2$ Converted

Exp No	Inlet SO_2 (ppm)	RH (%)	Amount lime (g)	Time (Minutes) 5	10	15	20	25	30	35	40	45	50	55	60
27^a	1500	70	4.0	2.9	5.6	8.2	10.5	12.7	14.7	16.6	18.4	20.1	21.7	23.2	24.5
31	1650	70	4.0	3.2	6.3	8.8	11.1	13.1	15.0	16.8	18.4	19.9	21.3	22.6	23.8
28^a	1060	70	4.0	2.1	4.2	6.3	8.3	10.4	12.5	14.6	16.6	18.6	20.4	22.0	23.4
30	1150	70	4.0	2.3	4.5	6.8	9.1	11.3	13.5	15.5	17.5	19.3	21.0	22.6	24.2
34^a	2150	70	4.0	4.0	7.2	9.9	12.2	14.2	16.1	17.9	19.5	21.0	22.4	23.7	24.8
44	2050	50	4.0	3.7	6.5	8.6	10.3	11.5	12.6	13.5	14.1	14.7	15.2	15.6	15.9
46^a	2050	50	4.0	4.0	7.2	9.9	12.0	13.7	15.1	16.2	17.0	17.7	18.2	18.6	18.8
47	2040	50	4.0	4.0	7.8	10.5	12.3	13.5	14.3	14.8	15.2	15.5	15.8	16.1	16.3
37^a	2000	19	4.0	2.8	4.1	4.8	5.3	5.6	5.8	5.9	5.9	5.9	5.9	5.9	5.9
48^a	2100	50	2.0	6.3	9.8	12.1	13.8	14.9	15.6	16.2	16.7	17.1	17.4	17.8	18.1
40	2070	50	2.0	6.3	10.2	12.7	14.4	15.6	16.5	17.3	18.1	18.7	19.3	19.9	20.4
45	1980	50	2.0	6.4	11.1	13.7	15.3	16.4	17.2	17.9	18.5	19.0	19.5	19.9	20.2
43^a	2000	50	1.0^b	8.7	11.8	14.6	16.4	17.5	18.5	19.4	20.2	20.9	21.5	22.1	22.6
50^a	2000	50	1.0^b	8.7	11.4	13.1	14.2	15.2	16.1	16.9	17.7	18.4	19.2	19.8	20.5
56^a	1000	50	1.0^b	6.6	9.3	11.4	12.7	13.5	14.1	14.5	14.9	15.2	15.5	15.7	16.0
53^a	940	50	2.0	3.7	7.2	9.7	11.2	12.3	13.0	13.5	13.9	14.2	14.6	14.8	15.1
42^a	4000	50	4.0	5.4	9.0	11.7	13.8	15.3	16.5	17.5	18.4	19.1	19.7	20.1	20.5
57	4000	50	4.0	6.7	10.3	12.8	14.6	15.8	16.7	17.3	17.7	18.1	18.5	18.7	19.0
58	4000	50	4.0	6.4	10.1	12.8	14.7	16.0	17.0	17.7	18.3	18.8	19.3	19.7	19.9
52^a	1100	50	4.0	2.2	4.3	6.5	8.5	10.2	11.3	12.3	13.0	13.6	14.0	14.4	14.7

a Experimental runs modelled b Mixed with 40 g silica sand

Table B-2: Experimental Data, Lime A

4.6 l/min N_2, 1 g lime A, 40 g silica sand

Percentage of $Ca(OH)_2$ Converted

Exp	SO_2	RH	Temp	Time (Minutes)												Chemical
No	(ppm)	(%)	(°C)	5	10	15	20	25	30	35	40	45	50	55	60	Analysis
63	490	78	66	4.0	7.6	10.8	13.5	15.9	18.0	20.0	21.8	23.4	24.9	26.2	27.3	-
64	530	78	55.3	4.2	8.0	11.1	13.6	15.8	17.7	19.5	21.0	22.4	23.6	24.7	25.7	
77[a]	510	74	64.4	4.0	7.8	10.9	13.5	15.6	17.4	18.9	20.1	21.8	22.5	23.2	21.2	
96	490	74	64.4	3.9	7.7	11.5	14.9	17.3	18.7	19.5	20.2	20.7	21.1	21.5	21.9	18.2
99	500	74	64.4	3.9	7.9	11.6	14.9	17.1	18.4	19.3	20.0	20.6	21.2	21.6	22.1	18.3
66	530	45	66	3.8	6.3	7.9	8.8	9.3	9.6	9.9	10.1	10.2	10.4	10.5	10.7	-
67	570	45	66	4.2	6.4	7.7	8.5	8.9	9.2	9.4	9.5	9.6	9.7	9.8	9.8	-
82[a]	500	74	30.4	3.7	6.9	9.5	11.6	13.4	14.8	15.9	16.8	17.6	18.2	18.9	19.5	16.3
83	560	74	30.5	4.1	7.4	10.1	12.2	13.8	15.2	16.2	17.1	17.8	18.5	19.1	19.7	19.3
84	500	74	30.4	3.6	6.8	9.5	11.6	13.3	14.8	15.9	16.8	17.6	18.3	19.0	19.6	18.8
136[a]	505	54	66	3.7	6.5	8.5	9.7	10.4	10.8	11.2	11.4	11.5	11.6	11.7	11.8	13.4

[a] Experimental runs modelled

Table B-3: Experimental Data, Lime with Organic Additives

74% RH, 64.4°C, 4.6 l/min N_2, 1 g lime A, 40 g silica sand

Percentage of $Ca(OH)_2$ Converted

Exp No	SO_2 (ppm)	Additive (Wt%)	Time (Minutes) 5	10	15	20	25	30	35	40	45	50	55	60	Chemical Analysis
101	500	1% AA + 7% $CaCl_2$	3.8	7.3	10.3	12.8	15.0	16.8	18.3	19.6	20.9	22.0	22.9	23.8	20.5
108	515	1% AA + 7% $CaCl_2$	4.1	8.1	11.8	15.2	18.1	20.3	21.7	22.8	23.6	24.3	24.9	25.4	27.3
109	515	1% AA + 7% $CaCl_2$	4.1	8.1	11.7	14.8	17.2	18.7	19.7	20.5	21.0	21.6	22.0	22.4	23.7
112	490	1% AA + 7% $CaCl_2$	3.8	7.4	10.4	13.2	15.6	17.6	19.1	20.2	21.1	21.7	22.1	22.5	21.4
110	505	1% AA	3.8	7.1	10.0	12.5	14.6	16.1	16.9	17.3	17.7	18.0	18.4	18.7	18.5
111	540	1% AA	4.3	8.6	12.1	14.8	16.8	18.3	19.3	20.0	20.6	21.1	21.5	21.9	22.5
116	500	5% GA	2.3	3.2	4.0	4.9	5.7	6.5	7.2	7.9	8.6	9.4	10.1	10.7	11.4
118	510	5% GA	2.6	3.7	4.8	5.8	6.8	7.7	8.5	9.3	10.0	10.7	11.3	11.9	13.0
114	490	5% TEG	3.6	6.9	9.9	12.4	14.1	15.4	16.4	17.2	17.7	18.2	18.6	18.9	18.6
115	480	5% TEG	3.7	7.4	10.8	13.6	15.7	17.3	18.5	19.4	20.2	20.9	21.5	22.1	21.3
117	504	5% EG	3.8	7.4	10.5	13.2	15.2	16.5	17.3	17.8	18.2	18.5	18.8	18.9	19.2
119	515	5% EG	4.1	8.1	11.8	15.0	17.5	19.0	19.9	20.5	20.9	21.2	21.4	21.6	21.1
121	500	5% MEA	4.1	8.3	12.0	14.9	16.7	17.7	18.3	18.8	19.2	19.5	19.8	20.0	20.9
122	490	5% MEA	4.2	7.8	10.6	13.0	15.0	16.3	17.2	17.8	18.3	18.6	19.0	19.2	19.8

AA = Adipic Acid GA = Glycolic Acid EG = Ethylene Glycol

TEG = Tri-Ethylene Glycol MEA = Monoethanolamine

Table B-4: Experimental Data, Lime with Salts Additives at 74% RH

74% RH, 64.4°C, 4.6 l/min N_2, 1 g lime A, 40 g silica sand

Percentage of $Ca(OH)_2$ Converted

Exp No	SO_2 (ppm)	Additive (Mole%)	Time (Minutes) 5	10	15	20	25	30	35	40	45	50	55	60	Chemical Analysis
97	510	7% $CaCl_2$	4.0	8.0	12.0	16.1	19.9	23.6	26.4	29.0	30.8	32.0	32.8	33.6	27.8
98	515	7% $CaCl_2$	4.1	8.1	12.2	16.0	19.6	23.1	26.2	29.0	31.4	33.6	35.4	37.0	28.7
100	500	7% $CaCl_2$	3.9	7.9	11.8	15.6	19.0	22.1	24.9	27.4	29.4	31.1	32.4	33.6	27.1
127	510	10% NaOH	3.8	7.6	11.5	15.3	19.1	22.8	26.3	29.6	34.5	35.0	37.1	38.8	35.0
128	510	5% Na_2SO_3	3.9	7.5	10.8	14.0	16.9	19.4	21.7	23.8	25.6	27.2	28.6	29.8	30.8
129	507	5% Na_2SO_4	4.0	8.0	11.8	15.1	18.0	20.3	22.3	24.0	25.4	26.4	27.4	28.3	26.6
130	520	10% NaCl	4.1	8.2	12.3	16.2	19.9	23.4	26.7	29.7	32.4	34.8	36.8	38.5	39.0
131	510	10% $NaNO_3$	4.0	8.0	12.0	16.1	19.9	23.7	27.5	30.9	34.1	37.0	39.5	41.5	40.7
132	510	10% $NaNO_2$	4.0	8.0	12.0	15.7	19.2	22.6	25.9	29.0	32.0	34.8	37.5	40.0	31.5
133	502	5% $Ca(NO_3)_2$	4.0	7.9	11.9	15.8	19.7	23.7	27.6	31.1	34.1	36.4	38.1	39.4	40.1

Table B-5: Experimental Data, Lime with Salts Additives at 54% RH

54% RH, 66°C, 4.6 l/min N_2, 1 g lime A, 40 g silica sand

Percentage of $Ca(OH)_2$ Converted

Exp	SO_2	Additive	Time (Minutes)												Chemical
No	(ppm)	(Mole%)	5	10	15	20	25	30	35	40	45	50	55	60	Analysis
136	505	None	3.7	6.5	8.5	9.7	10.4	10.8	11.2	11.4	11.5	11.6	11.7	11.8	13.4
135	500	5% $Ca(NO_3)_2$	3.7	7.2	9.9	11.3	11.8	12.1	12.4	12.6	12.7	12.8	13.0	13.1	-
137	520	5% $Ca(NO_3)_2$	3.7	6.6	8.7	9.8	10.4	10.7	11.0	11.1	11.3	11.4	11.5	11.5	11.2
134	520	10% $NaNO_3$	4.1	8.2	12.2	15.9	19.1	21.9	24.1	25.9	27.2	28.2	28.8	29.3	29.6
138	530	10% $NaNO_3$	4.1	8.1	11.6	14.5	17.1	19.2	21.0	22.4	23.5	24.2	24.7	25.1	23.5
139	510	10% NaOH	3.9	7.5	10.5	12.9	14.6	15.6	16.2	16.5	16.8	17.0	17.2	17.3	-
140	500	10% NaCl	3.9	7.9	11.8	15.6	19.1	21.9	24.1	25.7	26.8	27.5	28.0	28.4	21.5
140B	500	10% NaCl	3.9	7.8	11.4	14.8	17.5	19.8	21.6	23.0	23.9	24.6	25.2	25.7	17.8
141	500	5% Na_2SO_3	3.9	7.5	10.8	13.0	14.1	14.7	15.1	15.3	15.6	15.8	15.9	16.1	17.8
142	505	5% $Na_2S_2O_3$	4.0	8.0	11.5	14.2	16.1	17.7	18.9	19.8	20.5	21.0	21.3	21.6	-
143	500	3% $NaNO_3$	3.9	7.7	11.0	13.3	14.9	16.0	16.6	17.0	17.3	17.6	17.8	18.0	16.6
145	500	1% $NaNO_3$	4.0	7.4	9.8	11.2	11.9	12.4	12.8	13.0	13.2	13.3	13.4	13.5	16.7
148	512	15% $NaNO_3$	4.0	8.1	11.9	15.4	18.3	20.6	22.3	23.5	24.3	25.0	25.6	26.1	24.8
149	500	1% NaCl	3.5	6.3	8.7	10.7	12.4	13.8	14.6	15.1	15.3	15.7	15.9	16.0	14.0

Table B-5: Continuation

Percentage of $Ca(OH)_2$ Converted

Exp No	SO_2 (ppm)	Additive (Mole%)	Time (Minutes) 5	10	15	20	25	30	35	40	45	50	55	60	Chemical Analysis
162	515	10% NaCl[b]	4.1	8.1	12.1	15.8	18.8	21.2	23.1	24.5	25.6	26.3	26.8	27.1	25.1
150	500	3% NaCl	3.9	7.3	10.3	12.5	14.1	15.3	16.2	16.8	17.3	17.7	18.0	18.1	18.1
155B	520	15% NaCl	4.1	8.2	12.2	15.9	19.0	21.3	23.1	24.2	25.1	25.8	26.3	26.7	-
155	518	10% NaCl[a]	4.1	8.1	11.7	14.7	17.2	19.1	20.5	21.5	22.1	22.6	22.9	23.2	22.7
157	490	10% $NaNO_3$[a]	3.9	7.7	11.4	14.6	17.2	19.0	20.3	21.2	21.9	22.6	23.1	23.7	22.6
185	507	10% KCl[a]	3.9	7.5	10.7	13.1	14.7	15.7	16.6	17.3	17.9	18.4	18.9	19.3	20.4
176	515	5% BaCl	3.9	7.4	10.3	12.6	14.5	16.0	17.1	17.8	18.3	18.7	19.1	19.4	14.4
177	508	5% $Co(NO_3)_2$	3.8	7.1	9.4	10.7	11.6	12.1	12.4	12.6	12.8	12.9	13.1	13.2	12.6
178	507	10% NaBr	4.0	8.0	12.0	16.0	19.8	23.5	27.1	30.4	33.6	36.5	39.3	42.0	44.2
179	535	10% KCl	4.2	8.4	12.6	16.6	20.3	23.5	26.4	28.9	30.9	32.5	33.9	35.0	35.8
175	510	10% KCl	4.0	8.0	12.0	16.0	19.9	23.7	27.5	31.1	34.1	36.4	38.3	39.7	41.9
180	510	10% LiCl	4.0	8.0	12.0	16.1	20.1	24.1	27.9	31.5	34.8	37.8	40.7	42.9	47.2
183	600	5% $CaCl_2$	4.6	8.8	11.7	13.1	13.9	14.4	14.9	15.3	15.8	16.2	16.6	17.0	14.6
191	330	3% NaCl	2.6	5.0	7.4	9.5	11.2	12.6	13.6	14.4	15.0	15.5	15.9	16.2	20.3

[a] No Prehumidification of the bed at 98% RH

[b] O_2 free N_2

Table B-6: Experimental Data, Lime with Salts Additives at 35 and 17% RH

4.6 l/min N_2, 1 g lime A, 40 g silica sand, 10 mole% Additive

Percentage of $Ca(OH)_2$ Converted

Exp No	SO_2 (ppm)	Additive	Time (Minutes) 5	10	15	20	25	30	35	40	45	50	55	60	Chemical Analysis
34.6% RH, 77.5°C															
151	490	NaCl	3.9	7.6	10.6	12.4	13.6	14.4	15.3	15.9	16.4	16.7	17.0	17.3	15.9
144	520	$NaNO_3$	4.1	7.9	10.6	12.0	12.8	13.4	13.8	14.2	14.5	14.7	14.9	15.1	16.5
17.4% RH, 95°C															
152	510	NaCl	3.7	6.2	7.0	7.6	8.1	8.4	8.7	9.0	9.2	9.4	9.6	9.8	9.7
146	512	$NaNO_3$	3.6	5.6	6.6	7.2	7.6	7.9	8.2	8.4	8.6	8.8	8.9	8.9	11.9
147	512	None	2.2	2.5	2.7	2.9	3.1	3.2	3.3	3.4	3.4	3.4	3.4	3.4	4.0
184	508	NaBr	3.6	5.5	6.7	7.6	8.3	8.9	9.4	9.9	10.3	10.7	11.1	11.3	11.0
186	500	LiCl	3.7	6.0	6.8	7.3	7.7	8.1	8.4	8.7	8.9	9.2	9.4	9.6	9.1
182	500	KCl	-	-	-	-	-	-	-	-	-	-	-	3.4	2.9
187	510	NaCl[a]	-	-	-	-	-	-	-	-	-	-	-	3.3	4.0

[a] No prehumidification of bed at 98% RH

Table B-7: Experimental Data, Pressure Hydrated Dolomitic Lime

74% RH, 64.4°C, 4.6 l/min N_2, 1 g lime, 40 g silica sand

Percentage of Lime Converted Assuming 40% $Mg(OH)_2$

Exp No	SO_2 (ppm)	Type Lime (Mole%)	Time (Minutes) 5	10	15	20	25	30	35	40	45	50	55	60	Chemical Analysis
166	530	Ball Mill	3.8	7.6	11.3	14.4	16.8	18.6	19.9	21.1	22.1	23.1	23.9	24.6	22.3
167	510	Hydrator	3.7	7.3	11.0	14.3	16.2	17.6	18.8	20.1	21.1	22.1	23.0	24.2	21.6
171	510	Ball Mill (Sieved)	3.3	6.7	10.0	13.2	16.3	19.2	21.9	24.3	26.4	28.2	29.8	31.2	-
172	510	Ball Mill + 10% NaCl	3.5	7.0	10.4	14.0	17.4	20.9	24.3	27.7	30.9	34.0	36.8	39.3	-

Table B-8: Differential Experiments

0.125 g lime A, 500 ppm SO_2, 4.6 l/min N_2

Additive (Mole%)	RH (%)	Temp (°C)	Time (Minutes)	Conversion (%)
None	54	66	10	8.4
			30	14.1
			30	10.4
			60	17.6
None	74	64.4	10	16.6
			30	19.1
			60	24.3
			60	21.2
			60	23.9
			60	22.7
10% NaCl	54	66	10	27.3
			30	25.6
			60	28.1
5% $CaCl_2$	74	64.4	10	26.8
			10	27.5
			10	28.2
			30	28.6
			30	34.9
			30	33.6
			60	38.6
			60	37.0

Appendix C.

Model Computer Program

```
PROGRAM REARE0(INPUT,OUTPUT,TTY,TAPE1=INPUT,TAPE2=OUTPUT,
     &TAPE3=TTY)
C     ************************************************************
C     THIS IS A PROGRAM TO INTEGRATE THE REACTION OF SO2 WITH
C     CA(OH)2 ALONG THE REACTOR AND IN TIME.THE PROGRAM
C     ASSUMES A ZERO ORDER KINETICS IN SO2.
C     THIS PROGRAM USES DGEAR TO INTEGRATE IN TIME AND IN
C     DISTANCE AND IT USES VARIABLE STEP SIZE.
C     THE SURFACE AREA IS ALLOWED TO DECREASE WHEN THE
C     REACTION OCCURS. THE SURFACE AREA DECREASE
C     FOLLOWS THE EQUATION:
C
C     AREAF = (1.0 + EXP(13.428*XLIME-10.7424))/15.667
C
C     THIS EQUATION ASSUMES THAT THE ROUGHNESS IS 15.667 WHEN ALL
C     THE LIME IS UNREACTED AND THAT IS 2.0 WHEN 20 % OF THE
C     LIME HAS BEEN CONVERTED.
C     ************************************************************

      INTEGER NZ,IC,NZN,ICN,IPRINT
      REAL K1,K2,K3,CAG,VXLIME,VXSO2,VMC,X(3)
      REAL VZ,C,H,VZN(200),VXLN(200),NB,SO2EXP(12)
      COMMON /CONST1/ K1,K2,K3,CAG
      COMMON /CONST2/ VMC
      COMMON /CONST3/ H
      COMMON /CONST4/ NB
      COMMON /CONST5/ NZ,VZ(200),VXLIME(200)
      COMMON /CONST6/ C(200,3),IC
      COMMON /CONST7/ VXSO2(200)
      COMMON /CONST8/ IPRINT,XAVERA(12),CONC(12),TIME(12)
      COMMON /CONST9/ XLEXP(12),XDEV(12)
      READ(1,*) NUMEXP
      READ(1,*) DE,DKS,DKC
      READ(1,*) CAG,VMC,NB,TREAC
      DO 17 I=1,12
      READ(1,*) SO2EXP(I),XLEXP(I)
17    CONTINUE
      VMC=VMC*((273.25+TREAC)/273.15)
      K1=9.4E4*NB*DE/(3.958156*2.273E-4)
      K2=9.4E4*NB*2.2*DKS/74.1
      K3=DKC*NB*9.4E4
      NB=NB/74.1
      CAG=CAG*0.000001/(82.06*(273.15+TREAC))
      X(1)=K1
      X(2)=K2
      X(3)=K3
      CALL FUNCT(X,F)
      WRITE(2,900) NUMEXP
      WRITE(3,900) NUMEXP
900   FORMAT('                 EXPERIMENT NUMBER =',I4)
```

```
      WRITE(2,910) DE,DKS,DKC
      WRITE(3,910) DE,DKS,DKC
      WRITE(2,909) K1,K2
      WRITE(3,909) K1,K2
  909 FORMAT('                K1 =',E12.7,/,'                K2 =',
     &E12.7)
  910 FORMAT('                DE =',E12.7,/,'                KS =',E12.7
     &,/,'                KC =',E12.7)
      STDEV=(F/11.0)**0.5
      WRITE(2,920) F
      WRITE(3,920) F
  920 FORMAT('                SUM OF SQUARE ERRORS =',E12.7)
      WRITE(2,923) STDEV
      WRITE(3,923) STDEV
  923 FORMAT('                STANDARD DEVIATION =',F5.2,/)
      WRITE(2,*)'       TIME(I)     SO2EXP(I)    CONC(I)     XLEXP(I)     XAVE
     &RA(I)    XDEV(%)'
      WRITE(3,*)'       TIME(I)     SO2EXP(I)    CONC(I)     XLEXP(I)     XAVE
     &RA(I)    XDEV(%)'
      DO 500 I=1,IPRINT
      XDEV(I)=100.0*(XAVERA(I)-XLEXP(I))/XLEXP(I)
      WRITE(2,930) TIME(I),SO2EXP(I),CONC(I),XLEXP(I),XAVERA(I),XDEV(I)
      WRITE(3,930) TIME(I),SO2EXP(I),CONC(I),XLEXP(I),XAVERA(I),XDEV(I)
  500 CONTINUE
  930 FORMAT(8X,G10.5,4(1X,G10.5),F7.2)
      STOP
      END
```

```
SUBROUTINE FUNCT(X,F)
      ************************************************************
      THIS SUBROUTINE DOES THE ACTUAL INTEGRATION, THE MAIN
      PROGRAM ONLY READ DATA AND PRINT THE RESULTS
      ************************************************************
      DIMENSION VZN(200),VXLN(200),X(5)
      INTEGER NZ,IC,NZN,ICN,IER,IPRINT
      REAL K1,K2,K3,CAG,VXLIME,VXSO2,VMC
      REAL VZ,C,HZ,VZN,VXLN,NB,X,XAVERA,CONC,T,TINI,TEND
      REAL TDEL,TPRINT,DELTT
      COMMON /CONST1/ K1,K2,K3,CAG
      COMMON /CONST2/ VMC
      COMMON /CONST3/ H
      COMMON /CONST4/ NB
      COMMON /CONST5/ NZ,VZ(200),VXLIME(200)
      COMMON /CONST6/ C(200,3),IC
      COMMON /CONST7/ VXSO2(200)
      COMMON /CONST8/ IPRINT,XAVERA(12),CONC(12),TIME(12)
      COMMON /CONST9/ XLEXP(12),XDEV(12)
      K1=X(1)
      K2=X(2)
      K3=X(3)
 C    SET INITIAL VALUES OF NZ,VZ(I),VXLIME(I)
      NZ=11
      IC=NZ-1
      DO 10 I=1,NZ
      VZ(I)=0.1*FLOAT(I-1)
      VXLIME(I)=1.0
  10  CONTINUE
 C    SET VALUE OF TPRINT AND INITIAL VALUES FOR T,DELTT,IPRINT
      T=0.0
      TDEL=5.0
      TINI=T
      TEND=TDEL
      DELTT=(TEND-TINI)/100.0
      IPRINT=1
      TPRINT=300.0
      TMAX=3600.0
 C    NOW THE INTEGRATION IN THE Z DIRECTION WILL BE PERFORMED
       DO 100 J=1,2000
       WRITE(3,2) J
  2    FORMAT(I4)
       CALL INTEGZ(VXSO2,VXLN,VZN,NZN,ICN)
       NZ=NZN
       IC=ICN
        DO 20 I=1,NZ
        VZ(I)=VZN(I)
        VXLIME(I)=VXLN(I)
  20    CONTINUE
 C      NOW THE INTEGRATION IN TIME WILL BE PERFORMED
```

```
85     CALL INTEGT(TINI,TEND,VXLN,DELTT,INDEX,IER)
       WRITE(2,*)'            T        TINI         TEND          DELTT'
       WRITE(2,87) T,TINI,TEND,DELTT
       WRITE(3,87) T,TINI,TEND,DELTT
  87  FORMAT (3(1X,F10.3),E12.5)
      IF (TEND.EQ.TPRINT) GO TO 32
       CALL STPCHG(T,TEND,DELTT,INDEX,TPRINT)
 32    IF (INDEX.EQ.1) THEN
         DO 30 I=1,NZ
         VXLN(I)=VXLIME(I)
30       CONTINUE
        TINI=T
       TDEL=TEND
        DELTT=DELTT*0.1
        GO TO 85
       ELSE
         DO 35 I=1,NZ
         VXLIME(I)=VXLN(I)
35       CONTINUE
        IF(ABS(TEND-TPRINT).LE.1.0E-6) THEN
         WRITE(2,800) NZ
800      FORMAT('       NZ =',I4)
         WRITE(2,*)'       # Z POINTS   VZ(I)     VXSO2(I)           VXLIME(I)
    &    VXLN(I)'
         DO 500 IZ=1,NZ
         WRITE(2,550) IZ,VZ(IZ),VXSO2(IZ),VXLIME(IZ),VXLN(IZ)
550      FORMAT(4X,I10,4(1X,G12.5))
500      CONTINUE
         TIME(IPRINT)=TEND
         CONC(IPRINT)=1.0-VXSO2(NZ)
         XAVERA(IPRINT)=0.0
          DO 65 I=1,NZ-1
          XAVERA(IPRINT)=XAVERA(IPRINT)+(VZ(I+1)-VZ(I))*
    &                    (VXLIME(I)+VXLIME(I+1))/2.0
65        CONTINUE
         XAVERA(IPRINT)=(1.0-XAVERA(IPRINT))*100.0
         IF(ABS(TEND-TMAX).LE.1.0E-6)THEN
C          CALCULATION OF SUM OF SQUARE ERRORS
          F=0.0
           DO 95 I=1,IPRINT
           F=F+(XAVERA(I)-XLEXP(I))*(XAVERA(I)-XLEXP(I))
95         CONTINUE
          RETURN
         ENDIF
         IPRINT=IPRINT+1
         TPRINT=TPRINT+300.0
        ENDIF
        TINCRE=TEND-T
      IF(TINCRE.LT.DELTT) TINCRE=DELTT*2.2
        T=TEND
```

```
           TINI=T
           TDEL=T+TINCRE
           TEND=TDEL
           IF(TEND.GE.TPRINT) THEN
            TEND=TPRINT
            TDEL=TPRINT
           ENDIF
          ENDIF
 100      CONTINUE
         WRITE(3,*) 'INSUFFICIENT ITERATIONS IN TIME'
         RETURN
         END
```

```
SUBROUTINE INTEGZ(VXSO2,VXLN,VZN,NZN,ICN)
C     ****************************************************************
C     THIS SUBROUTINE USE DGEAR TO INTEGRATE THE FRACTION OF
C     SO2 REMAINING IN THE REACTOR AT ANY GRID POINT ALONG
C     THE REACTOR VXSO2(I), IT ALSO PROVIDES VALUES FOR THE
C     LIME FRACTION INTERPOLATED AT THE NEW GRID POINTS,
C     VXLN(I).
C     VARIABLES ENTERING THE SUBROUTINE THROUGH COMMON
C     BLOCKS ARE:
C
C     NZ = NUMBER OF GRID POINTS IN THE Z DIRECTION
C     VXLIME(I) = FRACTION OF LIME UNCONVERTED AT ALL GRID
C     POINTS
C     K1 = CONSTANT FOR THE DIFFUSION OF SO2 THROUGH THE ASH
C          LAYER
C     K2 = CONSTANT FOR CHEMICAL REACTION
C     K3 = CONSTANT FOR DIFFUSION THROUGH THE GAS FILM
C     CAG = SO2 CONCENTRATION ENTERING THE REACTOR
C     VMC = N2 FLOW RATE (CC/SEC) AT THE REACTOR TEMPERATURE
C     THE FOLLOWING VARIABLES ARE USED INSIDE THE SUBROUTINE:
C
C     HZ = STEP SIZE IN THE Z DIRECTION
C     H = STEP SIZE FOR DGEAR
C     N = NUMBER OF DIFFERENTIAL EQUATIONS TO BE INTEGRATED
C     XSO2 = FRACTION OF SO2 REMAINING IN THE GAS
C     THE FOLLOWING VARIABLES EXIT THE SUBROUTINE:
C
C     NZN = NEW NUMBER OF GRID POINTS
C     ICN = NEW NUMBER OF SPLIT SPINE COEFFICIENTS
C     VZN(I) = Z COORDINATE OF NEW GRID POINTS
C     VXLN(I) = FRACTION OF LIME REMAINING AT NEW GRID POINTS
C     ****************************************************************
      DIMENSION VXSO2(1001),VZN(1001),VXLN(1001)
      COMMON /CONST1/ K1,K2,K3,CAG
      COMMON /CONST2/ VMC
      COMMON /CONST3/ H
      COMMON /CONST5/ NZ,VZ(200),VXLIME(200)
      COMMON /CONST6/ C(200,3),IC
      INTEGER METH,MITER,INDEX,IWK(2),IER,K,IC,NZ,N
      REAL K1,K2,K3,CAG,XLIME,H
      REAL VXSO2,Z,HZ,XSO2,ZEND,TOL,WK(35),VZ,C
      EXTERNAL FCN,FCNJ
C     CALL THE INTERPOLATION ROUTINE ICSCCU TO DETERMINE THE
C     SPLINE COEFFICIENTS C, FROM THE VXLIME(I) OF THE
C     PREVIOUS TIME
      CALL ICSCCU(VZ,VXLIME,NZ,C,IC,IER)
C     INITIALIZE VARIABLES FOR DGEAR
      N=1
      METH=2
      MITER=2
      INDEX=1
      TOL=1.0E-4
      Z=0.0
      ZMAX=1.0
      XSO2=1.0
      VZN(1)=0.0
      VXSO2(1)=1.0
      VXLN(1)=VXLIME(1)
      HZ=VZ(2)-VZ(1)
      ZGI=Z
      ZEND=Z+HZ/100.0
      H=(ZEND-ZGI)/1000.0
      ZEGI=ZEND
      TMPSO2=XSO2
      IZ=1
       DO 10 J=1,200
        IF (ABS(ZMAX-ZGI).LE.1.0E-6) THEN
         NZN=IZ
         ICN=IZ-1
         RETURN
        ENDIF
        IF (ZEGI.GE.ZMAX) THEN
         ZEGI=ZMAX
         ZEND=ZMAX
        ENDIF
        IF (XSO2.GT.1.0E-12) THEN
C        DGEAR IS CALLED TO PERFORM THE INTEGRATION
         CALL DGEAR(N,FCN,FCNJ,ZGI,H,XSO2,ZEGI,TOL,METH,MITER,INDEX,
     &              IWK,WK,IER)
        ELSE
         INDEX=0
         IER=0
         H=0.05
         XSO2=0.0
        ENDIF
        IF (XSO2.LT.0.0) XSO2=0.0
C       STPCHG IS CALLED TO CHECK IF THE STEP SIZE USED FOR
C       DGEAR IS SMALL ENOUGH
        CALL STPCHG (Z,ZEND,H,INDEX,ZMAX)
        IF (INDEX.EQ.1) THEN
         ZEGI=ZEND
         ZGI=Z
         XSO2=TMPSO2
         H=H*.1
        ELSE
         TMPSO2=XSO2
         IZ=IZ+1
         VZN(IZ)=ZEND
         VXSO2(IZ)=XSO2
C        THE INTERPOLATION SUBROUTINE XINTER IS CALLED TO
```

```
C          DETERMINE THE FRACTION OF LIME AT THE NEW GRID
C          POINT, VXLN(I)
           CALL XINTER(VZ,VXLIME,NZ,C,IC,VZN(IZ),VXLN(IZ),IER)
           DELTZ=ZEND-Z
           Z=ZEND
           ZEND=Z+DELTZ
           ZGI=Z
           ZEGI=ZEND
          ENDIF
   10  CONTINUE
       NZN=IZ
       ICN=IZ-1
       RETURN
       END
```

```
SUBROUTINE STPCHG(Z,ZEND,H,INDEX,ZMAX)
C     **************************************************************
C     THIS SUBROUTINE DETERMINE IF THE DIFFERENCE BETWEEN Z AND
C     ZEND IS SMALL ENOUGH TO ENSURE AN ACCURATE INTEGRATION.
C     THE CRITERIA USED IS THAT DELTZ = ZEND -Z MUST BE LESS THAN
C     5 TIMES BUT GREATER THAN 2 TIMES H, THE STEP SIZE USED
C     FOR DGEAR.
C     VARIABLES ENTERING THE SUBROUTINE ARE:
C
C     Z = VALUE OF Z AT WHICH THE INTEGRATION IS STARTED
C     ZEND = VALUE OF Z AT WHICH THE INTEGRATION END
C     H = INTEGRATION STEP SIZE USED BY DGEAR
C     INDEX = DGEAR PARAMETER EQUAL TO 1 FOR FIRST CALL TO
C             DGEAR AND EQUAL TO 0 FOR OTHER CALLS.
C     ZMAX = MAXIMUN POSSIBLE VALUE OF ZEND, REACTOR LENGTH
C     VARIABLES USED INSIDE SUBROUTINE:
C
C     DELTZ = ZEND - Z, INTEGRATION STEP SIZE
C     VARIABLES LEAVING SUBROUTINE:
C
C     ZEND = NEW VALUE FOR ENDING THE INTEGRATION OF DGEAR IF
C            STEP SIZE WAS CHANGED, OTHERWISE THE SAME ENTERING
C            VALUE
C     INDEX = PARAMETER WITH VALUE 1 IF STEP SIZE WAS CHANGED
C             AND VALUE 0 IF THE STEP SIZE WAS NOT CHANGED
C     **************************************************************
      INTEGER INDEX
      REAL Z,ZEND,H,DELTZ
      DELTZ=ZEND-Z
       IF(DELTZ.GT.5.0*H) THEN
        ZEND=Z+DELTZ*0.7
        INDEX=1
       ENDIF
       IF (DELTZ.LT.(H*2.0).AND.(ZMAX-ZEND).GT.2.0E-6) THEN
        ZEND=Z+DELTZ*1.6
        INDEX=1
       ENDIF
       IF (ZEND.GE.ZMAX) ZEND=ZMAX
      RETURN
      END
      SUBROUTINE FCN(N,Z,XSO2,DXSO2)
C     ************************************************************
C     THIS SUBROUTINE IS AN EXTERNAL FUNCTION OF DGEAR.
C     IT CALCULATE THE DERIVATIVE DXSO2/DZ AT ANY POINT
C     Z ALONG THE REACTOR.
C     THIS SUBROUTINE IN TURN CALL THE SUBROUTINE XINTER THAT
C     DETERMINE THE VALUE OF VXLIME AT THE  GIVEN Z.
C     VARIABLES ENTERING THE SUBROUTINE ARE:
C
C     N = NUMBER OF DIFFERENTIAL EQUATIONS TO BE SOLVED
C         BY DGEAR
C     Z = Z COORDINATE ALONG THE REACTOR
C     XSO2 = FRACTION OF SO2 REMAINING IN THE GAS
C     VARIABLES ENTERING THE SUBROUTINE BY COMMON BLOCKS:
C
C     K1 = CONSTANT FOR DIFFUSION OF SO2 THROUGH ASH LAYER
C     K2 = CONSTANT FOR CHEMICAL REACTION
C     K3 = CONSTANT FOR DIFFUSION OF SO2 THROUGH THE GAS FILM
C     CAG = SO2 CONCENTRATION ENTERING THE REACTOR
C     VMC = VOLUMETRIC NITROGEN FLOW RATE (CC/SEC)
C     NZ = NUMBER OF GRID POINT AT WHICH VXLIME IS KNOWN FROM
C          PREVIOUS INTEGRATION
C     VZ(I) = Z COORDINATE OF GRID POINT AT WHICH VXLIME IS
C             KNOWN
C     VXLIME(I) = VALUES OF FRACTION OF LIME AT GRID POINTS,
C                 KNOWN FROM PREVIOUS INTEGRATION
C     C(I,J) = SPLINE COEFFICIENTS DETERMINED FOR VXLIME BY THE
C              IMSL INTERPOLATION ROUTINE ICSCCU
C     IC = NZ-1, ONE OF THE DIMENSIONS OF THE SPLINE COEFFICIENTS
C          MATRIX
C     VARIABLES USED INSIDE THE SUBROUTINE:
C
C     XINT = FRACTION OF LIME AT Z, INTERPOLATED BY XINTER
C     VARIABLES EXITING THE SUBROUTINE:
C
C     DXSO2 = DERIVATIVE OF XSO2 WITH RESPECT TO DISTANCE, AT Z
C     ************************************************************
      INTEGER N,IER,NZ,IC
      REAL Z,XSO2(N),DXSO2(N),K1,K2,K3,CAG,VMC
      REAL VZ,VXLIME,C,XINT,H
      COMMON /CONST1/ K1,K2,K3,CAG
      COMMON /CONST2/ VMC
      COMMON /CONST3/ H
      COMMON /CONST5/ NZ,VZ(200),VXLIME(200)
      COMMON /CONST6/ C(200,3),IC
      CALL XINTER(VZ,VXLIME,NZ,C,IC,Z,XINT,IER)
      AREAF=(1.0+EXP(13.428*XINT-10.7424))/15.667
      RATE1=K2*AREAF*XINT**(2./3.)
      ALFA=(XINT**(-1./3.)-1.0)/(K1*SQRT(AREAF))
      RATE2=CAG*XSO2(1)/(ALFA+(1./K3))
      IF(RATE2.LT.RATE1) THEN
       DXSO2(1)=-(1./(VMC*CAG))*RATE2
      ELSE
       DXSO2(1)=-(1./(VMC*CAG))*RATE1
      ENDIF
      RETURN
      END


      SUBROUTINE FCNJ(N,Z,XSO2,PD)
      *********************************************************
C     THIS SUBROUTINE ESTIMATE THE PARTIAL DERIVATIVES OF XSO2.
C     NOT NEEDED IN OUR PROBLEM, SO A DUMMY SUBROUTINE WILL BE
C     USED.
      *********************************************************
      INTEGER N
      REAL XSO2(N),PD(N,N),Z
      RETURN
      END
```

```
SUBROUTINE XINTER(VZ,VXLIME,NZ,C,IC,ZINT,XINT,IER)
C      ************************************************************
C      THIS SUBROUTINE PROVIDE AN INTERPOLATED VALUE OF VXLIME
C      AT ANY GIVEN VALUE VALUE OF Z
C      THE VARIABLES ENTERING THE SUBROUTINE ARE:
C      VZ = VECTOR OF DISTANCES ALONG THE REACTOR WERE XLIME IS
C           AVAILABLE
C      VXLIME = FRACTION OF LIME REMAINING AT ANY GIVEN VZ
C      NZ = NUMBER OF GRID POINTS IN THE Z DIRECTION
C      IC = NZ-1
C      C = SPLINE COEFFICIENTS DETERMINED BY THE INTERPOLATION
C          ROUTINE ICSCCU. C IS A MATRIX OF NZ-1 BY 3
C      ZINT = VALUE OF Z WERE THE VXLIME IS DESIRED
C      THE OUTPUT OF THE PROGRAM ARE:
C      XINT = VALUE OF FRACTION OF LIME REMAINING AT Z = ZINT
C      IER = ERROR PARAMETER
C      **************************************************************
      INTEGER NZ,IC,IER,ISAV
      REAL VZ(NZ),C(IC,3),VXLIME(NZ),ZINT,XINT,D
      ISAV=0
      DO 10 I=1,NZ-1
      IF((VZ(I).LE.ZINT).AND.(ZINT.LT.VZ(I+1))) THEN
       ISAV=I
       GO TO 20
      ENDIF
   10 CONTINUE
   20 CONTINUE
       IF (ZINT.EQ.VZ(NZ)) ISAV=NZ-1
       IF (ISAV.EQ.0) THEN
        IER=60
         IF (ZINT.GE.VZ(NZ)) ISAV=NZ-1
         IF (ZINT.LT.0.0) ISAV=1
        DSLP=(VXLIME(ISAV+1)-VXLIME(ISAV))/(VZ(ISAV+1)-VZ(ISAV))
        XINT=VXLIME(ISAV+1)+DSLP*(ZINT-VZ(ISAV+1))
       ELSE
        IER=0
        D=ZINT-VZ(ISAV)
        XINT=((C(ISAV,3)*D+C(ISAV,2))*D+C(ISAV,1))*D+VXLIME(ISAV)
       ENDIF
      IF (XINT.LT.0.0) XINT=0.0
      IF (XINT.GT.1.0) XINT=1.0
      RETURN
      END
```

```
SUBROUTINE INTEGT(TINI,TEND,VXLN,DELTT,INDEX,IER)
C     ***********************************************************
C     THIS SUBROUTINE USE DGEAR TO INTEGRATE THE FRACTION
C     OF LIME REMAINING IN THE REACTOR AT TIME TEND, FOR
C     ALL GRID POINTS GIVEN THE FRACTION OF LIME REMAINING
C     AT EACH POINT AT TIME TINI.
C
C     THE VARIABLES ENTERING THE SUBROUTINE ARE:
C     TINI       = INITIAL TIME OF THE INTEGRATION
C     TEND        = FINAL TIME OF THE INTEGRATION (SEC)
C
C     VARIABLES ENTERING THROUGH COMMON BLOCK ARE:
C     NZ        = NUMBER OF POINT IN THE GRID
C     VZ(I)      = Z COORDINATE FOR ALL GRID POINTS
C     VXLIME(I) = FRACTION OF LIME REMAINING AT EACH GRID POINT
C                 AT TIME TINI
C     VXSO2(I)  = FRACTION OF SO2 REMAINING IN THE GAS AT EACH
C                 GRID POINT
C     K1        = CONSTANT FOR THE DIFFUSION OF SO2 THROUGH THE
C                 ASH LAYER
C     K2        = CONSTANT FOR THE CHEMICAL REACTION
C     K3        = CONSTANT FOR DIFFUSION OF SO2 THROUGH THE GAS
C                 FILM
C     CAG        = SO2 CONCENTRATION ENTERING THE REACTOR
C     NB         = MOLES OF LIME PLACED IN REACTOR
C                 SURFACE
C
C     VARIABLES EXITING THE SUBROUTINE ARE:
C     VXLN(I) = FRACTION OF LIME AT EACH GRID POINT AT TIME TEND
C     DELTT      = TIME STEP SIZE FROM DGEAR
C     IER        = ERROR PARAMETER FROM DGEAR
C     ******************************************************************
      DIMENSION VXLN(200),IWK(200),WK(3420)
      COMMON /CONST1/ K1,K2,K3,CAG
      COMMON /CONST4/ NB
      COMMON /CONST5/ NZ,VZ(200),VXLIME(200)
      COMMON /CONST6/ C(200,3),IC
      COMMON /CONST7/ VXSO2(200)
      EXTERNAL FTN,FTNJ
      INTEGER NZ,METH,MITER,INDEX,IER,IWK
      REAL TINI,TEND,DELTT,TOL,CAG,NB
      REAL VZ,VXSO2,VXLIME,VXLN,K1,K2,K3
      REAL WK
      DO 10 I=1,NZ
      VXLN(I)=VXLIME(I)
   10 CONTINUE
C      INITIALIZE VARIABLES IN DGEAR
      N=NZ
      METH=1
      MITER=0
```

```
 INDEX=1
 TOL=1.0E-6
 DELTT=(TEND-TINI)/10.0
 CALL DGEAR(N,FTN,FTNJ,TINI,DELTT,VXLN,TEND,TOL,METH,MITER,
&INDEX,IWK,WK,IER)
 RETURN
 END
```

```
SUBROUTINE FTN(N,TINI,VXLN,DXLIME)
C     ****************************************************************
C     THIS SUBROUTINE IS CALLED BY DGEAR IN THE TIME INTEGRATION
C     IT CALCULATE THE DERIVATIVE OF XLIME WITH RESPECT TO TIME
C     FOR EVERY GRID POINT.
C     ****************************************************************
      COMMON /CONST1/ K1,K2,K3,CAG
      COMMON /CONST4/ NB
      COMMON /CONST5/ NZ,VZ(200),VXLIME(200)
      COMMON /CONST6/ C(200,3),IC
      COMMON /CONST7/ VXSO2(200)
      INTEGER IER
      REAL TINI,VXLN(200),DXLIME(200),K1,K2,K3,CAG,NB,VXSO2
      DO 10 I=1,N
      AREAF=(1.0+EXP(13.428*VXLN(I)-10.7424))/15.667
      RATE1=K2*AREAF*VXLN(I)**(2./3.)
      ALFA=(VXLN(I)**(-1./3.)-1.0)/(K1*SQRT(AREAF))
      RATE2=CAG*VXSO2(I)/(ALFA+(1./K3))
      IF(RATE2.LT.RATE1) THEN
       DXLIME(I)=-(1./NB)*RATE2
      ELSE
       DXLIME(I)=-(1./NB)*RATE1
      ENDIF
 10   CONTINUE
      RETURN
      END


      SUBROUTINE FTNJ(N,TINI,VXLN,PD)
C     ****************************************************************
C     THIS SUBROUTINE IS CALLED BY DGEAR IN THE INTEGRATION
C     IN TIME IT ESTIMATE THE PARTIAL DERIVATIVES OF XLIME
C     WITH RESPECT TO TIME. NOT NEEDED IN OUR CASE, SO A
C     DUMMY SUBROUTINE WILL BE USED.
C     ****************************************************************
      REAL TINI,VXLN(200),PD(200,200)
      INTEGER N
      RETURN
      END
```

```
SUBROUTINE STPCHT(T,TEND,DELTT,INDEX,TPRINT)
C      **************************************************************
C      THIS SUBROUTINE DETERMINE IF THE DIFFERENCE BETWEEN T AND
C      TEND IS SMALL ENOUGH TO ENSURE AN ACCURATE INTEGRATION.
C      THE CRITERIA USED IS THAT DELTA = TEND -T MUST BE LESS
C      THAN 3 TIMES BUT GREATER THAN 1 TIMES DELTT, THE STEP
C      SIZE USED FOR DGEAR.
C      VARIABLES ENTERING THE SUBROUTINE ARE:
C
C      T = VALUE OF T AT WHICH THE INTEGRATION IS STARTED
C      TEND = VALUE OF T AT WHICH THE INTEGRATION END
C      DELTT = INTEGRATION STEP SIZE USED BY DGEAR
C      INDEX = DGEAR PARAMETER EQUAL TO 1 FOR FIRST CALL TO
C              DGEAR AND EQUAL TO 0 FOR OTHER CALLS.
C      TPRINT = MAXIMUN POSIBLE VALUE OF TEND
C      VARIABLES USED INSIDE SUBROUTINE:
C
C      DELTA = TEND - T, INTEGRATION STEP SIZE
C      VARIABLES LEAVING SUBROUTINE:
C
C      TEND = NEW VALUE FOR ENDING THE INTEGRATION OF DGEAR IF
C             STEP SIZE WAS CHANGED, OTHERWISE THE SAME ENTERING
C             VALUE
C      INDEX = PARAMETER WITH VALUE 1 IF STEP SIZE WAS CHANGED
C              AND VALUE 0 IF THE STEP SIZE WAS NOT CHANGED
C      **************************************************************
       INTEGER INDEX
       REAL T,TEND,DELTT,DELTA
       DELTA=TEND-T
        IF(DELTA.GT.3.0*DELTT) THEN
         TEND=T+DELTA*0.7
         INDEX=1
        ENDIF
        IF (DELTA.LT.(DELTT).AND.(TPRINT-TEND).GT.1.0E-6) THEN
         TEND=T+DELTA*1.7
         INDEX=1
        ENDIF
        IF (TEND.GE.TPRINT) TEND=TPRINT
       RETURN
       END
```

Appendix D.

Sample Calculation for Lime Conversion

The raw data from the experiments are concentrations of SO_2 leaving the reactor vs time. Figure D-1 shows the raw data obtained for Experiment 132, run at 74% RH, 64.4°C, using 1.0 g lime A with 10 mole% $NaNO_2$ as additive.

The SO_2 reacts with $Ca(OH)_2$ according to the reaction:

$$Ca(OH)_2 + SO_2 \rightarrow CaSO_3 \cdot 1/2H_2O + 1/2H_2O \qquad (D.1)$$

The fraction of $Ca(OH)_2$ converted, x_{lime} is given by;

$$x_{lime} = \frac{\text{gmol } Ca(OH)_2 \text{ reacted}}{\text{initial moles of } Ca(OH)_2} \qquad (D.2)$$

For each mol of SO_2 removed one mol of $Ca(OH)_2$ will react. Thus, Equation (D.2) can also be written as:

$$x_{lime} = \frac{\text{gmol } SO_2 \text{ removed}}{\text{initial moles of } Ca(OH)_2} \qquad (D.3)$$

The initial moles of $Ca(OH)_2$ can be calculated as

$$\text{initial amount of } Ca(OH)_2 \text{ (gmol)} = \frac{m}{\text{MW of } Ca(OH)_2} \qquad (D.4)$$

m being the amount of $Ca(OH)_2$ in the reactor in grams.

The amount of SO_2 removed can be obtained from a mass balance in the reactor as;

$$SO_2 \text{ removed (gmol)} = \int_0^t (C_{SO_2,in} - C_{SO_2,out})\, v_m \, dt \qquad (D.5)$$

Where:

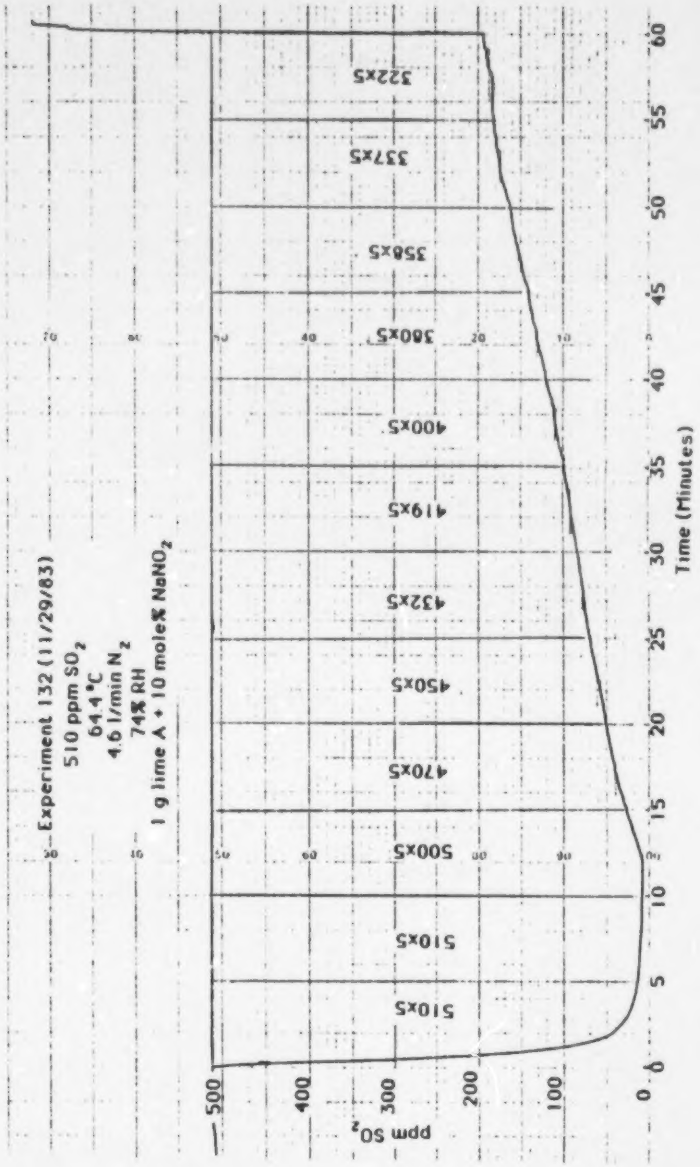

Figure D-1: Raw Data from Experiment 132

$C_{SO_2,in}$ = concentration SO_2 entering reactor (gmol/cm^3)

$C_{SO_2,out}$ = concentration SO_2 leaving reactor (gmol/cm^3)

v_m = volumetric flow rate of gas (cm^3/minutes)

t = time (minutes)

Assuming the gas phase behaves as an ideal gas, the SO_2 concentration can be expressed as;

$$C_{SO_2} = \frac{P_{SO_2}}{R\,T} = \frac{P\,x_{SO_2}}{R\,T} \qquad (D.6)$$

Where:

P_{SO_2} = partial pressure of SO_2 (atm)

P = total pressure (atm)

R = gas constant (atm cm$_3$/gmol K)

T = temperature (K)

x_{SO_2} = mole fraction of SO_2 = ppm $SO_2/10^6$

Substituting Equations (D.4) and (D.6) in Equation (D.5) one gets:

$$x_{lime} = \frac{P\,v_m}{R\,T\,m}\int_0^t (x_{SO_2,in} - x_{SO_2,out})\,dt \qquad (D.7)$$

The integral is given by the area A_t between the data curve in Figure D-1 and the horizontal line corresponding to the inlet SO_2 concentration. A_t has to be multiplied by 10^{-6} to convert ppm to mole fraction.

After substituting,

$P = 1$ atm

$T = 273$ K

$v_m = 4600$ cm^3/min

$m = 1$ g

$MW = 74.1$

The equation for conversion of $Ca(OH)_2$ as a function of A_t is:

$$Ca(OH)_2 \text{ Converted } (\%) = 1.573\, 10^{-3}\, A_t \qquad (D.8)$$

Integrating graphically the area A_t, the values of lime conversion shown in Table D-1 are obtained.

Table D-1: Conversion of $Ca(OH)_2$ versus reaction time

Experiment 132

74% RH, 64.4°C, 4.6 l/min N_2, 1 g lime A, 10 mole% $NaNO_2$

Time (minutes)	$Ca(OH)_2$ Converted (%)
5	4.0
10	8.0
15	12.0
20	15.7
25	19.2
30	22.6
35	25.9
40	29.0
45	32.0
50	34.8
55	37.5
60	40.0

Appendix E.

Error Analysis and Reproducibility

E.1 Error Analysis

The experimental results were presented as $Ca(OH)_2$ conversion versus time curves. $Ca(OH)_2$ conversion was determined by a gas phase material balance (explained in detail in Appendix D) and/or solids analysis. In the calculation of $Ca(OH)_2$ conversion by gas phase material balance the following equation was obtained for the fraction of lime converted:

$$x_{\text{lime}} = \frac{P\, v_m}{R\, T\, m} \int_0^t \left(x_{SO_2,\text{in}} - x_{SO_2,\text{out}}\right) dt = \frac{P\, v_m}{R\, T\, m} A_t \qquad (E.1)$$

Where:

x_{lime} = molar fraction of $Ca(OH)_2$ converted at any given time t

P = atmospheric pressure (mm Hg)

v_m = volumetric flow rate of gas at 24°C and 1 atm (cm^3/min)

R = gas constant (mm Hg cm_3/gmol K)

T = temperature (K)

m = amount of $Ca(OH)_2$ in the reactor (g)

t = time (min)

x_{SO_2} = mole fraction of SO_2 = ppm $SO_2/10^6$

A_t = area representing the integral (ppm min)

Using Equation (E.1) the fractional error of x_{lime} will be given by:

$$\frac{\Delta x_{\text{lime}}}{x_{\text{lime}}} = \frac{\Delta P}{P} + \frac{\Delta v_m}{v_m} + \frac{\Delta T}{T} + \frac{\Delta m}{m} + \frac{\Delta A_t}{A_t} \qquad (E.2)$$

The atmospheric pressure was measured with a mercury barometer having a precision of 0.1 mm Hg (0.01%) and an accuracy of 0.05%. The gas flowrate was measured with a rotameter (LabCrest Century) that has a precision of 2% and 5% accuracy according to the manufacturer. As the rotameter was calibrated in the laboratory using a wet test meter with 0.5% accuracy and the measured calibration curve was used instead of the one provided by the manufacturer, the accuracy of the gas flowrate measurement is believed to be far better than 5%. A conservative value of 3% for the accuracy of the gas flowrate measurement will be used in the calculations. The temperature was measured with a mercury thermometer with 0.1°C precision and 0.5°C accuracy. Finally, the SO_2 concentration was measured with 1% precision and 2% accuracy with a Thermoelectron pulsed fluorescent SO_2 analyzer calibrated weekly with a SO_2/N_2 standard gas (± 1%). With a typical SO_2 concentration of 500 ppm, a 2% error in the SO_2 concentration will lead to an error in the area $\Delta A_t = 0.02(500 \text{ ppm})(60 \text{ min}) = 600$ ppm min. In the worst case, when the lime conversion after one hour of reaction was 12%, which corresponds to 25% average SO_2 removal, $A_t = .25(500 \text{ ppm})(60 \text{ min}) = 7500$ ppm min.

Substituting the values of the variables in Equation (E.2):

$$\frac{\Delta x_{lime}}{x_{lime}} = \frac{0.0005\,P}{P} + \frac{0.03\,v_m}{v_m} + \frac{0.05}{24 + 273.15} + \frac{0.00005}{1} + \frac{600}{7500} \qquad \text{(E.3)}$$

$$= 0.112$$

So, with relatively large amounts of $Ca(OH)_2$ (1 g or more) giving high SO_2 removal, conversion will be calculated with 11 % accuracy. With smaller amounts of $Ca(OH)_2$ and reduced SO_2 removal (differential experiments), integrating the SO_2 concentration curve introduces larger errors. Therefore, $Ca(OH)_2$ conversion in differential experiments can only be determined by solids analysis.

The chemical analysis was performed by combined iodometric and acid/base titration. The analysis was made with the entire amount of products solids, so selective sampling was not a problem. It determines total sulfite and total free $Ca(OH)_2$. The conversion is calculated assuming there is no $CaSO_4$ formed. It is difficult to determine the accuracy of this chemical analysis, but when tested with known samples of $CaSO_3$ and $Ca(OH)_2$, the method predicted the compositions with less than 2% error. It is believed then, that using O_2 free nitrogen to prevent oxidation, an accuracy of at least 10% can be expected.

$Ca(OH)_2$ conversion is a strong function of relative humidity. The relative humidity was calculated as:

$$RH(\%) = \frac{p}{p^*} 100 \qquad (E.4)$$

Where:

p = partial pressure of water vapor (mm Hg)

p^* = saturation pressure of water at reactor temperature (mm Hg)

The partial pressure of water vapor (p) was calculated as:

$$p = \frac{H P_e}{\frac{MW_{water}}{MW_{nitrogen}} + H} \qquad (E.5)$$

Where:

H = absolute humidity (g water/g nitrogen)

P_e = total pressure at reactor entrance (mm Hg)

MW_{water} = molecular weight of water = 18

$MW_{nitrogen}$ = molecular weight of nitrogen = 28

With absolute humidity given by:

$$H = \frac{m_{water}}{m_{nitrogen}} \tag{E.6}$$

The mass flowrate of water (m_{water}) is given directly by the syringe pump, and the mass flowrate of nitrogen ($m_{nitrogen}$) is calculated from the volumetric flowrate of nitrogen at 24°C and atmospheric pressure, assuming ideal gas behavior:

$$m_{nitrogen} = \frac{P\, v_m\, MW_{nitrogen}}{R\, T} \tag{E.7}$$

According to Equation (E.7), the error in the mass flowrate of nitrogen is given by:

$$\frac{\Delta m_{nitrogen}}{m_{nitrogen}} = \frac{\Delta P}{P} + \frac{\Delta v_m}{v_m} + \frac{\Delta T}{T} \tag{E.8}$$

Substituting in Equation (E.8) one gets:

$$\frac{\Delta m_{nitrogen}}{m_{nitrogen}} = \frac{0.0005\Delta P}{P} + \frac{0.03\Delta v_m}{v_m} + \frac{0.5}{24 + 273.15} = .0355 \tag{E.9}$$

The fractional error of the absolute humidity is obtained from Equation (E.6) as:

$$\frac{\Delta H}{H} = \frac{\Delta m_{water}}{m_{water}} + \frac{\Delta m_{nitrogen}}{m_{nitrogen}} \tag{E.10}$$

Using the results of Equation (E.9) and the fact that the water was injected with a calibrated Sage syringe pump with 2% precision and 3% accuracy, one gets:

$$\frac{\Delta H}{H} = 0.03 + 0.0355 = .0655 \qquad (E.11)$$

The fractional error of the partial pressure of the water can be obtained from Equation (E.5) as:

$$\frac{\Delta p}{p} = \frac{1}{H} + \frac{1}{\dfrac{MW_{water}}{MW_{nitrogen}} + H} \quad \Delta H + \frac{\Delta P_e}{P_e} \qquad (E.12)$$

The total pressure at the reactor entrance was obtained by adding the barometric pressure (typically 746.3 mm Hg, measured with 0.05% accuracy) to the pressure drop across the system (typically 86 mm Hg) measured with a mercury manometer with an accuracy of 5 mm Hg (5%). The uncertainty in the pressure at the reactor entrance will be then the sum of the error of the two pressure measurements, or 5.4 mm Hg. Substituting these values of the variables and a typical value of 0.0964 for the absolute humidity in Equation (E.12) one gets:

$$\frac{\Delta p}{p} = \frac{1}{0.0964} + \frac{1}{\dfrac{18}{28} + H} \quad 0.0655(0.0964) + \frac{5.4}{746.3 + 86} = 0.08 \qquad (E.13)$$

Finally, the fractional error of the relative humidity can be obtained from Equation (E.4), and is given by:

$$\frac{\Delta RH}{RH} = \frac{\Delta p}{p} + \frac{\Delta p^*}{p^*} \qquad (E.14)$$

The temperature in the reactor was typically 66°C, measured with 0.1°C accuracy. At this temperature the vapor pressure of the water is 196.09 mm Hg, and 0.1°C of change in the temperature will cause a variation of 0.855 mm Hg in the vapor pressure. Substituting these values in Equation (E.14) one gets:

$$\frac{\Delta \mathrm{RH}}{\mathrm{RH}} = \frac{8.65}{107.37} + \frac{0.855}{196.09} = 0.085 \tag{E.15}$$

The error in the calculated relative humidity is then ± 8.5%.

E.2 Reproducibility of Results

During actual operation of the apparatus, when multiple experiments at identical conditions were performed, the deviation of the lime conversion from the average conversion of multiple experiments was below ± 8%. The maximum deviation of the lime conversion between experiments was below 15%. Figures E-1 and E-2 illustrate two sample cases, one for three experimental runs made using pure $Ca(OH)_2$, and the other for experimental runs made using 10 mole% NaCl as additive. All these experiments were run on different days. We can see from the figure that the deviation between the experimental runs is in general much less than 15%.

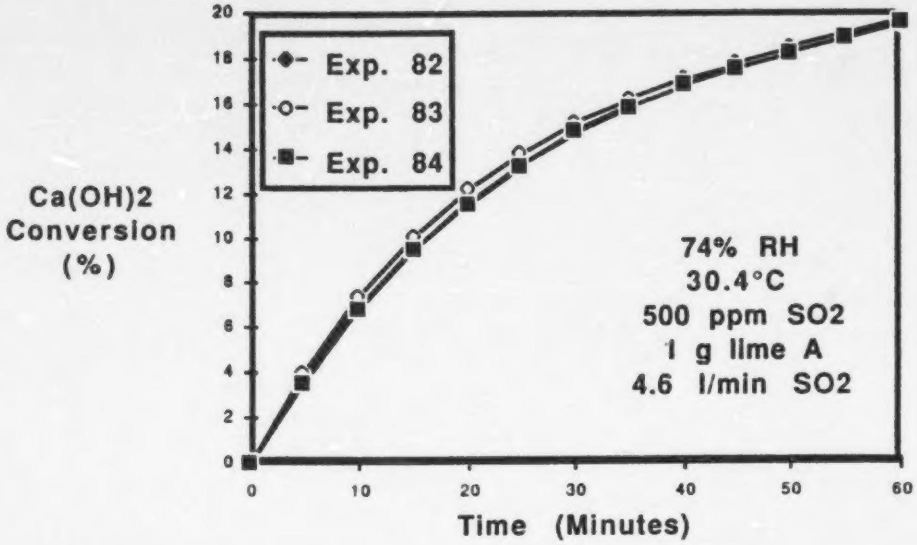

Figure E-1: Reproducibility of results, pure $Ca(OH)_2$

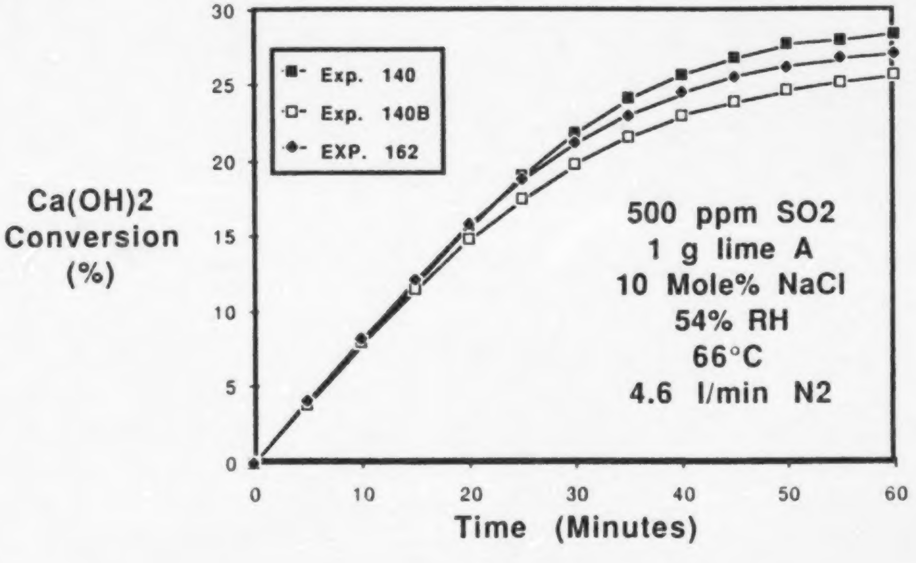

Figure E-2: Reproducibility of results, $Ca(OH)_2$ with 10 mole% NaCl

E.3 Quality Assurance

Current EPA policy requires a quality assurance project plan for all extramural projects. Since no formal plan for this project was on record at the time these data were obtained, the following disclaimer is added:

"Quality assurance/quality control requirements are applicable to this project. The data contained in this report are not supported by QA/QC documentation as required by U. S. EPA Quality Assurance Policy".

Bibliography

Ablin, D. W. "Dry Injection: The Development of An Emerging Technology," in *Proceedings: First Annual Pittsburgh Coal Conference.* Pittsburgh,Pennsylvania: United States Department of Energy, 1984, pp. 272-279.

Akhtar, S., Friedman, S. and Yavorsky, P. M. "Process for Hydrosulfurization of Coal in Turbulent Flow Fixed Bed Reactor." *AIChE Symposium Series*, 70, No. 137 (1974), pp. 106-113.

Bagwell, F. A., Cox, L. F. and Push, E. A. "Design and Operation Experience: A Filterhouse Installed on an Oil Fired Boiler." *Journal of the APCA*, 19 (1969), pp. 149.

Barthel, Y., Bonnifay, P., Dutriau, R. and Renault, P. "Relative Economics of Residual Desulfurization vs Stack Gas Cleanup." *AIChE Symposium Series*, 70, No. 137 (1974), pp. 155-159.

Bechtel Corporation. *Evaluation of Dry Alkalis for Removing Sulfur Dioxide from Boiler Flue Gases* (Project Final Report EPRI FP-207). Electric Research Institute, October 1976.

Belt, R. J. and Roder, M. M. "Low Sulfur Fuel by Pressurized Entrainment Carbonization of Coal," in *Pollution Control and Energy Needs*, Ed. Jimeson, R. M. and Spindt, R. S., *Advances in Chemistry Series.* Washington, D. C.: American Chemical Society, 1973, pp. 121-134.

Bjerle, I., Klingspor, J. and Karlsson, H. T. *Sulfur Capture by Promoted Limestone.* Presented at the 11th Annual Stack Gas Meeting, October 5-7, Paducah, Kentucky, 1983.

Blythe, G. M. and Rhudy, R. G. "EPRI Spray Dryer/Baghouse Pilot Plant Status and Results," in *Proceedings: Eighth Symposium on Flue Gas Desulfurization, New Orleans, LA, November 1983, Volume 2.* Report EPA-600/9-84-017b, NTIS No. PB 84-223 049, 1984, pp. 708-734.

Blythe, G. M., Dickerman, J. C. and Kelly, M. E. *Survey of Dry SO_2 Control Systems.* Report EPA-600/7-80-030, NTIS No. PB 80-166 853, Environmental Protection Agency, February, 1980.

Blythe, G. M., Burke, J. M., Kelly, M. E., Rohlack, L. A. and Rhudy, R. G. "EPRI Spray Drying Pilot Plant Status and Results," in *Proceedings: Symposium on Flue Gas Desulfurization, Volume 2.* Report EPA-600/9-83-020b, NTIS No. PB84-110 584, 1983, pp. 595-627.

Blythe, G. M., Burke, J. M., Lewis, D. L., Thompson, C., Brna, T. G. and Rhudy, R. G. *Field Evaluation of a Utility Dry Scrubbing System* (Final Report EPRI CS-3954). Electric Power Research Institute, May 1985.

Blythe, G. M., Burke, J. M., Brna, T. G. and Rhudy, R. G. "Field Evaluation of a Utility Dry Scrubbing System," in *Proceedings: Eighth Symposium on Flue Gas Desulfurization, New Orleans, LA, November 1983, Volume 2.* Report EPA-600/9-84-017b, NTIS No. PB 84-223 049, 1984a, pp. 736-757.

Bobman, M. H., Weber, G. F. and Keener, T. C. *Additive Enhancement of Pressure-Hydrated Lime for Control of SO_2/NO_x Emissions.* Presented at AIChE 1985 Spring National Meeting, March 24-28, Houston, Texas, 1985.

Borgwardt, R. H., Roache, N. F. and Bruce, K. R. "Surface Area of Calcium Oxide and Kinetics of Calcium Sulfide Formation." *Environm. Progr.*, 3, No. 2 (May 1984), pp. 129-35.

Bresowar, G. E., Borsare, D. C. and Walki, K. W. *Dry Scrubber Design and Application. The C-E Approach.* Presented at the Joint Power Generation Conference, St. Louis, Missouri, October 1981.

Brunauer, S., Emmett, P. H. and Teller, E. "Adsorption of Gases in Multimolecular Layers." *J. Am. Chem. Soc.*, 60 (1938), pp. 309-319.

Brzozowski, K. J. and Kumins, C. A. "Barrier Properties of Earth Lining for Pollution Control." *Polym. Sci. Technol.*, 6 (1974), pp. 321-330.

Burbank, D. A., Wang, S. C., McKinsey, R. R. and Williams, J. E. "Test Results of Adipic Acid-Enhanced Limestone Scrubbing at the EPA Shawnee Test Facility--Third Report," in *Proceedings: Symposium on Flue Gas Desulfurization-Houston, October 1980, Volume 1.* Report EPA-600/9-81-019a, NTIS No. PB 81-243156, 1981, pp. 233-286.

Burke, J. M., Metcalfe, R. P., Cmiel, R. and Mobley, J. D. "Technical and Economic Evaluation of Organic Acid Addition to the San Miguel FGD System. Part 1. Results of Parametric Tests," in *Proceedings: EPA's Industry Briefing on the Organic-Acid-Enhanced Limestone FGD Process (July 1984).* Report EPA 600/9-85-009, NTIS No. PB 85-181 105, 1985, pp. 1-35.

Burnett, T. A. and O'Brien, W. E. *Preliminary Economic Analysis of a Lime Spray Dryer FGD System.* Report EPA-600/7-80-050, NTIS No. PB 80-190 051, Environmental Protection Agency, March 1980.

Burnett, T. A., Anderson, K. D. and Torstrick, R. L. "Spray Dryer FGD: Technical Review and Economic Assessment," in *Proceedings: Symposium on Flue Gas Desulfurization-Houston, October 1980, Volume 2.* Report EPA-600/9-81-019b, NTIS No. PB 81-243 164, 1981, pp. 713-729.

Burnett, T. A., Larkin, L. and Torstrick, R. L. *Economic Analysis and Comparison of Wet and Dry Scrubbing for Utility Application.* Presented at the Seminar on Dry Scrubbing Sponsored by Western Precipitation/Niro Atomizer, June 26-29, Minneapolis, Minnesota, 1981a.

Cavallaro, J. A., Deurbrouck, A. W. and Baker, A. F. "Physical Desulfurization of Coal." *AIChE Symposium Series*, 70, No. 137 (1974), pp. 114-122.

Chan, P. K. *$CaCO_3$ Dissolution in SO_2 Scrubbing Solutions; Mass Transfer Enhanced by Chemical Reactions*. Master's thesis, University of Texas at Austin, 1981.

Chan, P. K. and Rochelle, G. T. "Limestone Dissolution; Effects of pH, CO_2, and Buffers Modelled by Mass Transfer." *ACS Symposium Series*, 188 (1982), pp. 75-97.

Chang, C. S. and Rochelle, G. T. "Effect of Organic Acid Additives on SO_2 Adsorption into $CaO/CaCO_3$ Slurries." *AIChE J.*, 28, No. 2 (1982), pp. 261-265.

Chopra, O. K., Smith, G. W., Lenc, J. F., Shearer, K. M., Myles, K. M. and Johnson, I. "Effect of Salt Treatment of Limestone on Sulfation and on the Corrosion Behavior of Materials in AFBC Systems," in *The Proceedings of the Sixth International Conference on Fluidized bed Combustion*. Atlanta, Georgia, 1980.

Clarke, A. J. *Emission of Sulfur Dioxide, Nitrogen Oxides, and Particulate Matter from Coal-Burning Power Stations,* 1st. [Environmental Effects of Utilizing More Coal.] Kent: Whitstable Litho Ltd., 1980.

Coulter Electronics, Inc. *Coulter Counter Model TAII Operator's Manual*. Haileah, Fl.: January 1980.

Dick, J. G. *Analytical Chemistry*. N. Y.: McGraw-Hill Book Co., 1973.

Donnelly, J. R., Wilson, S., Matis, L. P., Eriksen, R., Emerson, R. D. and Fooks, J. C. "Spray Dryer FGD Experience. Joy-Niro Installations," in *Ninth Symposium on Flue Gas Desulfurization, Cincinnati, Ohio, June 1985, Volume 2*. Report EPA-600/9-85-033b, NTIS No PB 86-138658, 1985, pp. 580-601.

Downs, W., Sanders, W. J. and Miller, C. E. *Control of SO_2 Emissions by Dry Scrubbing*. Presented to the American Power Conference, April 21-23, Chicago,Illinois, 1980.

Environmental Protection Agency. *National Air Pollutant Emission Estimates, 1970-1981*. Report EPA-450/4-82-012, September 1982.

Farber, P. S. "Dry Scrubbing for High-Sulfur-Coal Utilization," in *Proceedings: First Annual Pittsburgh Coal Conference*. Pittsburgh, PA: University of Pittsburgh, 1984, pp. 280-288.

Felsvang, K., Gude, K. and Kaplan, S. "SO_2 Spray Absorption with Dry Wastes," in *Proceedings: Symposium on Flue Gas Desulfurization-Hollywood, FL, November 1977, Volume II*. Report EPA-600/7-78-058b, NTIS No. PB 282-091, 1978, pp. 1017-1021.

Felsvang, K., Morsing, P. and Veltman, P. "Acid Rain Prevention Thru New SO_2/NO_x Dry Scrubbing Process," in *Proceedings: Eighth Symposium on Flue Gas Desulfurization, New Orleans, LA, November 1983, Volume 2*. Report EPA-600/9-84-017b, NTIS No. PB 84-223 049, 1984, pp. 650-667.

Felsvang, K. S., Hansen, O. E. and Rasmussen, E. I. *Process for Flue Gas Desulfurization*. U.S. Patent 4,279,873, July 21, 1981.

Ferron, G. A. "The Size of Soluble Aerosol Particles as a Function of the Humidity of the Air. Application to the Human Respiratory Tract." *J. Aerosol Sci.*, 8 (1977), pp. 251-267.

Forsythe, R. C. and Kaiser, R. A. *Hydrate Addition at Low Temperature SO_2 Removal in Conjunction with a Baghouse*. Presented at the Third Conference on Fabric Filter Technology for Coal-Fired Power Plants, 1986.

Genco, J. M. and Rosenberg, H. M. "Sorption of SO_2 on Ground Nahcolite Ore." *Journal of the APCA*, 26, No. 10 (1976), pp. 989-90.

Genco, J. M., Rosenberg, H. S., Anastas, M. Y., Robar, C. C. and Dulin, J. M. "The Use of Nahcolite Ore and Bag Filters for Sulfur Dioxide Emission Control." *Journal of the APCA*, 25, No. 12 (1975), pp. 1244-53.

Getler, J. L. and Furlong, H. L. "Modeling the Spray Absorption Process for SO_2 Removal." *Journal of the APCA*, 29, No. 12 (December 1979), pp. 1270-1274.

Glover, R. L., Brown, G. E., Dickerman, J. C. and Hargrove O. W. "Results of the First Two Years of Commercial Operation of an Organic-Acid-Enhanced FGD System," in *Proceedings: EPA's Industry Briefing on the Organic-Acid-Enhanced Limestone FGD Process (July 1984)*. Report EPA 600/9-85-009, NTIS No. PB 85-181 105, 1985, pp. 46-57.

Goldstein, J. I., Yakowitz, H., Newbury, D. E., Lifshin, E., Colby, J. W. and Coleman, J. R. *Practical Scanning Electron Microscopy*, 3rd. N. Y.: Plenum Press, 1975.

Green, L. Jr. "Emission Control Alternatives," in *Proceedings: First Annual Pittsburgh Coal Conference*. Pittsburgh, PA: University of Pittsburgh, 1984, pp. 21-31.

Gregoli, A. A. and Hartos, G. R. "Hydrodesulfurization of Residuals," in *Pollution Control and Energy Needs*, Ed. Jimeson, R. M. and Spindt, R. S., *Advances in Chemistry Series*. Washington, D. C.: American Chemical Society, 1973, pp. 98-104.

Grutle, R. O. M. and Gehri, D. C. "Perspectives on the Development of Dry Scrubbing - The Coyote Story," in *Proceedings:Symposium on Flue Gas Desulfurization-Houston, October 1980, Volume* 2. Report EPA-600/9-81-019b,NTIS No. PB 81-243 164, 1981, pp. 1009-1020.

Gunther, G. W., Meyler, J. A. and Hansen, S. K. *The Riverside Station Dry Scrubbing System*. Presented at the Third Symposium on the Transfer and Utilization of Particulate Control Technology, July 1981.

Gustke, J. M., Morgan, W. E. and Wolf, S. H. "Overview and Evaluation of Two Years of Operation and Testing of the Riverside Spray Dryer System," in *Proceedings: Eighth Symposium on Flue Gas Desulfurization, New Orleans, LA, November 1983, Volume 2*. Report EPA-600/9-84-017b, NTIS No. PB 84-223049, 1984, pp. 758-787.

Hellinckx, J. R. "Combustion Rate of Coal Shale." *Chem. Eng. Sci.*, 3 (1954), pp. 201-208.

Hill, C. G. Jr. *An Introduction to Chemical Engineering Kinetics & Reactor Design*, 2nd. N. Y.: John Wiley & Sons, 1977.

Hills, A. D. W. "The Mechanism of the Thermal Decomposition of Calcium Carbonate." *Chem. Eng. Sci.*, 23 (1968), pp. 297.

Hollett G. T. Jr. *Dry Removal of SO_2 - Application to Industrial Coal-Fired Boilers*. Presented at the 72nd Annual Meeting of the Air Pollution Control Association, June 24-29, Cincinnati, Ohio, 1979.

Horn, R. J. and Bent, J. F. "Performance of Dry FGD on a Petroleum Coke Kiln Application." *Journal of the APCA*, Vol. 34, No. 9 (September 1984), pp. 982-86.

Hunter, T. W. "Low Sulfur Coal Supplies for Environmental Purposes," in *Pollution Control and Energy Needs*, Ed. Jimeson, R. M. and Spindt, R. S., *Advances in Chemistry Series*. Washington, D. C.: American Chemical Society, 1973, pp. 17-23.

Hurst, T. B. and Bielawski, G. T. "Dry Scrubber Demonstration Plant - Operating Results," in *Proceedings:Symposium on Flue Gas Desulfurization - Houston, October 1980, Volume 2*. Report EPA-600/9-81-019b, NTIS No. PB 81-243 164, 1981, pp. 853-860.

Jankura, B. J., Doyle, J. B. and Flynn, T. J. "Dry Scrubber, Flue Gas Desulfurization on High-Sulfur, Coal-Fired Steam Generators: Pilot-Scale Evaluation," in *Proceedings: Eighth Symposium on Flue Gas Desulfurization, New Orleans, November 1983, Volume 2*. Report EPA-600/9-84-017b, NTIS No. PB 84-223049, 1984, pp. 689-707.

JCPDS. *Powder Diffraction File: Inorganic Phases*. Swarthmore, Pennsylvania: JCPDS International Diffraction Data, 1984.

Johnson, A. R., Wolk, A. R., Hippeli, R. F. and Nongbri, G. "H-Oil Desulfurization of Heavy Fuels," in *Pollution Control and Energy Needs,* Ed. Jimeson, R. M. and Spindt, R. S., *Advances in Chemistry Series*. Washington, D. C.: American Chemical Society, 1973, pp. 105-120.

Jones, B. F., Lowell, P. S. and Meserole, F. B. *Experimental and Theoretical Studies of Solid Solution Formation in Limestone and Limestone SO_2 Scrubbers*. Volume I, Report EPA-600/2-76-273a, NTIS No. PB 264954, October 1976.

Jorgensen, C., Chang, J. C. S. and Brna, T. G. *Evaluation of Sorbents and Additives for Dry SO_2 Removal.* Presented at the Spring National AIChE Meeting, April 6-10, New Orleans, 1986.

Jozewicz, J. and Rochelle, G. T. "Fly Ash Recycle in Dry Scrubbing." *Env. Prog.*, 5 (1986), pp. 218-223.

Kaplan, S. M. and Felsvang, K. "Spray Absorption of SO_2 from Industrial Boiler Flue Gas." *AIChE Symposium Series*, Vol. 76, No. 201 (1980), pp. 23.

Kaplan, S. M., Chen, Y., Hyde, R. C., Sannes, C. A. Jr. and Skinner, M. F. "Dry Scrubbing at the Northern States Power Company Riverside Generating Plant," in *Proceedings: Symposium on Flue Gas Desulfurization, Volume 2*. Report EPA-600/9-83-020b, NTIS No. PB 84-110 584, 1983, pp. 650-672.

Karlsson, H. T., Klingspor, J., Linne, M. and Bjerle, I. "Activated Wet-Dry Scrubbing of SO_2. *Journal of the APCA*, 33, No. 1 (1983), pp. 23

Kelly, M. E. and Dickerman J. C. "Current Status of Dry Flue Gas Desulfurization Systems," in *Proceedings:Symposium on Flue Gas Desulfurization-Houston, October 1980, Volume 2*. Report EPA-600/9-81-019b, NTIS No. PB 81-243 164, 1981, pp. 761-776.

Kelly, M. E. and Shareef, S. A. *Third Survey of Dry SO_2 Control Systems*. Report EPA-600/7-81-097, NTIS No. PB 81-218 976, Environmental Protection Agency, June 1981.

Kelly, M. E. and Shareef, S. A. *Second Survey of Dry SO_2 Control Systems*. Report EPA-600/7-81-018, NTIS No. PB 81-157 919, Environmental Protection Agency, February 1981a.

Kelly, M. E., Kilgroe, J. D. and Brna, T. G. "Current Status of Dry SO_2 Control Systems," in *Proceedings: Symposium on Flue Gas Desulfurization, Volume 2*. Report EPA-600/9-83-020b, NTIS No. PB84-110 584, 1983, pp. 550-573.

Kirk-Othmer, ed. Vol. 11: *Encyclopedia of Chemical Technology*, 3rd. N. Y.:John Wiley & Sons, 1980.

Klingspor, J, Karlsson, H. T. and Bjerle, I. "A Kinetic Study of the Dry SO_2 - Limestone Reaction at Low Temperature." *Chem. Eng. Commun.*, 22 (1983), pp. 81-103.

Klingspor, J., Stromberg, A., Karlsson, H. T. and Bjerle, I. "Similarities Between Lime and Limestone in Wet-Dry Scrubbing." *Chem. Eng. Process.*, 18, No. 5 (1984), pp. 239-247.

Lange, N. A., ed. *Lange Handbook of CHemistry*, 10th. N. Y.: Mc Graw Hill, 1961.

Lewis, M. F. and Gehri, D. C. "Atomization - The Key to Dry Scrubbing at the Coyote Station," in *Proceedings: Symposium on Flue Gas Desulfurization, Volume 2*. Report EPA-600/9-83-020b, NTIS No. PB84-110584, 1983, pp. 673-687.

Lindau, L. and Ahman, S. *Removing Acid Gas Components from Gases, Specially Sulfur Dioxide from Flue Gas*. SE Patent Appl. 80/6,603, 22 Sept., 1980. Chemical Abstracts 96:222605 (1982).

Lisauskas, R. A., Itse, D. C. and Masser, C. C. *Evaluation of a Prototype Burner for Combined NO_X/SO_2 Control*. Presented at AIChE 1985 Spring National Meeting, March 24-28, Houston, Texas, 1985.

Lu, W. and Bistsianes, G. "The General Rate Equation for Gas-Solid Reactions in Metallurgical Processes. II With the Restriction of Reversibility of Chemical Reaction and Gaseous Equimolal Counterdiffusion." *Trans. Met. Soc.* AIME, 236 (1966), pp. 531.

Lutz, S. J., Christman, R. C., McCoy, B. C., Mulligan, S. W. and Slimak, K. M. *Evaluation of Dry Sorbents and Fabric Filtration for FGD*. Report EPA-600/7-79-005, NTIS No. PB 289-921, Environmental Protection Agency, January 1979.

MacDonald, R. W. and Huang, Y. M. "Permeation of Gases through Modified Polymers Films. V. Permeation and Diffusion of Helium, Nitrogen, Methane, Ethane and Propane through γ-Ray Crosslinked Polyethylene." *J. Appl.Polym. Sci.*, 26 (1981), pp. 2239-2263.

Maloney, K. L. "Sulfur Capture in Coal Flames." *AIChE Symposium Series*, Vol. 76, No. 201 (1980), pp. 31-37.

Marchello, J. M. *Chemical Processing and Engineering Series of Monographs and Textbooks. Control of Air Pollution Sources*. N. Y.: Marcel Dekker Inc., 1976.

Martin, J. R., Ferguson, W. B. and Frabotta, D. *C-E Dry Scrubber System: Application to Western Coals*. Presented at the 42nd Annual American Power Conference, Chicago, Illinois, April 1980.

Masters, K. "Spray Drying in Environmental Control with Special Reference to Flue Gas Desulfurization," in *Proceedings of the 2nd International Symposium Drying'80*. Ed. Arun S. Mujumdar. N. Y.: Hemisphere Publishing Co., 1980, pp. 401-404.

Mc Clellan, A. L. and Harnsberger, H. F. "Cross-Sectional Areas of Molecules Adsorbed on Solid Surfaces." *J. Colloid and Interface Sci.*, 23 (1967), pp. 577-599.

McBride, J. S., Massaro, T. A. and Cooper, S. L. "Diffusion of Gases Through Polyurethane Block Polymers." *J. Appl. Polym. Sci.*, 33 (1979), pp. 201-214.

McKewan, W. M. "Reduction Kinetics of Hematite in Hydrogen-Water Vapor-Nitrogen Mixtures." *Trans. Met. Soc. AIME*, 224 (1962), pp. 2.

Melia, M. T., McKibben, R. S. and Pelsor, B. W. *Utility FGD Survey July 1982-March 1983* (Project Summary EPRI Contract No.RP982-32). Electric Power Research Institute, August 1983.

Minoura, N., Fujiwara Y. and Nakagawa T. "Gas Permeability of Copolypeptide Membranes Composed of γ-Methyl L-glutamate and γ-Benzil L-glutamate." *J. Appl. Polym. Sci.*, 26 (1981), pp. 1301-1308.

Moriber, G. *Environmental Science*. Boston: Allyn and Bacon Inc., 1974.

Morrell, G. P., Oliver, D. R. and Reed, J. L. "The Supply of Oil for Future U. S. Needs and the Subsequent Effects in the Environment," in *Pollution Control and Energy Needs,* Ed. Jimeson, R. M. and Spindt, R. S., *Advances in Chemistry*. Washington, D. C.: American Chemical Society, 1973, pp. 24-32.

Mortimer, C. T. "Differential Scanning Calorimetry," in *Thermochemistry and Its Applications to Chemical and Biochemical Systems*, Ed. M. A. V. Rebeiro da Silva, NATO ASI Series. Dordrecht, Holland: Reidel Publishing Co., 1984, pp. 47-60.

Mueller, A. W. and Winston, A. E. "The Chemistry of Sodium Dry Sorbent Injection," in *Ninth Symposium on Flue Gas Desulfurization, Cincinnati, Ohio, June 1985, Volume 2*. Report EPA-600/9-85-033b, NTIS No PB 86-138658, 1985, pp. 902-921.

Muzio, L. J., Arand, J. K. and Shah, N. D. "Dry SO_2-[2] Removal with Nahcolite and Trona," in *Proceedings of Second Conference on Air Quality Management in the Electric Power Industry*. Austin, Texas: University of Texas at Austin, 1980.

Muzio, L. J., Sonnichsen, T. W., Hooper, R. G., Green, G. P., Brines, H. G. and Shah, N. D. "Demonstration of SO_2 Removal on a Coal-Fired Boiler by Injection of Dry Sodium Compounds," in *Proceedings: Symposium on Flue Gas Desulfurization, Volume 2*. Report EPA-600/9-83-020b, NTIS No. PB84-110 584, 1983, pp. 628-648.

Narsimhan, G. "Thermal Decomposition of Calcium Carbonate." *Chem. Eng. Sci.*, 16 (1961), pp. 7-20.

National Research Council. Vol. 3: *International Critical Tables*. New York: Mc Graw Hill, 1930.

NGPSA, ed. *Engineering Data Book*, Eighth Edition. Tulsa, Oklahoma: Natural Gas Processors Suppliers Association, 1966.

Olsen, E. D. *Modern Optical Methods of Analysis*. N. Y.: McGraw Hill Book Co., 1975.

Parsons, E. L., Hemenway, L. F., Kragh, O. T., Brna, T. G. and Ostop, R. L. "SO_2 Removal by Dry FGD," in *Proceedings:Symposium on Flue Gas Desulfurization-Houston, October 1980, Volume 2*. Report EPA-600/9-81-019b, NTIS No. PB 81-243 164, 1981, pp. 801-854.

Parsons, E. L., Boscak, V., Brna, T. G. and Ostop, R. L. "SO_2 Removal by Dry Injection and Spray Absorption Techniques," in *Third Symposium on the Transfer and Utilization of Particulate Control Technology, Volume I*. Report EPA-600/9-82-005a, NTIS No. PB83-149 583, 1982, pp. 303-312.

Perry, R. H., Chilton, C. H., ed. *Chemical Engineer's Handbook*, 5th. N. Y.: McGraw Hill, 1973.

Qader, S. A. and Hill, S. A. "Production of Low Sulfur Fuel from Utah Coals," in *Pollution Control and Energy Needs*, Ed. Jimeson, R. M. and Spindt, R. S., *Advances in Chemistry*. Washington, D. C.: American Chemical Society, 1973, pp. 91-97.

Ranz, W. E. and Marshall, W. R. Jr. "Evaporation from Drops." *Chem. Eng. Prog.*, 48, No. 3 (March 1952), pp. 141-146.

Rase, H. F. Vol. 1: *Chemical Reactor Design for Process Plants*, 1st. N. Y.: John Wiley & Sons, 1977.

Reinauer, T. V., Monat, J. P. and Mutsakis, M. "Dry FGD on an Industrial Boiler." *Chem. Eng. Progr.*, March 1983, pp. 74-80.

Rhudy, R. G. and Blythe, G. M. "Recent Results from the EPRI 2-1/2 MW Spray Dryer Pilot Plant," in *Ninth Symposium on Flue Gas Desulfurization, Cincinnati, Ohio, June 1985, Volume 2*. Report EPA-600/9-85-033b, NTIS No PB 86-138658, 1985, pp. 643-669.

Robards, R. F., Aldred, R. W., Burnett, T. A., Humphries, L. R. and Widico, M. J. "High-Sulfur Spray Dryer Evaluations," in *Ninth Symposium on Flue Gas Desulfurization, Cincinnati, Ohio, June 1985, Volume 2*. Report EPA-600/9-85-033b, NTIS No PB 86-138658, 1985, pp. 621-642.

Rochelle, G. T. and King, J. C. "The Effect of Additives on Mass Transfer in $CaCO_3$ or CaO Slurry Scrubbing of SO_2 from Waste Gases." *Ind. Eng. Chem. Fund.*, 16, No. 1 (1977), pp. 67-75.

Rochelle, G. T., Weens, W. T., Smith R. J. and Hsiang, M. W. "Buffer Additives for Lime/Limestone Slurry Scrubbing." *ACS Symp. Ser.*, 188 (1982), pp. 243-265.

Roop, R. N. and Pflug, L. Jr. "Operating Experience with Dry FGD System." *Tappi J.*, 67, No. 9 (1984), pp. 82-5.

Samuel, E. A., Lugar, T. W., Lapp, D. E., Fortune, O. F., Brna, T. G. and Ostop, R. L. "Dry FGD Pilot Plant Results: Lime Spray Absorption for High Sulfur Coal and Dry Injection of Sodium Compounds for Low Sulfur Coal," in *Proceedings: Symposium on Flue Gas Desulfurization, Volume 2*. Report EPA-600/9-83-020b, NTIS No. PB84-110 584, 1983, pp. 574-594.

Samuel, E. A., Lugar, T. W., Lapp, D. E., Murphy, K. R., Fortune, O. F., Brna, T. G. and Ostop, R. L. "Process Characterization of SO_2 Removal in Spray Absorber/Baghouse Systems," in *Proceedings: Eighth Symposium on Flue Gas Desulfurization, New Orleans, LA, November 1983, Volume 2*. Report EPA-600/9-84-017b, NTIS No. PB 84-223 049, 1984, pp. 668-688.

Schwartz, S. "The Economics of Reduction Sulfur Dioxide Emissions from Existing Power Plants," in *Proceedings: First Annual Pittsburgh Coal Conference*. Pittsburgh, PA: University of Pittsburgh, 1984, pp. 32-50.

Seidell, A. and Linke, W. F. Vol. 1: *Solubilities of Inorganic and Metal Organic Compounds*, 4th Ed. Washington, D. C.: Van Nostrand Co. Inc., 1958.

Seinfeld, J. H. *Air Pollution: Physical and Chemical Fundamentals*, 1st. Ed. N. Y.: McGraw Hill, 1975.

Setoyama, K. and Takahashi, S. "Solid Solution of Calcium Sulfite Hemihydrate and Calcium Sulfate." *Yogyo-Kyokai-Shi*, 86, No. 5 (1978), pp. 244-250.

Shah, N. D. "Dry Scrubbing of SO_2." *Chem. Eng. Progr.*, June 1982, pp. 43-46.

Shen, J. and Smith, J. M. "Diffusional Effects in Gas-Solid Reactions." *Ind. Eng. Chem., Fundam.*, 4 (1965), pp. 293.

Sherwood, T. K., Pigford, R. L. and Wilke, C. R. *Mass Transfer*. New York: McGraw Hill Book Co., 1975.

Smith, J. M. *Chemical Engineering Kinetics*, 3rd. N. Y.: McGraw Hill Book Co., 1981.

Spitzer, R. H., Manning, F. S. and Philbrook, W. O. "Generalized Model for the Gaseous Topochemical Reduction of Porous Hematite Spheres." *Trans. Met. Soc. AIME*, 233 (1966), pp. 1715.

St. Clair, H. W. "Rate of Reduction of an Oxide Sphere in a Stream of Reducing Gas." *Trans. Met. Soc. AIME*, 233 (1966), pp. 1145.

Stevens, N. J. "Dry SO_2 Scrubbing Pilot Plant Results," in *Proceedings: Symposium on Flue Gas Desulfurization-Houston, October 1980, Volume 2*. Report EPA-600/9-81-019b, NTIS No. PB 81-243 164, 1981, pp. 777-800.

Stevens, N. J., Manavizadeh, G. B., Taylor, G. W. and Widico, M. J. "Dry Scrubbing SO_2 and Particulate Control," in *Third Symposium on the Transfer and Utilization of Particulate Control Technology, Volume I*. Report EPA-600/9-82-005a, NTIS No. PB83-149 583, 1982, pp. 313-322.

Stokes, R. H. and Robinson, R. A. "Standard Solutions for Humidity Control at 25°C." *Ind. Eng. Chem.*, 41 (1949), pp. 2013.

Stouffer, M. R., Rosenhoover, A. W. and Statnick, R. M. *Laboratory and Field Development of Coolside SO_2 Abatement Technology*. Presented at the Second Annual Pittsburgh Coal Conference, Pittsburgh, Pa., September, 1985.

Tang, I. N. "Phase Transformation and Growth of Aerosol Particles Composed of Mixed Salts." *J. Aerosol Sci.*, 7 (1976), pp. 361-371.

Tang, I. N. and Munkelwitz, H. R. "Aerosol Growth Studies. III Ammonium Bisulfate Aerosols in a Moist Atmosphere." *J. Aerosol Sci.*, 8 (1977), pp. 321-330.

Tang, I. N., Munkelwitz, H. R. and Davis, J. G. "Aerosol Growth Studies. II Preparation and Growth Measurements of Monodisperse Salts Aerosols." *J. Aerosol Sci.*, 8 (1977), pp. 149-159.

Tang, I. N., Munkelwitz, H. R. and Davis, J. G. "Aerosol Growth Studies. IV Phase Transformation of Mixed Salt Aerosols in a Moist Atmosphere." *J. Aerosol Sci.*, 9 (1978), pp. 505-511.

Toprac, A. J. *Limestone Dissolution in Stack Gas Desulfurization Processes - Effect of Type and Grind.* Master's thesis, University of Texas at Austin, 1981.

Tseng, C. P. *Calcium Sulfate Hemihydrate Dissolution and Crystallization.* Doctoral dissertation, University of Texas at Austin, 1984.

Veazie, F. M. and Kielmeyer, W. H. *Feasibility of Fabric Filter as Gas-Solid Contactor to Control Gaseous Pollutants*. Report EPA-APTD 0595, NTIS No. PB-195 884, August 1970.

Vieth, W. R. and Amini, M. A. "Generalized Dual Sorption Theory." *Polym. Sci. Technol.*, 6 (1974), pp. 49-61.

von Rosenberg, D. U., Chambers, R. P. and Swan, G. A. "Numerical Solution of Surface Controlled Fixed-Bed Adsorption." *Ind. Eng. Chem., Fundam.*, 16, No. 1 (1977), pp. 154-157.

Wark, K. and Warner, C. F. *Air Pollution. Its Origin and Control*, 2. New York: Harper & Row, 1981.

Weber, G. F., Schelkop, G. L. and Ness, H. M. "Pilot Scale Studies of Simultaneous Control of SO_x/NO_x Emissions Derived from the Combustion of Low-Rank Coal," in *Proceedings: First Annual Pittsburgh Coal Conference*. Pittsburgh, PA: University of Pittsburgh, 1984, pp. 241-262.

Wen, C. Y. and Wei, L. Y. "Simultaneous Nonisothermal Noncatalytic Solid-Gas Reactions." *AIChE J.*, 17 (1971), pp. 272.

Winkler, P. "The Growth of Atmospheric Aerosol Particles as a Function of the Relative Humidity. II An Improved Concept of Mixed Nuclei." *J. Aerosol Sci.*, 4 (1973), pp. 373-387.

Yagi, S. and Kunii, D. "Fluidized Solid Reactors with Continous Solids Feed - II Conversion for Overflow and Carryover Particles." *Chem. Eng. Sci.*, 16 (1961), pp. 372.

Yavorsky, P. M., Akhtar, S. and Friedman, S. "Process Developments: Fixed Bed Catalysis of Coal to Fuel Oil." *AIChE Symposium Series*, 70, No. 137 (1974), pp. 101-105.

Yeh, J. T., Demski, R. J., Gyorke, D. F. and Joubert, J. I. "Experimental Evaluation of Spray Dryer Flue Gas Desulfurization for Use with Eastern U. S. Coals," in *Proceedings: Symposium on Flue Gas Desulfurization, Volume 2*. Report EPA-600/9-83-020b, NTIS No. PB84-110584, 1983, pp. 821-839.

Zareski, G. K. "The Gas Supplies of the United States," in *Pollution Control and Energy Needs*, Ed. Jimeson, R. M. and Spindt, R. S., *Advances in Chemistry*. Washington, D. C.: American Chemical Society, 1973, pp. 1-16.